AD-A144 049 COOLING OF HIGH POWER GENERATORS AND MOTORS FOR ELECTRIC PROPULSION(U) NAVAL POSTGRADUATE SCHOOL MONTEREY CA J L SZATKOWSKI ET AL. MAR 84 1/2

UNCLASSIFIED F/G 13/10 NL

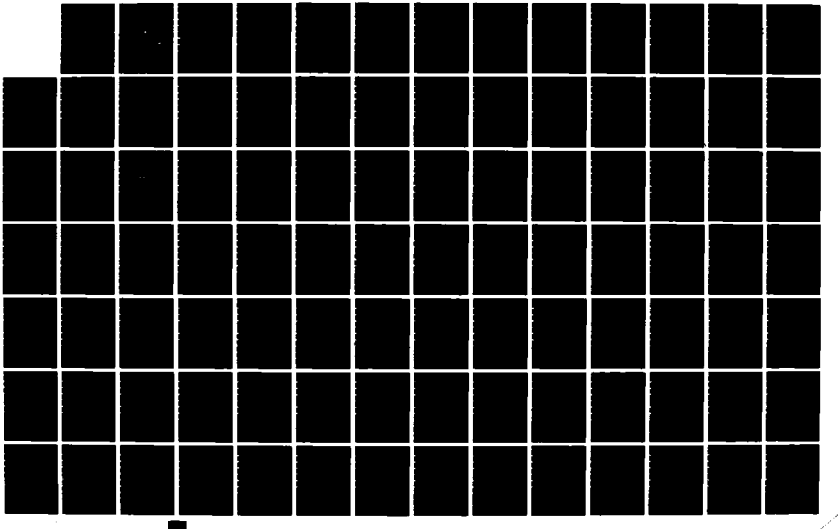

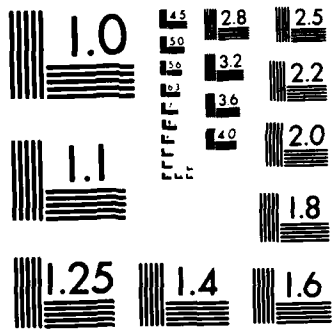

NAVAL POSTGRADUATE SCHOOL
Monterey, California

THESIS

COOLING OF HIGH POWER GENERATORS
AND MOTORS FOR ELECTRIC PROPULSION

by

James LeRoy Szatkowski

March 1984

Thesis Advisor: Paul J. Marto

Approved for Public Release, Distribution Unlimited

UNCLASSIFIED

SECURITY CLASSIFICATION OF THIS PAGE (When Data Entered)

REPORT DOCUMENTATION PAGE		READ INSTRUCTIONS BEFORE COMPLETING FORM
1. REPORT NUMBER	2. GOVT ACCESSION NO. A144 049	3. RECIPIENT'S CATALOG NUMBER
4. TITLE (and Subtitle) Cooling of High Power Generators and Motors for Electric Propulsion		5. TYPE OF REPORT & PERIOD COVERED Master's Thesis, March 1984
		6. PERFORMING ORG. REPORT NUMBER
7. AUTHOR(s) James LeRoy Szatkowski in conjunction with Paul J. Marto		8. CONTRACT OR GRANT NUMBER(s)
9. PERFORMING ORGANIZATION NAME AND ADDRESS Naval Postgraduate School Monterey CA 93943		10. PROGRAM ELEMENT, PROJECT, TASK AREA & WORK UNIT NUMBERS
11. CONTROLLING OFFICE NAME AND ADDRESS Naval Postgraduate School Monterey, CA 93943		12. REPORT DATE March 1984
		13. NUMBER OF PAGES 134
14. MONITORING AGENCY NAME & ADDRESS(if different from Controlling Office)		15. SECURITY CLASS. (of this report) UNCLASSIFIED
		15a. DECLASSIFICATION/DOWNGRADING SCHEDULE

16. DISTRIBUTION STATEMENT (of this Report)

Approved for Public Release, Distribution Unlimited

17. DISTRIBUTION STATEMENT (of the abstract entered in Block 20, if different from Report)

18. SUPPLEMENTARY NOTES

19. KEY WORDS (Continue on reverse side if necessary and identify by block number)

Electric motor cooling
Forced convection cooling
Thermosyphons
Heat pipes

20. ABSTRACT (Continue on reverse side if necessary and identify by block number)

This study reviews the history and development of marine electric propulsion drives, the types of electric propulsion, and the inherent losses which occur within the synchronous AC machines typically used for high-power propulsion systems.

A thorough review of the literature pertaining to heat transfer in electrical machinery is made. In particular, the use of liquid cooling in various flow configurations, including buoyancy-driven thermosyphons and two-phase thermosyphons, is analyzed. contd.

DD FORM 1473 EDITION OF 1 NOV 65 IS OBSOLETE

S/N 0102-LF-014-6601

UNCLASSIFIED

SECURITY CLASSIFICATION OF THIS PAGE (When Data Entered)

Forced-liquid cooling is feasible, but the required rotating seals are a problem in reliability. Closed-loop thermosyphon cooling appears feasible at high rotational speeds, although a secondary heat exchange through the shaft is required. Closed, two-phase thermosyphons and heat pipes are also feasible, but require forced-air circulation for heat rejection to the ambient. Since all of these concepts deserve additional attention, areas for further research and development are recommended.

Approved for public release; distribution unlimited.

Cooling of High Power Generators and Motors for Electric Propulsion

by

James L. Szatkowski
Lieutenant, United States Navy
B.S.E.E., University of Utah, 1976

Submitted in partial fulfillment of the requirements for the degree of

MASTER OF SCIENCE IN MECHANICAL ENGINEERING

from the

NAVAL POSTGRADUATE SCHOOL
March 1984

Author: _____

Approved by: _____
Thesis Advisor

_____
Second Reader

_____
Chairman, Department of Mechanical Engineering

_____
Dean of Science and Engineering

ABSTRACT

This study reviews the history and development of marine electric propulsion drives, the types of electric propulsion, and the inherent losses which occur within the synchronous AC machines typically used for high-power propulsion systems.

A thorough review of the literature pertaining to heat transfer in electrical machinery is made. In particular, the use of liquid cooling in various flow configurations, including buoyancy-driven thermosyphons and two-phase thermosyphons, is analyzed.

Forced-liquid cooling is feasible, but the required rotating seals are a problem in reliability. Closed-loop thermosyphon cooling appears feasible at high rotational speeds, athough a secondary heat exchange through the shaft is required. Closed, two-phase thermosyphons and heat pipes are also feasible, but require forced-air circulation for heat rejection to the ambient. Since all of these concepts deserve additional attention, areas for further research and development are recommended.

TABLE OF CONTENTS

LIST OF TABLES

LIST OF FIGURES

NOMENCLATURE

Latin Symbols

a tube radius (m)

Ac $H\ \Omega^2/g$

Cp specific heat (kJ/kg.K)

d tube diameter (m)

f friction factor

F_c condensation factor for equation (3.6)

P stress ratio = $\tau_w / \delta g\ \rho_l$

g acceleration of gravity (m/s^2)

Gr Grashof number = $g\ \beta\ \Delta T d^3 / \nu^2$

Grr Rotational Grashof number = $H\ \Omega^2\ \beta\ \Delta T d^3 / \nu^2$

hfg heat of vaporization (kJ/kg)

H radius of rotation (m)

j volumetric flux (m^3/s)

j* dimensionless volumetric flux = $j_g \rho_g^{1/2} \{gD(\rho_f - \rho_g)\}^{-1/2}$

J Rotational Reynolds number = $\Omega d^2 / \nu$

k thermal conductivity (W/m.K)

Ktcr-critical transition value (for equations 2.11-2.15)

Kl = JRe (for equation 2.14)

Kt = J^2/Re (for equations 2.11 & 2.12)

L length of tube (m)

p pressure (Pa)

P pressure (Pa)

Pr Prandtl number

q specific heat flux (W/m^2)

Q Heat load (W)

Ra Rayleigh number (Gr*Pr)

Rar Rotational Rayleigh number (Grr*Pr)

Re Reynolds number = Vd/ν

Ro Rossby number = V / Ωd

S swirl number = 1/ Ro

t temperature (K or °C)

V velocity (m/s)

Greek Symbols

α void fraction or thermal diffusivity (unitless or m^2/s)

β coefficient of thermal expansion (1/K)

δ film thickness (m)

γ ratio of specific heats

Δ difference in values

τ temperature gradient (K/m)

ρ density (kg/m^3)

μ viscosity ($N.s/m^2$)

σ surface tension (N/m)

ν kinematic viscosity (m^2/s)

Ω angular velocity (1/s)

Subscripts

0 stationary reference

am arithmetic mean temperature difference

b bulk condition

B boiling section

c cooled section

cr critical value

E entrainment value

h heated section

l laminar conditions

l liquid state

s sonic value (M=1)

sat saturation value

t turbulent conditions

v vapor state

w wall condition

m mean condition

ACKNOWLEDGMENT

The author wishes to express his sincere appreciation for the guidance, support, and understanding given by his advisor, Professor P. J. Marto, in the preparation of this thesis. Thanks are also given to Dr. A. S. Wanniarchchi for his expert assistance during the study. Finally, a special acknowledgment is also due my wife, Lesley, for the exceptional amount of patience shown during the preparation of this thesis.

I. INTRODUCTION

The marine engineer and naval architect are charged with creating a design of a vessel from a broad set of requirements for the ship system prepared by the customer. This requires a very structured procedure for preparing the design-based comparisions and economic trade-off studies at each and every stage of the development of the design. The end result is a complete set of design requirements from which to construct the final product (this result should meet the original design requirements!).

This structured procedure has the form of the well-known "design spiral" [Ref. 1], which is shown in Figure 1.1 for the propulsion machinery. This procedure encompasses the total ship design, including (but not limited to):

Main Propulsion System

Shaft horsepower

Propeller RPM

Specific fuel consumption and bunker capacity

Space and weight objectives

Adaptability to ship configuration

Auxiliary Ship Systems

Power and lighting

Steam-galley, deck, and heating systems

Heating, ventilating, and air conditioning

Firefighting and ballasting

Fresh water

Hull Engineering Systems

Anchor handling

Steering engine and bridge telemetering control

Cargo handling gear

Crane systems

Electronic and Navigation Systems

Communication, exterior and interior

Radar

Loran, Omega, etc., navigation aids

Military electronics, sensors, command and control systems, weapons directors, tactical data systems, and electronic countermeasures.

In order to design the vessel within economic constraints, or to use the life cycle cost as the function to optimize, it is imperative to define initially the devices used to provide the power for the vessel. They must provide most for the least, in terms of the fuel that they expend and the volume and weight that they possess.

The selection of the main propulsion plant requires matching the power of the generating device with a transmission (in most cases), the propulsor, other ship systems and the hull. If one limits the choices of propulsors to fixed-pitch propellers and controllable and reversible-pitch propellers, which are currently realistic for large vessels, the number of possible permutations remains quite sizable, as shown in Figure 1.2. The horsepower and RPM requirements of modern warships require the use of a transmission to couple the high RPM of an economical prime mover with the low RPM required at the propulsor for high propulsive

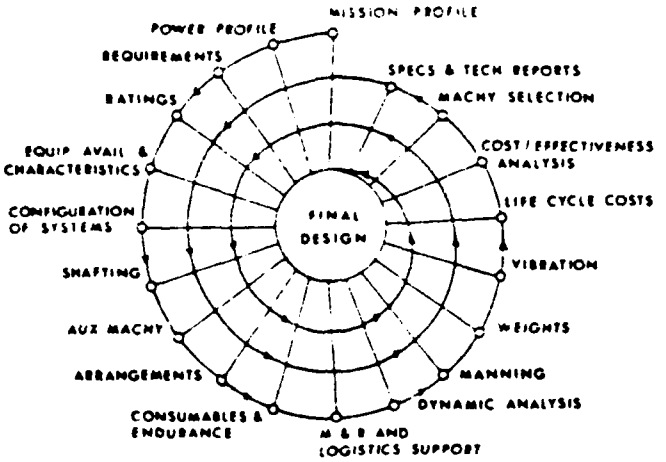

Figure 1.1 Preliminary Design Spiral for Propulsion Machinery.

efficiency. This transmission may be either mechanical or electrical. The mechanical reduction gear has been exploited in the past to minimize volume/space requirements. When coupled to a reversible prime mover, such as a steam turbine, it has been proven to be quite acceptable. However, the electrical transmission has several attractive features, such as ease of propulsor speed and direction control, flexibility in the the number and location of controls, freedom of installation and machinery layout, coupling of various prime movers independently to propulsor drives (as well as other auxiliary applications), and the ease of auxiliary thruster installation for maneuvering control.

The choice of the propulsion plant includes many important factors, such as:

1. Reliability
2. Maintainability
3. Space and arrangement requirements
4. Weight requirements
5. Type of fuel required

6. Fuel consumption
7. Fractional power and transient performance
8. Interrelations with auxiliaries
9. Reversing capability
10. Operating personnel
11. Rating limitations
12. Costs

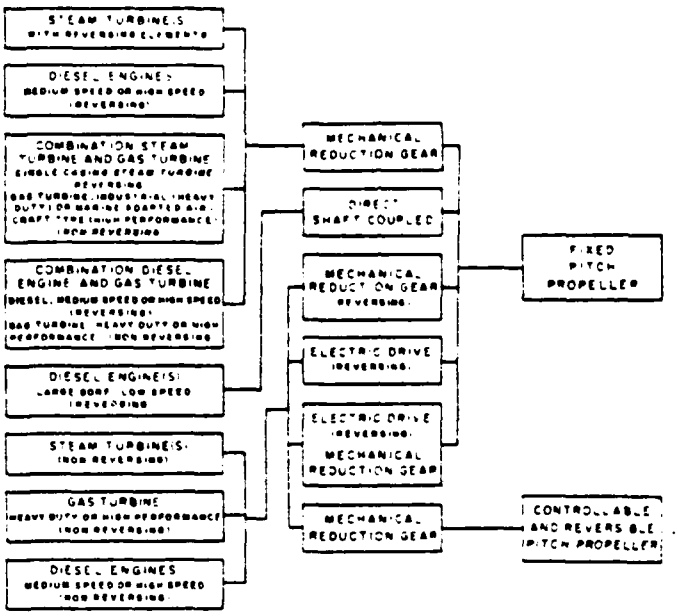

Figure 1.2 Propulsion Plant Alternatives.

These factors have gone through many cyclic changes based on the fluctuating economy. The recent emphasis on fuel costs and availability has driven the fuel consumption/prime mover efficiency to a much higher level of concern than it was previously given. The cost of acquisition of new vessels has skyrocketed, as well as the costs of maintenance and repair. These escalating costs are a challenge to the engineer of today. The economic considerations of the initial cost of a plant, the cost of maintenance and repair, and the cost to operate a plant from its

construction to its retirement, also coined "life cycle" cost, is the driving force that controls the design of the modern warship.

Of the list of prime movers shown in Figure 1.2, the life-cycle cost of the marine gas turbine is one of the lowest. The economy of operation is maximized within a rather narrow range of RPM's. This has been tolerated in the current employment of this device, since the cost of utilizing an electric transmission to accomplish the goal of operating the prime mover within its maximum economy range did not offset the loss of efficiency experienced by the gas turbine. This was due to the technology that existed within the field of electrical controls at the time. The advent of electronic frequency control of the output of the generator, independent of RPM or poles, and the frequency control of the synchronous motor, independent of its supply frequency, makes the use of the electrical transmission much more attractive. Although the initial cost will be higher, the cost of operation, maintenance, and repair of the system will rapidly offset the initial cost differential [Ref. 2], [Ref. 3], and [Ref. 4]. An analysis of the economic and engineering considerations involved with this mechanical vs. electrical drive selection was made by Eric Gott and S. O. Svensson [Ref. 5] in 1974; they clearly illustrated the nature of the problem and possible solutions. In their paper, it was evident that the selection of some of the possibly more appropriate forms of electric drives was discouraged due to the economics of the choice. High-power frequency-controlling equipment was very expensive and bulky. Recent advances in high-power, solid-state equipment have now again promoted these alternatives into viable contention.

A. HISTORICAL DEVELOPMENT

From the early attempts by the Russians in the 1890's to power small passenger launches, and the British and French experiments with small submersibles, to the present, the use of electric propulsion has made a slow evolution. The U.S. Navy began with the Jupiter in 1911. It was a 5500 hp/shaft vessel equipped with wound rotor induction motors, which fulfilled a 30-year lifespan (terminated by surface warfare activity in 1943, while serving as an aircraft carrier (Langely)). This led to several major programs, summarized below:

* AC drive installed on five battle ships of 30,000+hp(1918-1922)

* AC drive applied to carriers Saratoga and Lexington of 200,000hp (1920)

* Synchronous ac drive introduced on four Coast Guard cutters (1919)

* Synchronous ac drive in the liner Normandie at 160,000hp (1935)

* Synchronous ac drive and full dynamic braking in cutters (1940)

In the U.S.Navy Bureau of Ships Manual (BUSHIPS 250-660-2), dated 1 March 1945, the text states that the Navy's inventory of ships that used electric drive (in addition to above) was "....about two hundred destroyer escorts and about one hundred other ships including tankers, cargo transports, troop transports, and store ships." All of these applications were with steam turbines (which were speed-adjustable and reversible) and eventually this design lost favor to the less expensive mechanical reduction gear systems which were somewhat lighter. The weight of these

original electric drive systems was due to the basic frequency relationship of RPM to the number of poles. This led to the basic configuration of two pole generators (3600RPM) and twenty-eight to eighty pole motors (256-90RPM). The large number of poles required in motor the for speed reduction caused the motors to be extremely large and heavy. The advent of the use of synchronous motors reduced the weight slightly since the motor experienced much fewer slip losses. A good historical background on the early stages of electric propulsion is found in the book written by Commander S.M. Robinson, USN [Ref. 6].

Current applications in the U.S. Navy are shown in Table I.

TABLE I
U.S. Navy Electric Drive Ships

Type	# Ships	SHP	# Motors
AS	2	15,000	1
AS	2	11,520	8
TARC	1	10,000	2*
TAGOS	1	1,600	2**

* also has 4-1200 hp thrusters

** also has 1-550 hp thruster

B. ELECTRIC PROPULSION CONCEPTS

An area of current research in the field of rotating electric equipment that shows considerable promise with regard to electric propulsion is the use of acyclic (homopolar) superconductive DC devices. These devices produce exceptionally high torque and horsepower in a very small volume and weight. This is of great value in advanced

hullform propulsion. A large amount of research in this area to determine configuration, peak casualty potential, maintainability of the required cryogenic equipment, as well as the adaptibility of the systems for this cryogenic apparatus must be performed before actual implementation of this configuration can occur in a specific design. Thus, for rapid implementation in a short-term project (3-5yrs), the choices remaining in electric propulsion to be considered are direct-current (DC) and alternating-current (AC) devices. The category of AC devices is further subdivided into inductive and synchronous devices. All three devices have been used for marine propulsion and each has its own inherent advantages and disadvantages.

1. DC Machinery

The DC electric drive system has been used extensively in the past, primarily in low to medium power ranges (1000 - 6000 hp/shaft) with extremes of 400 hp/shaft and 19,600 hp/shaft noted. This employment of DC drives normally utilizes 1-4 prime movers powering one or more motors per shaft (duplicating the system if more than one shaft exists).

Primary advantages of this system include:

1. **Ease of Control.** Control being effected by varying the generator voltage through field control-a process that lends itself well to remote location(s).

2. **Multiple Control Stations.** The ease of which the generator voltage and polarity of the motor connections (either field or exciter) are varied allows multiple control stations to be designed for flexible ship control in tight maneuvering situations.

3. **Adaptability to varing propeller-hull characteristics.** The propeller-hull characteristics change

dramatically when the vessel is towing or ice-breaking. The ability to match the prime mover (running at optimum speed) to the propeller through the propulsion motor and still provide maximum torque is a specific advantage of this system, without excess engine or electrical capacity, through a wide range of propeller RPMs.

Primary disadvantages include:

1. **Limited Power Range.** The top-end range of approximately 10,000 hp/shaft limits the vessel size that can utilize this system.

2. **Generator Speed Limitations.** The maximum speed that the generator can be operated, due to problems primarily associated with commutation, is typically limited to under 1000 RPM. This limits the selection of the prime mover if one does not utilize mechanical reduction gearing to match the characteristics. Figure 1.3 shows the normal relationship of RPM vs. KW.

3. **Weight and Size.** The weight of the DC system increases dramatically with power rating as shown in Figure 1.4 (this figure shows weight in pounds/SHP); note that total weight becomes almost linear with SHP at higher SHP values. This precludes high power applications of conventional DC systems above 10,000 hp/shaft (acyclic-homopolar devices are excluded from this analysis). The physical size of the device also has this dramatic functional relationship to rating as shown in Figure 1.5.

From the above discussion of advantages and disadvantages, the consideration of DC electric propulsion for use in a warship design that would require on the order of 40,000 hp and utilize gas turbines in their most efficient

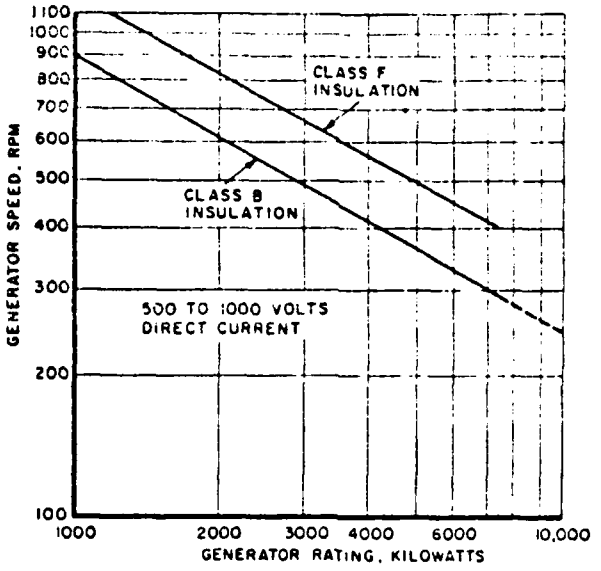

Figure 1.3 Variation of DC Generator Speed with Rating.

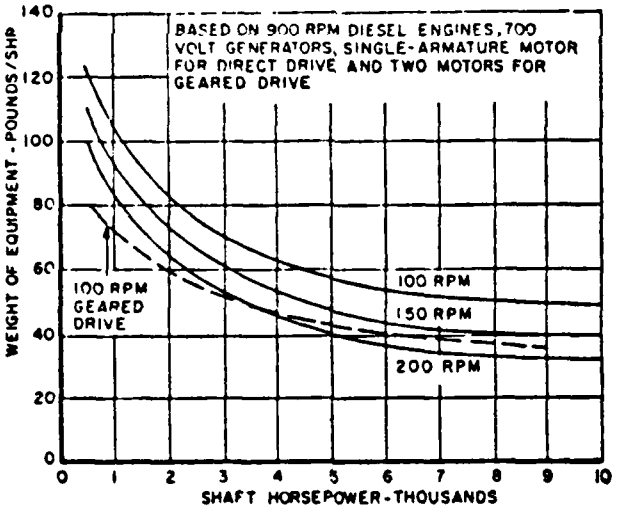

Figure 1.4 Variation of DC Generator Weight with Rating.

operating range is not realistic. Therefore, the remainder of this paper will only consider the AC systems. The

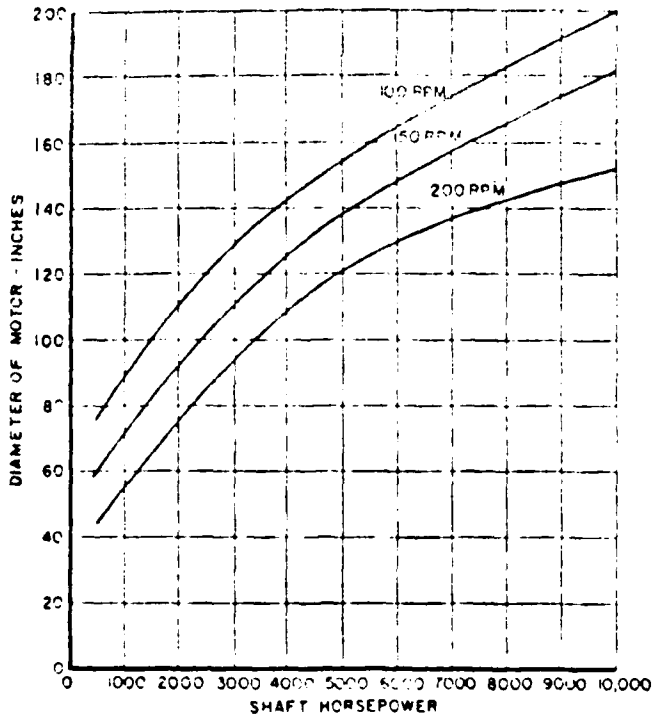

Figure 1.5 Variation of DC Generator Size with Rating.

inherent losses associated with these DC systems though are essentially the same as those in the AC systems. Figures 1.1 through 1.5 are from "Marine Engineering", R. L. Harrington, editor.

2. AC machinery

The devices included in the conventional AC machinery area fall into two categories: induction and synchronous. The principal difference between the two systems is in the motor application. The induction motor system provides exceptional torque at low RPM and maximum slip (200%). This high torque response at low RPM makes the induction motor system preferable in some applications. For naval applications, this system is not as efficient as the synchronous system by a few critical percentage points. The

induction motor has losses that are a function of the slip incurred between the rotor and the stator field. This slip is related to the RPM and load. The remaining losses in the induction motor are the same as the synchronous motor in general. Another critical difference between the two systems is the power factor difference. In the induction motor, the rotor current is induced from the stator field. This induced field that is created as a result of this current is the mechanism from which the mechanical rotation is derived. Since this current is induced from the stator (supplied current), it causes the current load seen by the supplying device to "lag" the supplying voltage and therefore cause the power factor (a measure of the amount of lag or lead) to be less than unity. A power factor of unity indicates that the load current and the load voltage are in phase and maximum real energy transfer is occurring. The induction motor is normally operated with a lagging power factor of approximately 80% [Ref. 6] and an overall efficiency of approximately 90%. In the synchronous system, the power factor is normally unity and is controllable by the external motor rotor excitation which results in the synchronous system's power factor being adjustable and a unity power factor being easily obtained. Note here also that the power factor in this system can be made to actually "lead" and thereby correct a system "lag" to other loads that might exist in the fully integrated system. The advantages of AC systems in general are:

1. **High Efficiency.** Losses in the synchronous system are approximately 6% (including excitation losses) as compared to the induction motor system losses that range from approximately 8 to 10%.

2. **Flexibility of Installation.** The direct drive motor can be installed in the vessel to minimize shaft

length to the propeller (since physically smaller than DC motors) and the generator can be installed without reduction gearing and operated directly coupled to the prime mover.

3. **Dual Use of Propulsion Power.** The AC system allows for the power from propulsion units to be used for other functions when not required for propulsion; this leads to the creation of a fully-integrated system.

4. **Available in large Power Ratings.** The conventional AC systems can be built in any power rating required with a reasonable upper limit of approximately 60,000 hp. The larger system's size is being reduced by raising the system voltage (which is not limited by the commutation requirements of DC systems). The system voltages typically in use are from 2,300 to about 7,500 volts. These voltages are easily transformed for other uses in addition to propulsion.

The selection of the main propulsion system therefore is not simple. The design environment must be specified and the prime mover is selected. Once these parameters are defined, the appropriate selection of transmission, control, and propulsor can be chosen. For the purpose of the propulsion of a vessel of approximately 8,000-ton displacement and the mission of a normal warship of the destroyer/cruiser variety using the marine gas turbine as the prime mover and life-cycle costs the design criteria, the selection of the AC synchronous drive (possibly fully integrated) appears as a very appropriate choice. Some of the design configurations possible within this choice, and the associated performance of each, are shown in Figure 1.6 as presented in [Ref. 7]. Additional possible configurations are shown in Figures 1.7 and 1.8 . The end result of the implementation of these technologies would result in substantial savings

over the current production configuration that utilizes the gas turbine main propulsion in the life-cycle analysis. Such a comparison is shown in Figure 1.9, also from the NAVSEA report [Ref. 7].

Additional propulsion plant arrangements are given in [Ref. 5] and the total number possible is only limited truly by the designer's imagination and creativity within the confines of the hullform.

3. Motor/Generator Losses

The concept of losses within the motor and the generator are comparative in magnitude and virtually identical in nature. The losses will, therefore, be discussed as a group which is applicable to both the motor and the generator. The approach of an energy balance is useful here to introduce these losses:

Energy into device on the mechanical side	+	Energy into device on the electrical side	=

Increase of stored kinetic/ potential mech. energy in device	+	Increase of stored energy in the elec.&mag. fields of device	+	Heat generated within device

(1.1)

The net quantity on the right-hand side of the equation is small and positive; the majority of the energy into the device is transmitted through the device as an output. As an example, when considering the motor, the energy into the device on the mechanical side is negative in sign and approximately equal to the electric energy into the device which is positive in sign. This amount must be balanced by the quantity on the right side of the equation.

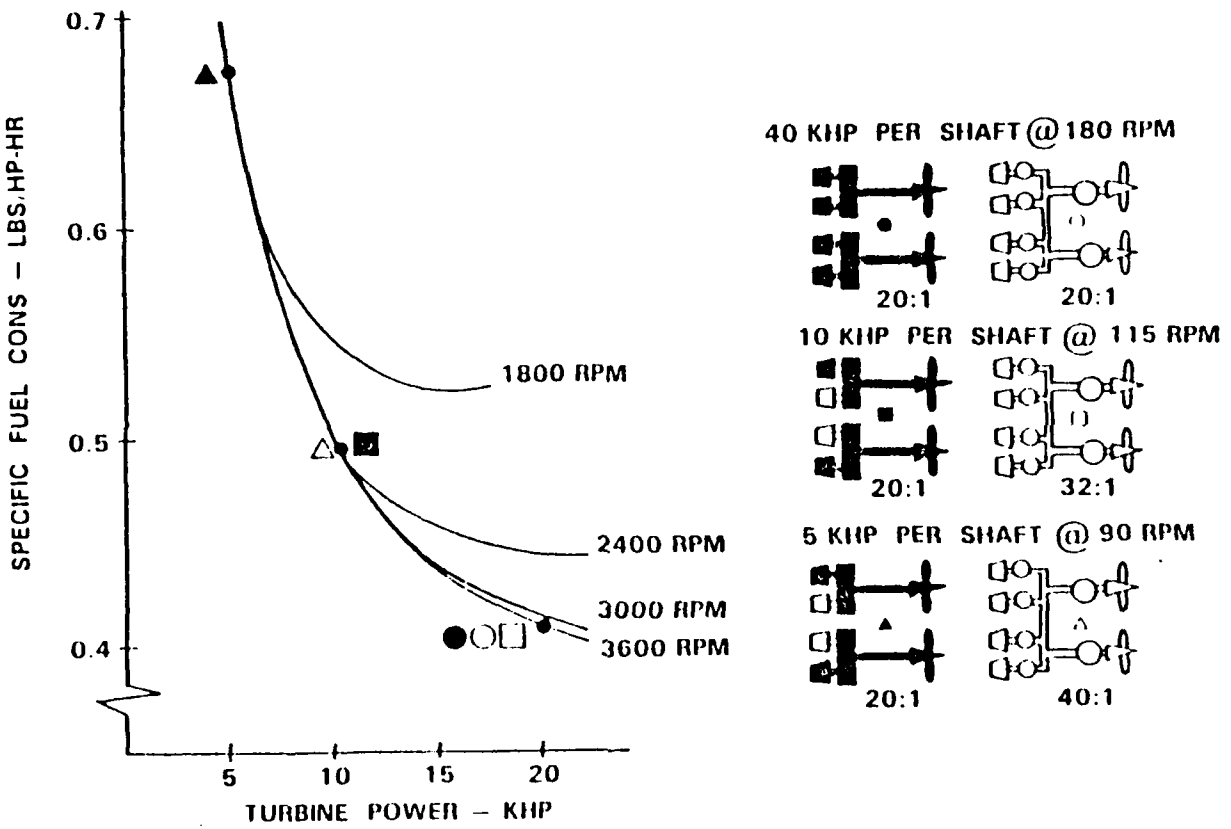

Figure 1.6 Performance for Various Configurations of AC Drives.

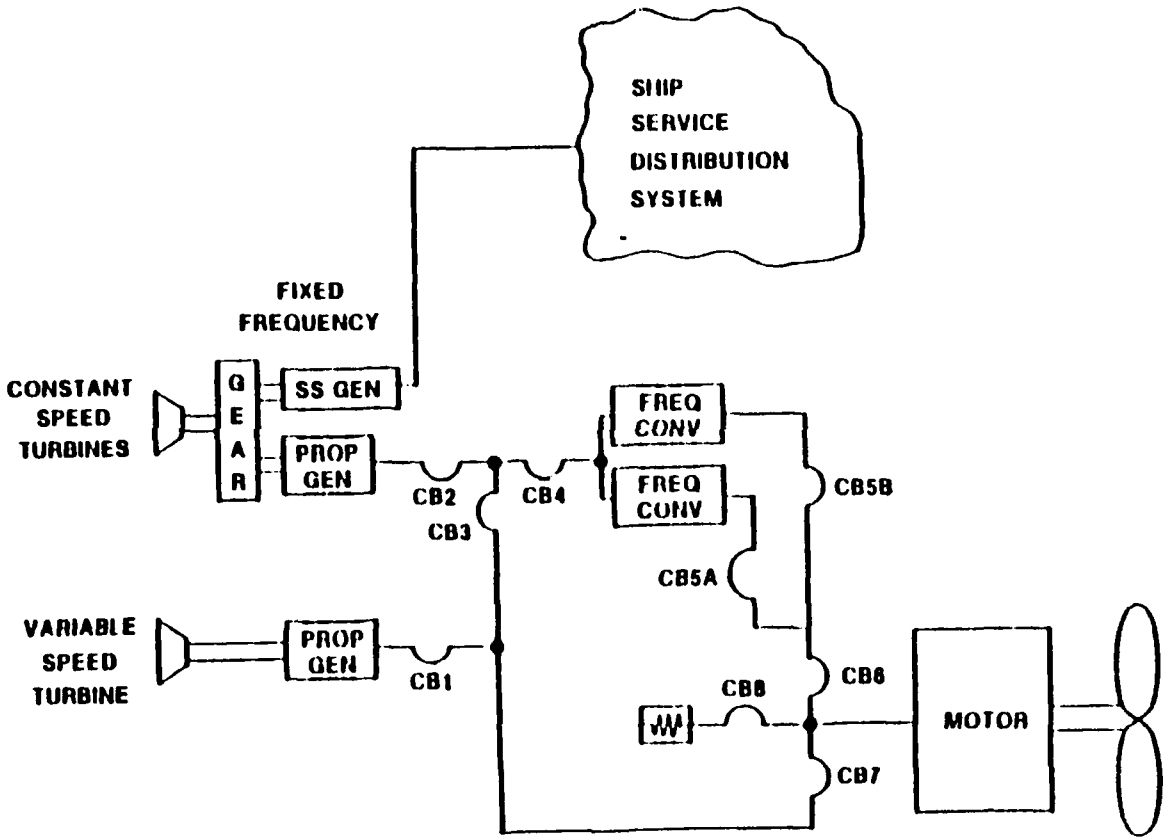

Figure 1.7 Integrated System Candidate, Fixed Frequency.

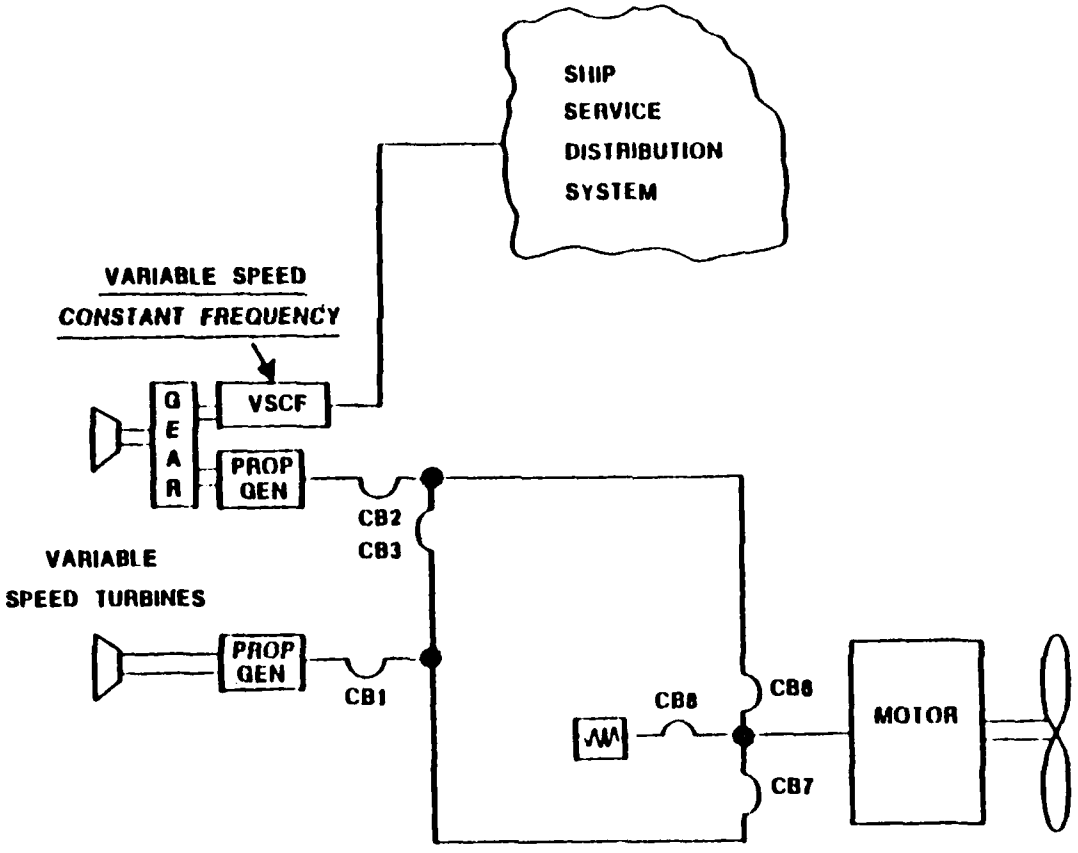

Figure 1.8 Integrated System Candidate, Variable Speed.

COMPARATIVE DESTROYER SIZE AND COST ★
DD963-LIKE MECHANICAL VS INTEGRATED ELECTRIC MACHINERY

MACHINERY ALTERNATIVE	SHIP IMPACT		LIFE CYCLE COST IMPACT	
	SIZE (M.TONS)	ACQUIS. COST	30YR FUEL ($M)	MANNING REQMT.
4 LM 2500 (DD963-LIKE)	7100	BASE	385	BASE
3 LM 2500 INTEGRATED ELECTRIC	6300	.97BASE	322	1.0BASE
IMPACT OF INTEGRATED ELECTRIC MACHINERY	-11%	-3% ★★	-16%	0

★ EXTRACTED FROM DDGX MACHINERY PLANT TRADEOFF SUMMARY PRESENTATION TO SENIOR REVIEW PANEL, 17 MARCH 1982.

★★ COST REDUCTION PERCENTAGE BASED ON TOTAL SHIP ACQUISITION COST (INCLUDING COMBAT SYSTEMS). SHIPBUILDING COST WOULD BE REDUCED ABOUT 6%.

Figure 1.9 Comparative Destroyer Size and Cost.

The terms on the right side are all usually small and may be zero. The first term represents the energy associated with a speed change and results from the inertia of the device. In the steady state it is zero. The second term would result from a change in current to the device and the electric field that existed would be a source of energy (the induction effect). The third term is the main point of interest here. It is comprised of the following:

* Mechanical friction losses
* Air friction losses (windage)
* Hysteresis and eddy-current losses
* Resistance losses in the armature, and
* Exciter losses (in the case of synchronous machines).

The object for the electrical engineer is to minimize these losses to the greatest extent possible. Since it is impossible to eliminate all these losses, the problem that remains is the removal of the resulting heat within the device [Ref. 8]. The size and weight of the device is largely dependent on the ability to remove this heat, since the capacity of the device is limited by the insulation used in the device. The method of heat removal is not limited to a single mode, but is a combination of many modes of heat transfer including:

* Conduction: stator to casing
  rotor to stator (through air gap)
  rotor to shaft
  shaft to casing
  shaft to external device (coupling, reduction gear, etc.)

* Convection (both forced and natural):
  casing to ambient
  stator to internal air (or gas)
  rotor to internal air (or gas)
  shaft surface to internal air (or gas)

shaft surface to external air

* Radiation: external surfaces to sinks

internal surfaces to casing

These modes are not all very controllable. Large amounts of research have been devoted to minimizing these thermal resistances. Efforts to improve convection heat transfer have found that the restrictions on the rotor-stator air gap have prevented exploitation of this mode as discussed as early as in 1926 by G.E. Luke [Ref. 9] and as late as in 1979 by O.N. Kostikiv, et al. [Ref. 10]. The improvement of the conduction heat transfer has been improved by minimizing the thermal resistance of the insulating compounds and the materials used in the construction of the device, including installing thermally-conductive materials in the coil ends.

The improvement of convection heat transfer is still being examined by using liquids and gases to cool the rotor and the stator of these devices. This procedure involves piping a liquid through the stator to remove heat by forced convection, and utilizing a material with high thermal conductivity directly adjacent to the piping to conduct it to the piping where it is removed by the passing liquid. This method is equally applicable to the rotor, provided the problem of the rotating seals can be overcome in order to channel the liquid from an external sink to the moving rotor and back out. The advantage of doing this over standard cooling schemes is that the capacity of a device may be increased due to the lower internal temperatures that could be maintained (or the physical size and weight of the device could be reduced for an existing capacity) as shown in Figure 1.10 for a 40,000 hp, 180 RPM synchronous motor. The use of a liquid in a bouyancy driven closed-loop, called a thermosyphon, is also possible. The amount of heat transfer

in this method is dependent on the specific heat capacity of the liquid being used, the temperature rise allowed, the pipe resistance in the loop, and the required flow rate; the heat-transfer areas then required may be prohibitively large.

The two-phase cooling method within a closed loop, in the form of a heat pipe, has also been extensively investigated. This method has an advantage over the conventional, liquid-cooling method in that it eliminates the necessity for rotating seals. These seals can be weak points in the design from a reliability stand point, especially if high RPMs are involved. The heat-pipe method typically involves a confined fluid acting as a two-phase medium for heat transfer, explciting the phase change as a vehicle for substantial heat transfer in order to remove heat from the rotor or the stator or both. This method then transfers the heat either to the ambient air or to some other gas, liquid or solid heat exchanger. The configuration most suitable for use within a motor/generator on the order of 40,000 hp would be either to ambient air or to a fresh water heat exchanger external to the motor in the case of stator cooling, or to internal forced air through extended surfaces in the case of rotor cooling.

C. PROBLEM DEFINITION

The purpose of this thesis is to analyze various methods of cooling motors and generators of warship propulsion plants and to discuss the economic and reliability perspectives associated with each system. The next two chapters will discuss the theory and application of these two methods: liquid cooling of the rotor, both forced convection and the thermosyphon, and two-phase cooling of the rotor.

A test apparatus for evaluation of various rotating cooling schemes has been designed and is currently under construction at the David W. Taylor Naval Ship Research and Development Center, Annapolis, Maryland. It is sketched in Figure 1.11 and will be used for the analysis within this study. The results/recommendations herein may thereby be experimentally evaluated.

For the purpose of this arbitrary configuration, the model for analysis is as follows:

1) The device will be a water-cooled frame, synchronous AC generator, 25,118 kVA @ 3,600 RPM.

2) A specific conduction bar shall be analyzed for a typical load for all cooling configurations. It has a length of 0.9144m and is 0.0116m squarewith a 4.763mm diameter hole bored through the length (herein referred to as the tube length and tube diameter). The losses per bar in this configuration are approximately 50W.

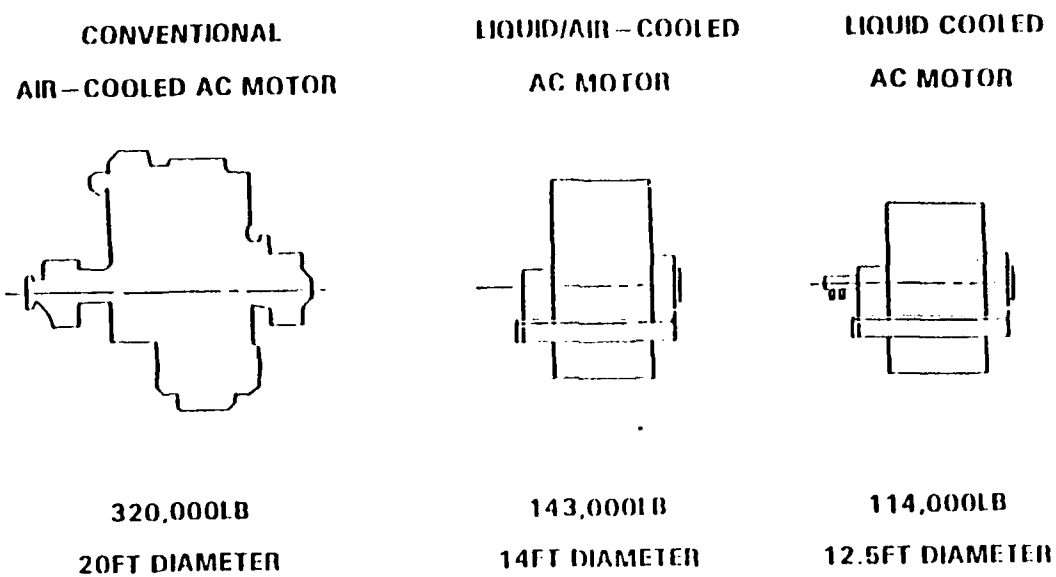

Figure 1.10 Motor Comparision with Various Cooling Schemes.

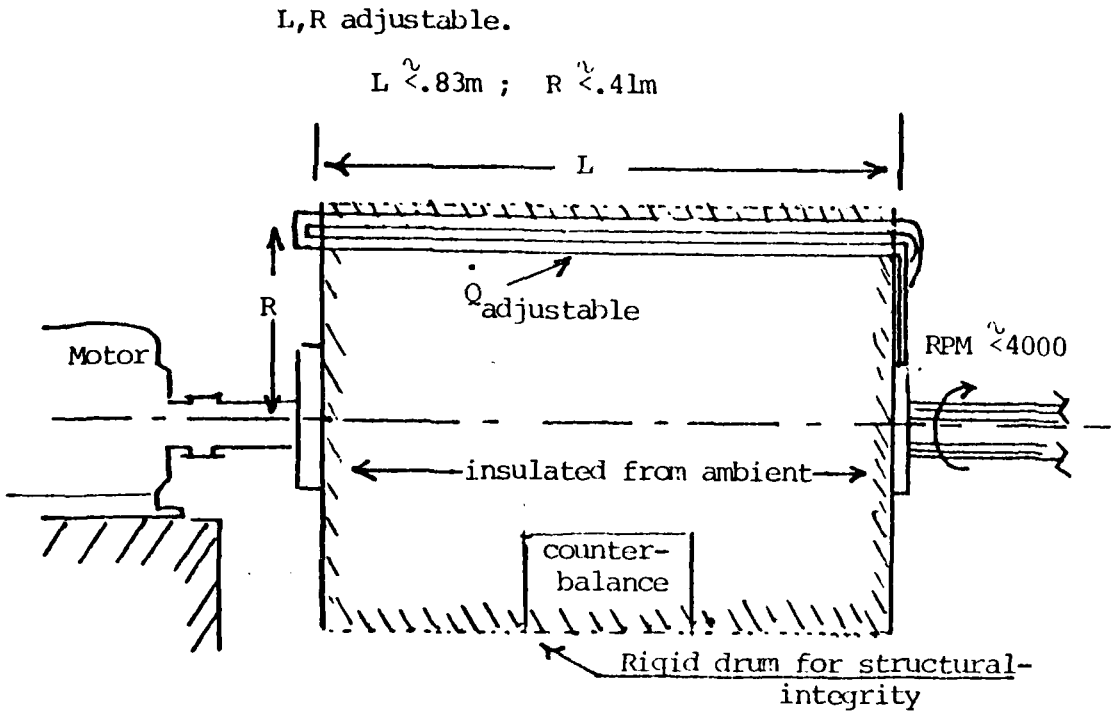

Figure 1.11 Test Rig for Analysis (DTNSRDC developed).

II. SINGLE-PHASE FLUID COOLING

Single-phase cooling has been extensively investigated with regard to rotating references. Work was stimulated early by the printing industry, with the need to cool printing roll mills. The work was further encouraged by the gas turbine industry with the need to cool high-temperature turbine blades, which rotate at high RPM, and by the electrical machine industry, where the need to cool large, powerful generators became a necessity. Research in the study of flow and heat transfer in a rotating reference system is applicable to forced-convection flow, buoyant flow in thermosyphons, and the single-phase flows of closed two-phase devices.

A theoretical analysis of flow in a heated, horizontal tube without rotation by Morton [Ref. 11] was completed in 1957. Although his analysis was limited to non-rotating flows, it gave considerable insight into buoyancy-induced secondary flows. His analysis was limited to laminar convection in horizontal, uniformly-heated tubes at low Rayleigh numbers (based on the temperature gradient along the pipe wall). The work was an extension of the study by Nusselt who ignored the gravitational (accelerational) effects and, therefore, was independent of orientation. This study was a numerical solution to the governing equations assuming small rates of heating and a notable variation of density along the pipe length giving rise to secondary flows. A similar study was completed by Kays [Ref. 12] in 1955. Morton studied this secondary flow driven by the buoyancy effects and the resultant temperature distribution by successive approximation in a power series (this is similar to the flow in a pipe rotating about a

perpendicular axis). Second-order terms were required to account for the secondary flow. The basic equations and development are presented in Appendix A, and are the basis for many later studies. This development is adapted to the rotating case by the substitution of centripetal acceleration for the gravitational acceleration term.

The configuration of the cooling loop has three distinct regions which must be considered: the **radial** sections of tubing (oriented along the line of the centripetal acceleration), the **entrance** regions of the axial sections, and the **axial** sections through the conductor bars (oriented parallel to the axis of rotation). Additionally, it must be determined whether the flow is **laminar** or **turbulent**. The development will be reviewed chronologically within each topic with sample calculations made for pertinent correlations in Appendices B and C as noted.

A. HISTORICAL DEVELOPMENT OF ONCE-THROUGH COOLING

In the 1968 publication, "Recent Advances in Heat Transfer" [Ref. 13], Kreith made a survey of virtually all the work to that date that had transpired in the field of convection heat transfer in rotating systems. His section on concentric cylinders and rotating tubes summarized the works mentioned herein, although principally evaluating the reports using gases as the fluid media. He presents the concept of utilizing a thermosyphon for the cooling of rotors, the theory of which is intimately related to the previous work with single-phase heat transfer, which will be discussed later. Kreith also describes the three different sections (radial, entrance, axial) of the device which this study is addressing. These have been analyzed individually both expermentally and theoretically. The inlet region has the swirl effect due to the Coriolis force, which is a

function of the Rossby number, or the swirl number (the reciprocal of the Rossby number); the radial and axial tube sections have, when a significant centrifugal acceleration term is present, noticeable hydrostatic effects and, additionally, buoyant effects when a density differential exists.

1. Radial Sections

Extending his research to a vertical tube rotating about a perpendicular axis, Morris [Ref. 14] confirmed that the approximate solutions must include second-order terms by studying low heating rates and using a method similar to Morton, but including tangential terms as well as radial acceleration terms. He identified the three components of convection:

1) Forced convection due to the externally-generated pressure gradient,
2) Gravitational buoyancy in the axial direction, and
3) Rotational buoyancy due to centrifugal and Coriolis forces.

The relative magnitude of the terms due to item 3) is characterized by the Rossby number. This is a ratio of the inertia force to the Coriolis force. Although the Rossby number exists in the velocity and temperature fields for solutions through the second order, it has no effect on the solutions for heat transfer or flow resistance. Since at the nominal rotation rates and eccentricity that exist in rotating electric machinery, the centrifugal acceleration is much much greater than the gravitational acceleration, the former will dominate.

In their 1968 report on heat transfer in rotating, radial, circular pipes in the laminar region, Mori and Nakayama [Ref. 15] continued their research by evaluating steady, fully-developed flow with analytical techniques.

Using the boundary-layer concept, they correlated their results with experimental work by Trefethen. They gave correlations for the (Nu/Nu_0) ratio as a function of the angular velocity, Reynolds, Prandtl, and rotational Reynolds numbers for fluids with Prandtl numbers above and below unity (i.e., gases, liquids, glycerol, and liquid metals). Their study confirms the stabilizing effect of the secondary flow on the critical Reynolds number and notes that laminar solutions are still valid when the Reynolds number is considerably large (12,600 @ Ω =500 rad/s).

As a second report on the subject of rotating radial pipes, Mori, et al. **[Ref. 16]** evaluated secondary flow effects due to the Coriolis force by assuming a boundary layer along the wall. With experimental results and correlations from previous work, they were able to show that the effect of secondary flow is less in the turbulent region than in the laminar region, although still on the order of a 10% increase over the value without secondary flow. The correlations they presented agree with their previous report **[Ref. 15]** and with experimental results with air; they are presented as a ratio of Nusselt numbers based on an exponential function of the Reynolds and Prandtl numbers and are given for a wide range of Prandtl numbers including gases and liquids.

Ito and Nanbu **[Ref. 17]** experimentally measured friction factors for flow in rotating, straight pipes of circular cross-section, and compared their results to those of Trefethen and Mori & Nakayama. Their empirical correlations for friction factor ratios for two ranges of Kt (where $Kt = J^2/Re$ and $J = \Omega d^2/\nu$) are shown in equations (2.1) and (2.2) for the turbulent region, $Kt \geq Ktcr$. These are as follows:

$$f/f_0 = \begin{cases} 0.942\ Kt^{0.282}, & 1 \le Kt \le 500, \quad (2.1) \\ 0.942\ Kt^{0.05}, & Kt > 500. \quad (2.2) \end{cases}$$

Below a Kt of 1, the friction factor practically coincides with the stationary friction factor given by Blasius:

$$f_{0_t} = 0.316\ Re^{-0.25}. \quad (2.3)$$

For laminar flow, which occurs when Kt is below Ktcr, the following correlation applies:

$$f/f_{0_1} = 0.0883\ Kl^{0.25}(1 + 11.2\ Kl^{-0.325}), \quad (2.4)$$

where Kl = J*Re. Equation (2.4) is valid for $2.2*10^2 < Kl < 10^7$ and $(J/Re) < 0.5$. The friction factor without rotation is given by:

$$f_{0_1} = 64/Re \quad (2.5)$$

Transition occurs at:

$$Ktcr = 1.07\ J^{1.23}*10^3 \quad (2.6)$$

or

$$Re_{cr} = 1.07\ J^{0.23}*10^3 \quad (2.7)$$

for the range $28 < J < 2*10^3$. Calculation of the pressure drop would be required in the detailed calculations for design of a cooling system, especially of the closed, rotating-loop system.

2. Axial Sections

Kuo, et al. [Ref. 18] analyzed the heat-transfer characteristics of water flowing through a partially-filled pipe which was rotating about its own axis and which was maintained at a constant heat flux. They also summarized the previous pertinent works that were available at the time the paper was written. The paper illustrates how the transition from gravitational to centrifugal force is accompanied by instabilities as previously discussed by Taylor [Ref. 19] and [Ref. 20]. The authors calculated a critical Taylor number at which the Nusselt number changes its functional dependence on the Reynolds number. The paper also shows how the heat transfer is accomplished within a layer around the periphery of the pipe. A correlation for this film thickness is provided, and experimental results confirm its validity and illustrate how the increasing depth of the film in the rotating pipe, up to completely full, does not enhance the heat transfer beyond the critical depth value. The range of the rotational Reynolds numbers used in the experimental work was between 4,000 and 20,000; the enhancement (Nu/Nu_0) was approximately up to 240%.

Oliver [Ref. 21] analyzed natural convection in a horizontal tube with no rotation, following the work of Colburn [Ref. 22]. This study, while pointing out several problems with the original research and basic criticisms noted by Martinelli [Ref. 23], combines the work of many authors to obtain a correlation (equation (2.8)) for the Nusselt number in terms of the Graetz, Grashof, and Prandtl numbers and the L/D ratio. The paper also points out that the Grashof number must be evaluated using the temperature gradient along the pipe axis instead of the gradient from the pipe wall to the fluid mean temperature.

$$Nu\ (\mu_w/\mu_b)^{0.14} = 1.75\{Gz_m + 5.6 * 10^{-4} *$$

$$(Gr_m Pr_m (L/d))^{0.70}\}^{0.333}. \qquad (2.8)$$

The correlation is supposed to incorporate the effects of natural convection along with forced convection by vector addition, but he notes that the velocity profile of the fluid flow is critical in the analysis and that natural convection in the case of horizontal tubes should be independent of L/D beyond the entry region. For this concept, a correlation is also provided for the Nusselt number without the L/D term:

$$Nu \quad (\mu_w/\mu_b)^{0.14} = 1.75\{Gz_m + 0.0083(Gr_m Pr_m)^{0.75}\}^{0.333}. \qquad (2.9)$$

The study of the Taylor vortices was continued by Pattenden [Ref. 24] using a horizontal (axial) tube rotating about its own axis. Due to problems in the slip-ring apparatus used in the experimental work, the errors in the accurate measurement of the temperature precluded specific determination of exponents for the Reynolds number in the correlation for the heat-transfer-coefficient equation. Qualitative analysis of the enhancement due to tube rotation was made, noting that the axial-flow effects were small compared to the rotational effects. Taylor vortices were neither confirmed, nor denied; the flow was sufficiently turbulent to mask the effects that the vortices may have had. Rotation rates were varied to a maximum of 4,000 RPM.

Mori, et al. [Ref. 25] investigated further into the effects of buoyancy on forced-convective heat transfer in horizontally-oriented, heated tubes with laminar flow. His study extended the work of Graetz and Nusselt, and went beyond the limitation of small heat fluxes such as those studied by Colburn, McAdams, Martinelli, et al., Jackson, et

al., and Oliver. The majority of the experimental work by the authors was performed with a constant wall temperature and large L/D ratio. Their study involved a large temperature difference between the wall and the fluid such as would occur with large heat flux. The change in viscosity with temperature is approximately covered with the $(\mu_w/\mu_b)^{0.14}$ term in equation (2.8), but the effect of natural convection has not been included specifically. This effect was shown [Ref. 11] as a function of the ReRa product; it is applicable in the range of ReRa less than 3,000, but within this range the effect of natural convection does not exceed several percent. The Rayleigh number is a function of the fourth power of the diameter; therefore, the effect that natural convection makes in small-diameter channels is small. This illustrates that in the thin layer near the wall, the temperature and velocity change abruptly and are quite different from that in the inner part of the fluid. When the ReRa product is large, the secondary flow is strong and the velocity distribution in the axial direction is utterly different from the Poiseuille flow assumed in the previous works. The Nusselt number is then calculated by:

$$Nu = 2aq/\ k(t_w - t_m) \qquad (2.10)$$

where the stationary Nusselt number for constant heat-flux case is:

$$Nu_0 = 48/11. \qquad (2.11)$$

The experiments were conducted with air and fluids with higher Prandtl numbers; they were only considering heating in a gravitational field (not an acceleration field due to rotation). In this case, the layer near the wall becomes thinner and the Nusselt number increases with the increasing

ReRa. The local Nusselt number for the experimental correlation (for air) is given by:

$$Nu = 0.61(ReRa)^{0.2}(1+1.8/(ReRa)^{0.2}) \qquad (2.12)$$

This study was extended into the turbulent region, where the highest point of the temperature distribution was found to shift in the direction of gravity slightly. In this case, the effect of the secondary flow was not as significant as in the case of laminar flow. The Nusselt numbers calculated within this regime were in good agreement with those of Colburn [Ref. 22], where:

$$Nu = 0.0204\ Re^{0.8}. \qquad (2.13)$$

Mori and Nakayama used the theoretical analysis of their previous research [Ref. 26] and [Ref. 27] on straight pipes rotating about a parallel axis [Ref. 28]. Analyzing the body forces driving the secondary flow caused by density differences in the centrifugal field and the Coriolis force with regard to the flow, they used fundamental principles to characterize the flow and temperature fields. This was done assuming an effective secondary flow due to buoyancy and using the rotational Reynolds number. This would indicate a rapid divergence from the results of Morris [Ref. 14] and shows that Coriolis effects cannot be ignored. The paper gave correction factors as a function of Reynolds, rotational Reynolds, and rotational Rayleigh numbers, and concluded that the Coriolis effects diminish with increasing eccentricity (higher g-fields) to a negligible value when the ReRa product is greater than 10,000,000.

In 1968, Nakayama [Ref. 29] further analyzed a horizontal, straight pipe rotating about a parallel axis. He assumed, as previously [Ref. 15], that an effective

secondary flow in fully-developed conditions of flow and temperature fields existed, and included body-force terms explicitly. The correlations he obtained for both the ratio of friction factors and the ratio of Nusselt numbers are valid over a large range of Prandtl numbers for both liquids and gases, as well as for a wide range of Reynolds and Grashof numbers. The correlation for the Nusselt number for liquids in fully-developed flow is:

$$Nu = Re^{0.8} Pr^{0.4} \{0.033 (Re/\Gamma^{2.5})^{1/30} (1+0.014/(Re/\Gamma^{2.5})^{1/6})\} \quad (2.14)$$

where $\Gamma = Re^{22/13} (GrrPr^{0.6})^{-12/13}$. The Γ term is the ratio of inertia force to body force. Inertia force is represented by $Re^{22/13}$, and the remaining terms in Γ represent the body force. The body force is either the Coriolis force in the case of the inlet region, curved regions, or the radial arms, or the centrifugal force in the case of the axial section. The numerical result of his correlations for the model presented in Chapter I is included in Appendix B for both turbulent and laminar liquids.

Siegwarth, et al. [Ref. 30] further evaluated the effect that bouyancy-induced secondary flow would have on laminar flow in a heated, horizontal pipe without rotation. His work showed clearly that secondary flows did exist due to density variations and that the heat transfer was enhanced by them as a function of the Grashof and Prandtl numbers. This effect is somewhat negated in the presence of extreme acceleration as that in the periphery of a rotor, but remains nonetheless, provided the turbulence is below the critical Reynolds value.

With no assumptions as to the structure of the flow and temperature fields to simplify the governing equations, Woods and Morris presented a numerical solution to the case of the rotating cylindrical tube [Ref. 31] with laminar, fully-developed flow. Data were compared to the theoretical results for the case of air, water, and glycerol. The correlation obtained is in terms of the Rayleigh-Reynolds-Prandtl product as is given by:

$$Nu = Nu_0 \{0.262 (RaRePr)^{0.173}\}. \qquad (2.15)$$

The value for the test model is calculated and presented in Appendix B.

Stephenson again studied this parallel, rotating-pipe, heat-transfer problem for fully-developed turbulent flow. He compared his experimental results and correlation with the earlier work of Morris and Woods [Ref. 32] and they compared favorably within the turbulent entrance region. He noted that the rotational buoyancy was not a strong factor in the secondary-flow in the fully-developed region. Because of this, his results, when compared against Nakayama's results assuming a strong effect [Ref. 29], did not compare well. His correlation is listed below:

$$Nu = 0.0071\ Re^{0.88}\ J^{0.023} \qquad (2.16)$$

and is compared with previous correlations for the test model in Appendix B.

3. Entrance Regions

In 1969, the Institution of Mechanical Engineers, Thermodynamics and Fluid Mechanics Group, sponsored a symposium, on the subject of heat transfer and fluid flow in electrical machines. Included in the presentations was a

paper by Davidson [Ref. 33], which described a full-size, generator-rotor test rig for evaluating the heat-transfer characteristics of hydrogen cooling. His testing showed that enhancement in the turbulent flow regimes was not as high as theoretically predicted. It was hypothesized that the reason was the inability of the hydraulic-diameter concept to accurately account for the flow conditions in the non-circular ducts. The tests were able to give a good turbulent correlation with theoretical prediction when the cooling scheme was modified by shortening the axial path. This effect, although not explained, could have been due to the Coriolis swirl effect in the inlet region enhancing the heat transfer above that to be obtained in the fully-developed region.

The effects of the entry length, especially with low Prandtl numbers such as those of gases, are very difficult to eliminate and the Coriolis effects on the heat transfer may be noted even at high Reynolds numbers. As the Reynolds-Rayleigh product increases above about 1,000,000, there is a tendency for the amount of enhancement to diminish. This is attributed to the turbulent effects overiding the secondary flow enhancement. The effect of rotation on heat transfer is to enhance it in the entrance regions by the secondary flow due to the Coriolis effects and in the fully-developed, horizontal-tube regions by buoyancy effects. A similar survey of the technology was made by Petukhov and Polyakov in the USSR with much the same results [Ref. 34]. The heat-transfer problem in the entrance region of a tube, where the Coriolis terms dominate, is addressed by Morris and Woods [Ref. 32]. Correlations are presented for air and are applicable for other gases as well. These correlations, for both the laminar and the turbulent cases, are presented as functions of the product of the Reynolds number and the

rotational-Reynolds number. The Morris and Woods paper notes that further work is required in the case of liquids, although a similar approach is valid. Mori and Nakayama also presented a survey of the state-of-the-art technology regarding the heat-transfer characteristics of rotating pipes and ducts [Ref. 35]. The questions of the entrance effect and its length were emphasized as being generally unanswered, but they gave a general guideline for determining the extent of the entrance region as approximately 20 times the diameter of the pipe. They also verified correlations of previous works for helium and water.

4. Combinations of Radial, Horizontal, and Entrance Sections

Also presented in the 1969 Institution of Mechanical Engineers Symposium was a study by Lambrecht [Ref. 36], which discussed the problems associated with water cooling of rotors. His paper summarized the theoretical considerations, as well as reviewed his previous work and the work of fellow German researchers (Neidhoeffer and Ingenieure). He noted the superior cooling properties of water and the size and weight reduction, along with the improved efficiency of water-cooled machines. He listed values for the optimum cooling duct size based on the heat-transfer and electrical-loss characteristics for various gases. The method used for optimum duct calculation was based on the principle that the pressure drop in the duct decreases with increasing duct size and electrical losses increase with decreasing conductor area (increasing duct size). A suitable calculation of this type is necessary in any final design for cooling of these devices by any method devised for either the single- or the two-phase approach.

In 1970, Sakamoto and Fukui measured heat- and mass-transfer coefficients for air and oil, specifically for

use in cooling rotating electric machines [Ref. 37]. Noting that the most effective and economic method to increase the power output of electrical machines was to improve the cooling of the insulating material (especially in the rotor conductors and drums), a geometry similar to a typical rotor was fabricated and suitable coolants were tested. The convective heat transfer was characterized as a function of the L/d, Re, Grr, Pr variables, with the H/d parameter held constant. When the shape factor of eccentricity H/d is sufficiently large, the centrifugal acceleration may be assumed to be a uniform acceleration (^2H) acting on the tube axis, which is similar to the force gravity exerts on a horizontal tube. With a low Reynolds number, the empirical correlation was in the form:

$$Nu = Nu_0 (1+C(Rar)^m/Gz)^n, \qquad (2.17)$$

where the values of the constants were:

$C = 0.03$ $\quad m = 0.75$ $\quad n = 1/3$

and where $Nu = 1.86(RePrd/L)^{0.33}$ for large L/d values, and $Nu = 2.67\ Gz^{0.33}$ for small L/d values.

This was valid within +10% to -17% for Reynolds numbers between 162 and 2,700 and rotational Rayleigh numbers to 20,000,000. It was also found that the length of the entrance region seemed to have no effect on the correlation, which would imply that a secondary flow existed in both configurations. An interesting point in this paper is that the rotational Grashof number (hence the rotational Rayleigh number) was calculated using the temperature difference between the wall and the fluid instead of the axial temperature gradient.

Woods and Morris investigated laminar flow in the rotor windings of directly-cooled, electrical machines in 1974 [Ref. 38] and noted that if water was used as the

coolant in lieu of hydrogen (which is currently widely used), an efficiency improvement of >0.5% could be obtained. Given that the 0.5% of a large, say 1,000 MW, generator was the only consideration made (and neglecting the size and weight reduction and the extended operating life possible due to the cooler operation), they proceeded to analyze the fundamentals of the problem. They surveyed the previous works directly applicable to this area of cooling;

1) Morris [Ref. 14] used a series-expansion technique (valid for low rotation rate and low heating rates), and

2) Mori and Nakayama [Ref. 28] assumed a secondary flow (which was claimed to be valid for high rotation rates), and used an integral-type analysis.

Woods and Morris claimed both were inadequate due to the restrictions imposed by the nature of their solutions. They attempted a versatile and "exact" solution for laminar flow in the fully-developed region by solving the governing equations with a numerical procedure. Numerical solutions were presented for both the friction factors and the Nusselt numbers. Their analytical values were compared with experimental results and to correlations of previous works. Discrepancies were explained and the difficulty in obtaining fully-developed conditions in the experiments of their work and previous works was emphasized. The axial density-variation effects were noted, also, as a potential for error in their analysis at high values of rotational Rayleigh numbers.

Nakayama and Fuzicka evaluated the generator problem, where reasonably large radii of rotors (approximately 1 m) and high RPM (3600) create high centrifugal acceleration effects [Ref. 39]. This acceleration causes the centrifugal buoyancy term to be significant. It also

emphasizes the Coriolis term in the radial tube segments and curved inlet regions. They presented correlations for the ratio of friction factors and the ratio of Nusselt numbers, arriving at friction-factor ratios for each of the three regions (radial, curved inlet, and axial), and compared the results to experimental data. Their correlations are listed below:

$$f/f_0 = 2.2\ Ro^{-0.33} \quad \text{(radial)} \tag{2.18}$$

$$f/f_0 = 1.5\ Ro^{-0.3} \quad \text{(coil end)} \tag{2.19}$$

$$f/f_0 = 14.0\ Ro^{-0.8} \quad \text{(axial)} \tag{2.20}$$

$$Nu = Re^{0.8}\ Pr^{0.4}\{0.014(Re/Ro^{2.5})^{0.124}\} \quad \text{(radial)} \tag{2.21}$$

Their report confirms the results of Nakayama's correlation (equation (2.14)) for the axial sections.

The application of the technology of rotating cooling schemes is not limited to the printing industry and electric machine area; extensive research has been devoted to this field of study by the gas turbine industry. The Advisory Group for Aerospace Research and Development (AGARD) held a meeting in September, 1977, at Ankara, Turkey, to discuss High Temperature Problems in Gas Turbine Engines. Numerous papers were presented on the subject including a paper by W.D. Morris on flow and heat transfer in rotating coolant channels [Ref. 40]. He used a selection of experimental results to illustrate the influence of

rotation on heat transfer, and demonstrated that Coriolis and centripetal inertial effects significantly alter the heat-transfer characteristics compared to the stationary case. Using the governing equations, he illustrated how the Navier-Stokes equations are modified to include the acceleration effects of the Coriolis forces and the centripetal forces. For constant properties, these equations then show how at distances sufficiently downstream from the entry region, where the axial gradients of the velocity are negligible, the elimination of the pressure-gradient terms from the radial and tangential momentum equations causes the Coriolis terms to vanish identically as a source for the creation of secondary cross-stream flow; see also [Ref. 14].

In the entry region, the Coriolis terms interact with the developing axial velocity and create secondary flows perpendicular to the axial direction, even with the constant property condition. Finally, in the fully-developed region, the effect of the rotation manifests itself only as a cross-stream pressure distribution if buoyancy terms are neglected. If the density is allowed to vary with temperature, the centripetal acceleration terms need only be included as the Coriolis terms do not affect this action. This cross-stream, buoyancy-induced flow gives rise to greatly-enhanced heat transfer and an attendant increase in flow resistance. The effects of the eccentricity, with regard to the Coriolis terms, has little effect, provided that the ratio of the radius (H) to the diameter of the tube (d) is greater than 5 (only very small radius of rotation will have any noticeable effects).

Marto [Ref. 41] lists the papers presented at the 14th Symposium of the International Centre for Heat and Mass Transfer (ICHMT) held in Dubrovnik, Yugoslavia, in 1982. Papers of particular interest to this study included a paper by Johnson and Morris [Ref. 42], wherein the concept of

centripetal-acceleration-induced secondary flow was proven to be of little importance, and its influence was shown to be totally hydrostatic. Their work also confirmed the effect of Coriolis acceleration with regard to secondary flows, especially in sections with relatively small L/d ratios. No quantitative recommendations were presented.

5. Flow Transitions

Mori [Ref. 25] states, when considering turbulent flow, that it is not necessary to consider the influence of buoyancy on heat transfer. The secondary flow was found to suppress the turbulence level when the turbulence at the inlet region was high and an empirical formula for the critical Reynolds number, in terms of the Reynolds number and Rayleigh number product, was calculated:

$$Re_{cr} = 128(ReRa)^{0.25}. \qquad (2.22)$$

Contrary to this, when the turbulence at the inlet region was low, the critical Reynolds number was higher (7,700 vs. 2,000), and heating decreased the critcal value. The net result was that when the ReRa value was high, the secondary flow caused by buoyancy makes the critical value of Reynolds number tend toward the same value, whether the turbulence in the inlet is high or low. In the case of low turbulence in the inlet, the value for the critical Reynolds number was given by:

$$Re_{cr} = Re_{cr_0}/(1+0.14\ ReRa*10^{-5}). \qquad (2.23)$$

The graph shown as Figure 62 in the Krieth article [Ref. 13] is shcwn below as Figure 2.1. This graph shows the heat-transfer as a function of both the RPM and the flow-through Reynolds number. It is easy to see the flow's transitional

dependence on the Reynolds number as a function of RPM. For the experimental model being evaluated, where Re=7,400 and Ra=7,400, the transition is delayed to Re=11,000 for the correlation that assumes high turbulence at the entrance.

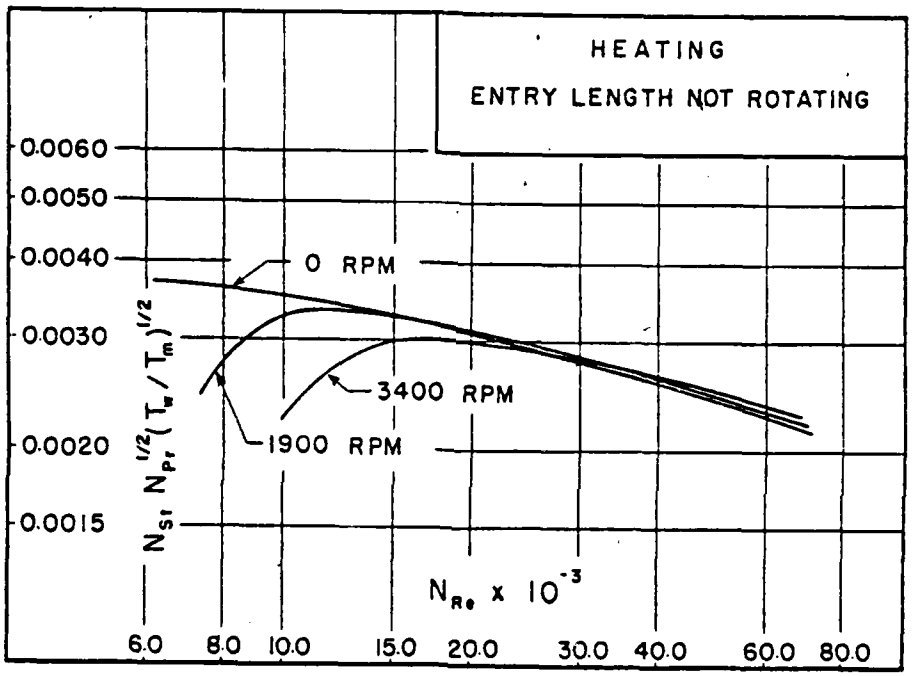

Figure 2.1 Effect of Rotational Speed in a Rotating Pipe.

The transition to turbulent flow is suppressed by rotation and has been qualitatively noted by numerous authors. An exact correlation for transition to turbulent flow in a rotating-reference frame with heating is not known to exist. From the available literature, it is clear that the transition follows a path from the laminar correlations

to the turbulent correlations. This path, in the case of the rotating reference, has a "dip" as shown qualitatively in a plot of the Nusselt number against the Reynolds number, Figure 2.2, whereas in the non-rotating case, no "dip" occurs.

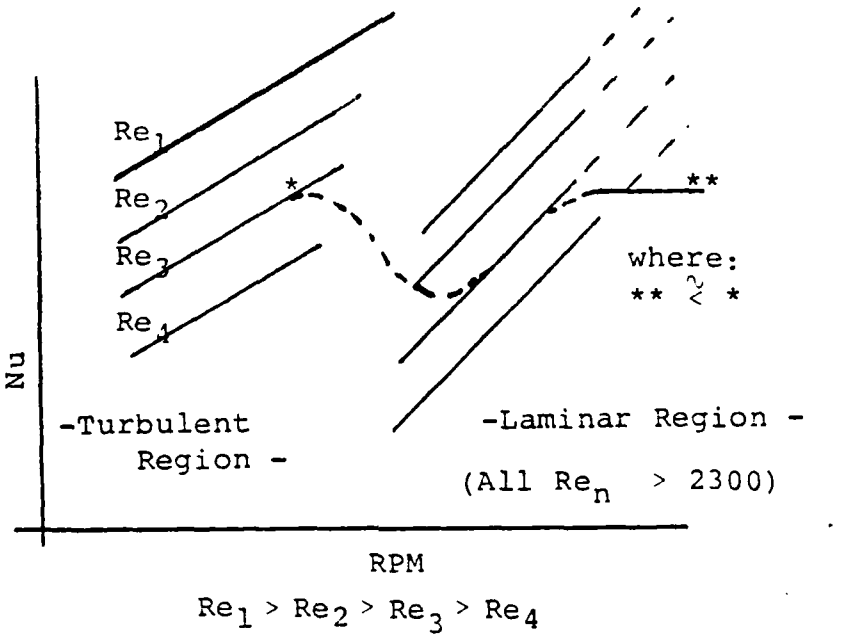

$Re_1 > Re_2 > Re_3 > Re_4$

Figure 2.2 Transitional Characteristics of Rotating Systems.

6. Summary

Based upon the information reviewed in the literature, it may be concluded that the three regions within the motor/generator application (shown in Figure 1.11) have very different heat-transfer characteristics.

1) In the radial section of the coolant path, the Coriolis forces tend to dominate the heat transfer and friction. This effect is to enhance the heat transfer and increase the pressure drop in these sections. The heat-transfer enhancement is substantial and could be effectively exploited for the heat rejection from the device by axial forced-air convection of the substantially-hollow, synchronous rotor.

2) In the coil-end regions (both at the radial connection points and the coil-end loops) the Coriolis force is strong and is coupled with the strong centripetal forces. The result is enhanced heat-transfer and friction-factor effects, but to a lesser degree than in the radial sections.

3) In the winding bars, the centripetal forces dominate; these forces result in hydrostatic effects which limit flows that would be affected by the Coriolis forces and result in some degree of secondary flow due to buoyancy. The amount of secondary flow is questionable and is somewhat affected by the degree of turbulence and the amount enhancement is less specific.

The enhancement in the laminar-flow heat transfer has been reported by numerous authors. This can be seen in Figure 2.3. Both the Nakayama [Ref. 29] and the Woods-Morris [Ref. 31] correlations for Nusselt number fall between the classical laminar value of 48/11 and the turbulent value of the Dittus-Boelter correlation. They have the same trend throughout the range of RPM shown and differ by only a few percentage points. Apparently, the effect of rotation in laminar flow enhances the heat transfer because of intense secondary flows due to centripetal forces. An interesting point is that, at the higher RPM values, the correlations of Nakayama, Woods-Morris, Stephenson, and Dittus-Boetler all are exceptionally close together.

The heat-transfer predictions for turbulent, fully-developed, parallel flows are shown in Figure 2.4. This figure illustrates that the resultant heat transfer is somewhere in the vicinity of the classical turbulent correlation of Dittus-Boelter for the current model.

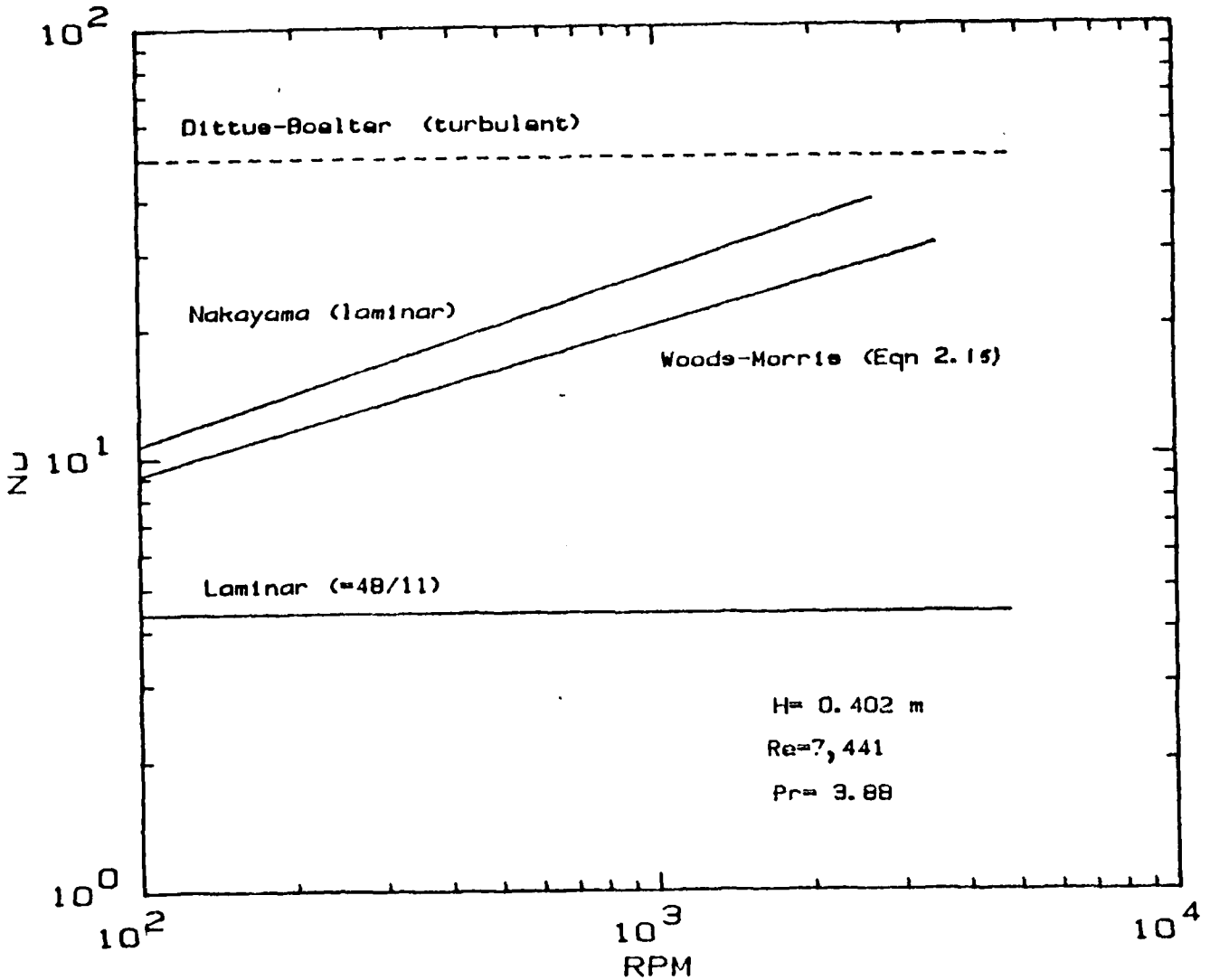

Figure 2.3 Variation of Laminar Nusselt Correlations with RPM.

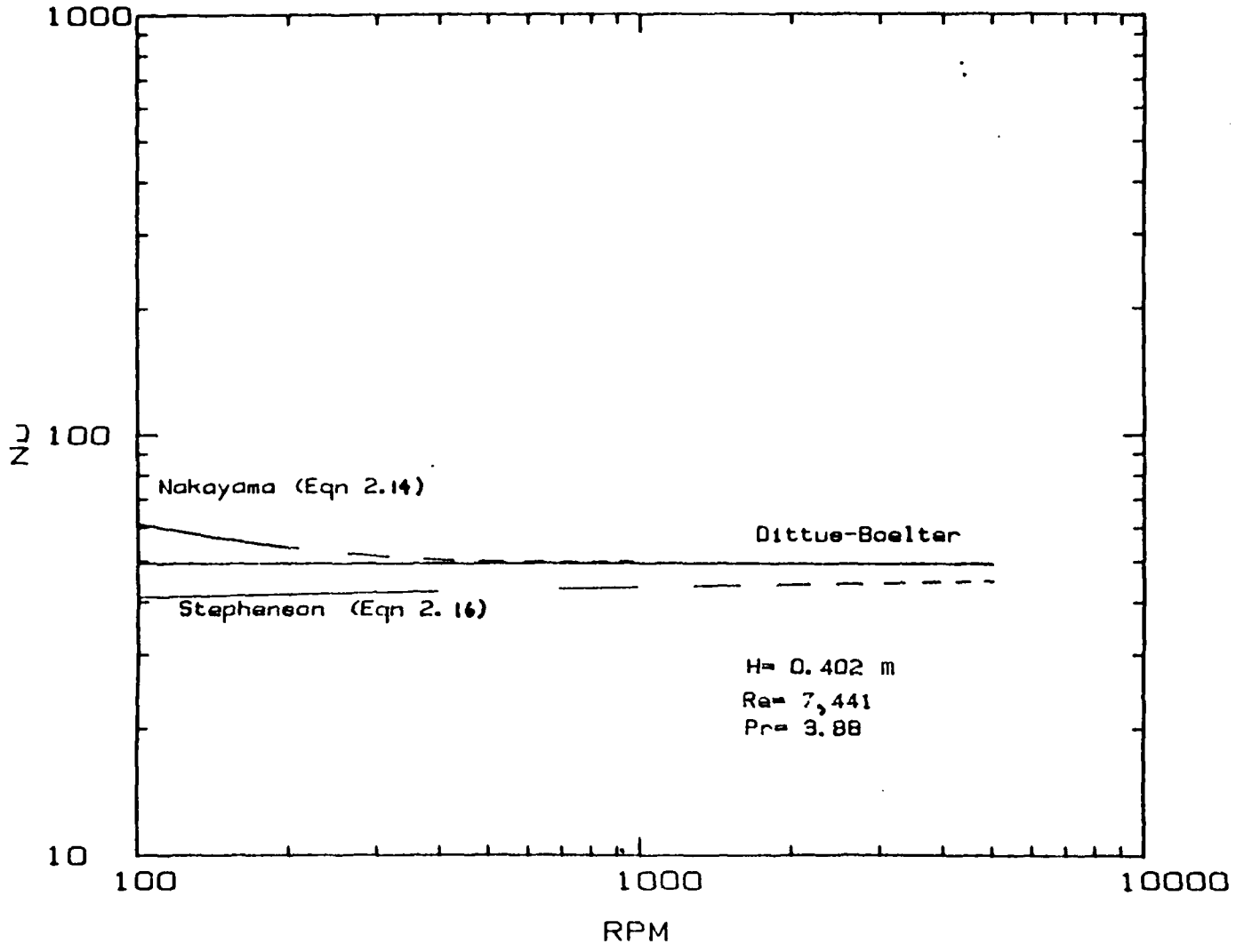

Figure 2.4 Variation of Turbulent Nusselt Correlations with RPM.

The heat transfer is either somewhat enhanced (on the order of 30%) in the lower RPM ranges (Nakayama [Ref. 29]), or somewhat suppressed by the high centripetal acceleration forces as shown by the correlation of Stephenson [Ref. 43].

The enhancement of the heat transfer in the Nakayama correlation [Ref. 29] in the lower RPM range is assumed to be due to the residual Coriolis effects from the entrance regions remaining longer in the lower centripetal acceleration field.

B. HISTORICAL DEVELOPMENT OF THERMOSYPHON COOLING

The thermosyphon is a device that creates the motion of the working fluid solely by buoyancy forces. It has a region where heat is supplied to the working fluid and a region where heat is rejected. The less buoyant, cooler portion of the fluid moves in the direction of the acceleration vector, while the opposite is occurring for the warmer portion. The thermosyphon also has a third region, the coupling region, with problems of fluid shear, mixing and entrainment. Figure 2.5 illustrates the conceptual arrangements of the three basic thermosyphon systems.

Kreith [Ref. 13] mentioned in his review that the thermosyphon (i.e., a liquid-filled container) had a great potential for cooling of electric rotating machinery. In motors and generators, the use of a thermosyphon would preclude the necessity of using rotating seals, which have marginal reliability in applications of high RPM and volumetric flow. In 1973, Japikse [Ref. 44] gave a thorough review of the literature regarding thermosyphon technology. Beginning with a reference to the Davies and Morris paper [Ref. 45], which will be discussed in detail later, Japikse categorizes thermosyphons as follows:

1) the nature of boundaries (either opened or closed to mass flow),

2) the regime of heat transfer (purely natural convection or mixed natural and forced convection),

3) the number and types of phases present, and

4) the nature of the body force present (gravitational or rotational).

These broad categories are then restricted to "....a prescribed circulating fluid system driven by thermal buoyancy forces."

The use of the closed thermosyphon in rotating references, such as in gas turbine cooling, has been studied in detail. In 1965, Bayley and Lock [Ref. 46] experimentally investigated the performance of closed thermosyphons. They utilized the theoretical development of the open thermosyphon, modified the theory, and experimentally verified their results. It was shown that the critical operating parameters include:

1) Length-to-Diameter Ratio. This ratio controls the characteristics of the flow and determines the extent of the coupling region.

2) Heated-Length-to-Cooled-Length Ratio. As this ratio tends toward zero, the analysis is identical to the open thermosyphon correlations. This restricts the use of the analysis for the closed thermosyphon to Lh/Lc ratio to be not much greater than one.

3) Coupling Region. This is the region that complicates the analysis and causes the Prandtl number to affect the heat transfer. It exists in three distinct modes; conduction, convection, and mixing. These are regarded as

ideals and actual coupling usually consists of a combination of all three.

Thermosyphon technology was also applied to transformer cooling, nuclear-reactor cooling, heat-exchanger fins, home and industrial furnaces, cryogenic cool-down apparatus, steam tubes for bakers' ovens, internal combustion engine cooling, and environmental control in the space vehicle program, as well as many others mentioned in the Japikse article.

In 1971, Bayley and Martin [Ref. 47] also reviewed the state-of-the-art technology, with particular emphasis on gas-turbine applications. They studied both the open and closed thermosyphon systems. The use of an open thermosyphon system in a rotating reference, such as in gas turbine cooling, as well as in the cooling of electric, rotating-machinery area, has problems regarding the fluid selection and its saturation temperature and pressure. In the open, rotating reference system, the region that receives the heat is under high acceleration forces with high resultant pressures. As the natural flow due to buoyancy occurs, the heated fluid moves from a high pressure to a relatively low pressure area where a phase change to vapor may occur, possibly even explosively, blocking the flow. They introduced the idea of using two-phase cooling within the closed thermosyphon as a way of exploiting this phenomenon, by using the high heat fluxes associated with the latent heats of evaporation and condensation and the lower temperature gradients associated with the phase change processes. This also has an added benefit of reduced weight over the single-phase liquid system. They noted that further research in the area of the Coriolis force effects on the heat-transfer chacteristics in a rotating reference needed to be accomplished.

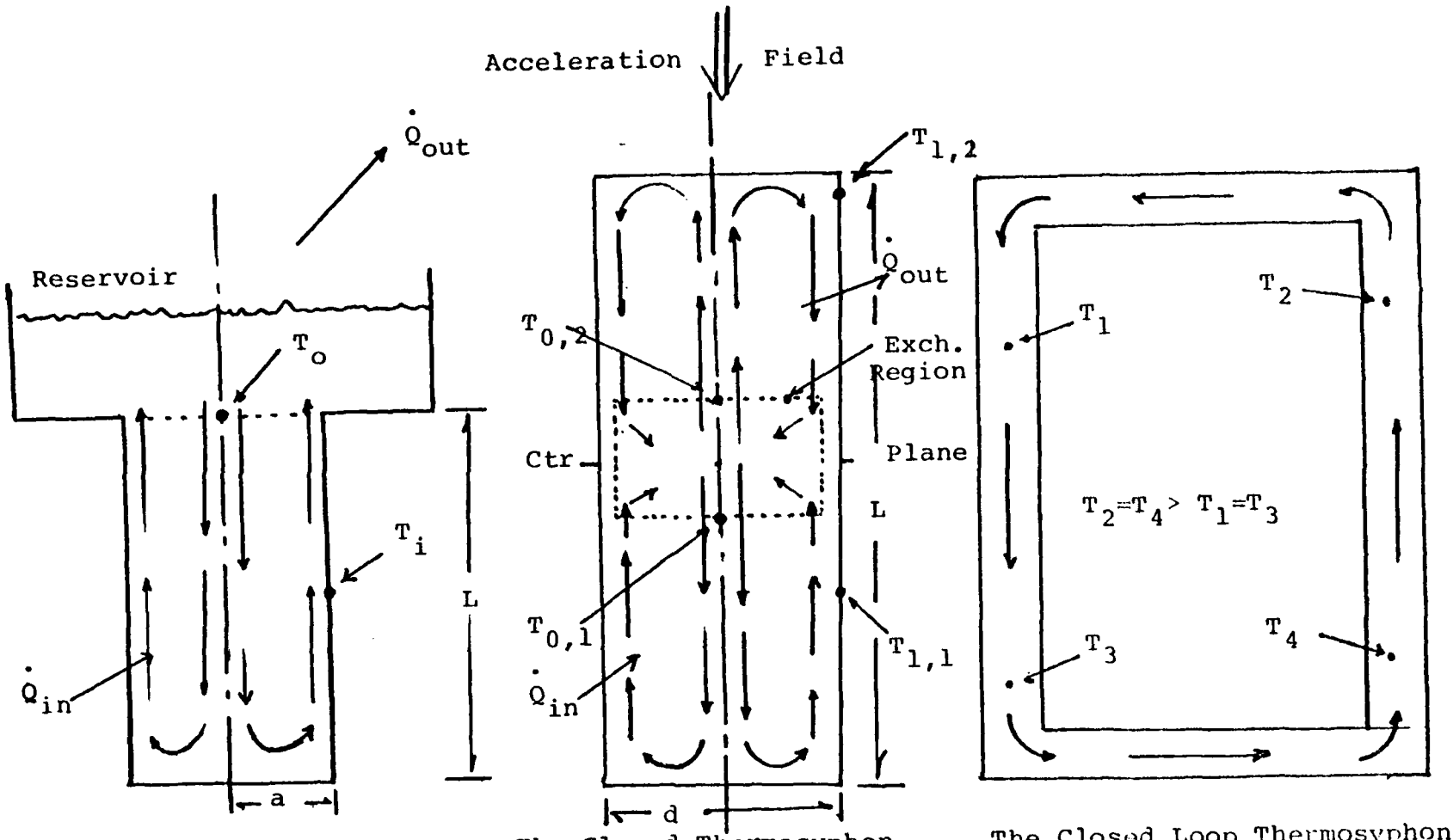

Figure 2.5 Various Thermosyphon Arrangements.

Applying the technology of the thermosyphon to electric machines, Morris and Davies [Ref. 45] adapted the principles of the closed thermosyphon to a closed rotating loop that could be placed into the rotor assembly of an electrical device. This configuration avoids the entry choking and mixing that occurs in the typical closed thermosyphon and generally avoids the complex mid-tube exchange process, as well as the adverse core-boundary layer interaction. The strong acceleration force present in the periphery of the rotor of electric rotating machinery, coupled with the heating due to the electrical losses, induces stong loop circulation. This heat can then be rejected either to the shaft of the rotor acting as a heat exchanger itself, to the air passing through the hollow rotor region and the air passing through the end-bell region of the rotor ends, or to both. The shaft, acting as a heat-exchanger itself, can be cooled with an internal, rotating heat-pipe (or two-phase thermosyphon) which could transfer the heat axially to another heat sink outside of the motor/generator casing. As an alternative, the shaft could be internally cooled by forced convection of water (or some other fluid) to an external heat exchanger through the non-coupling end of the shaft by the use of an axial rotating seal. The reliability and the casualty-control aspects of the axial rotating seal make it preferable to the radial rotating seal mentioned earlier.

Theoretical analysis of the loop-flow has used simple, one-dimensional force and energy balances, and need not be repeated here. The closed loop is shown in Figure 2.6 as conceptually applied to a rotor. Of course, numerous loops would be designed into the rotor to carry away the heat generated. Incorporation of a one-way valve was suggested as being necessary to insure one-directional flow created by the mean temperature difference and the pressure differences

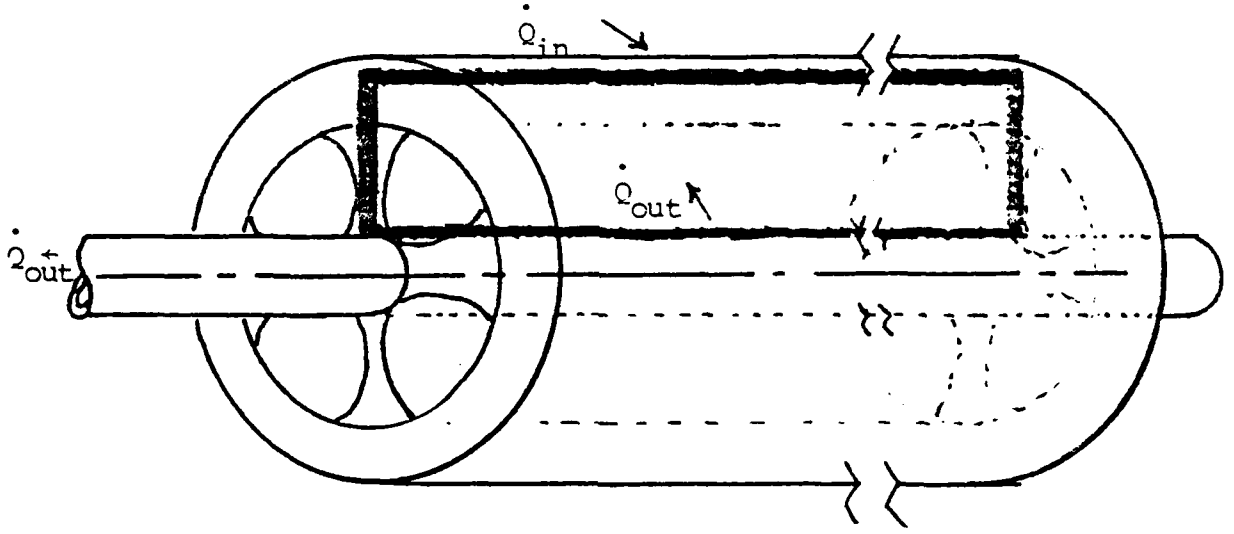

Figure 2.6 Rotating Loop Thermosyphon for a Rotor.

in the limbs of the circuit. Experimental testing was conducted in a test rig similar to the rig proposed for the evaluation of the systems studied herein and now under construction at DTNSRDC. A modest range of rotation rates was employed in the Morris and Davies test rig, typical of most motor applications. The details of their test section were very similar to the model used for analysis herein: 25.4 mm (one inch) diameter copper rod through which a 6.35 mm (0.25 inch) hole was bored. The experimental results were placed in the form:

$$Nu = f(Grr, Ro, Pr, Ac). \quad (2.24)$$

The ratio of angular acceleration to gravitational acceleration (Ac) was the authors' way of including the rotational effects (previous authors have used the rotational Grashof number). The final correlation was:

$$Nu = 0.1505\ Ac^{0.735}\ Re^{2.45}\ Pr/Gr \quad (2.25)$$

for the range of $10^3 < NuGr/Pr < 10^6$.

The critical consideration in the analysis of the closed-loop thermosyphon is the temperature rise in the heated limb (conductor bar). The model described in Chapter I was analyzed by using the governing relationships from the Davies and Morris [Ref. 45] paper iterated against the Woods and Morris [Ref. 31] correlation for laminar, fully-developed flow in a heated circular tube rotating about a parallel axis. It can be seen from Figure 2.7 that the heat transfer increases with RPM (the higher acceleration

TABLE II

Temperature Rise in the Closed-Loop Thermosyphon

RPM	Temp. Rise (C) *
300	209.0
1000	93.5
3000	41.0
3600	35.5
5000	27.0

* for a cold-side temperature of 45 C.

effect). For the conditions on the model which constructed Figure 2.7, the values of temperature rise is shown in Table II for various RPM's. This clearly shows that this method

of cooling, if selected, would be inappropriate for the motor device (i.e., low RPM); on the other hand, it could be very reasonable for the generator. The friction factor was assumed to be 64/Re and no correction was made for the rotation in the friction-factor calculation; the minor losses were neglected. If the friction factor is increased due to the rotation, as in equation (2.4), and minor losses (laminar) are included, the temperature rise will be increased slightly. The trend will be the same and the temperature rise at the higher RPM's will still be acceptable. The actual design of the closed-loop thermosyphon will require an optimization of the heat-transfer calculations and the friction-factor calculations. This optimization may indicate that a larger, single, closed-thermosyphon loop for a conductor bar group is preferable over individual conductor loops.

C. ADVANTAGES/DISADVANTAGES OF LIQUID COOLING

The main objectives of cooling are to remove the heat created by the electrical losses and improve the operating efficiency, extend the lifetime of the insulation, and reduce the overall weight and size of the device. The feature of liquid cooling (vs. gas cooling) is the superior capacity of liquids, especially water, to remove heat with a small rise in temperature. The principle disadvantage of using liquids, or gaseous fluids other than air, is the design of the piping, coupling, and secondary heat exchanger required to support the device cooled by the fluid. Since one of the main objectives is to reduce weight and size, the fluid chosen must be able to remove enough heat per unit mass to accomplish this goal within the device. Additionally, since the application under evaluation is marine combatants, the fluid should be non-toxic, and the

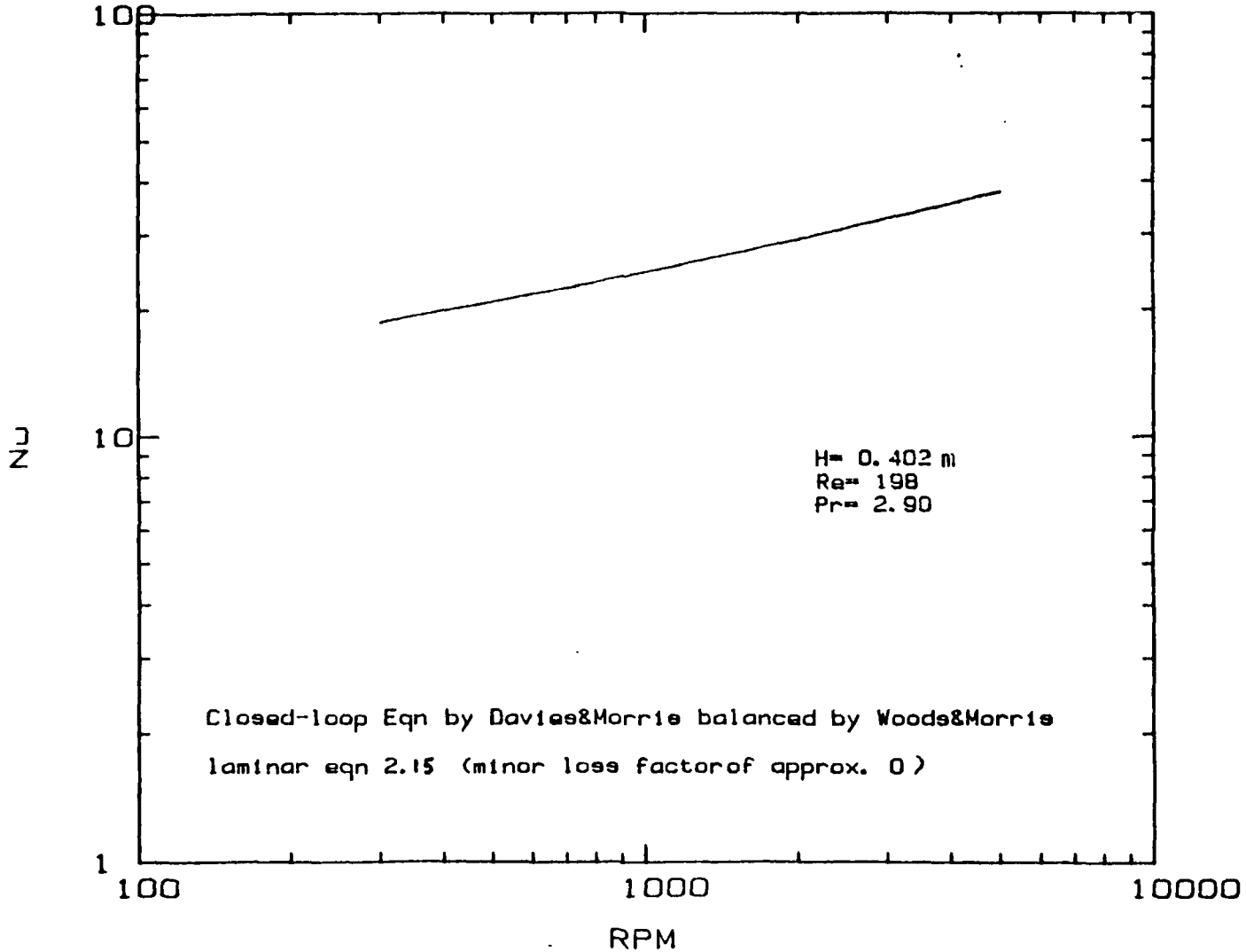

Figure 2.7 Thermosyphon Analysis for Nusselt number.

system should be durable enough to withstand damage and maintain operational safely. The popular fluid to date in land-based installations has been hydrogen which is clearly an unacceptable choice for the marine combatant due to its explosive nature and since the size reduction obtained is not sufficient to warrant system development. Of the remaining fluids, the obvious choice for its high heat capacity, availability, and safety, is water. The use of water has been tested both in stators and, on a limited scale, in rotors.

The principle problem to overcome in the use of water is in the rotary seals needed to direct the fluid into/out of the machine. Additionally, when the system inside the device is analyzed, the ability of a design to withstand damage is questionable. The design would be critically dependent on the fluid within the rotor for operation, even in a casualty mode. The supply of cooling water to a stator would not be as critical, since any casualty could be repaired easily with shipboard damage-control equipment, and emergency cooling of a stator could be accomplished by external means due to the thermal conductivity of the stator housing. For the rotor, this leaves a choice; either not utilize the enhanced cooling and suffer the weight and size penalties, or develop a closed system for cooling the rotor. The closed system for the rotor is not necessarily isolated. A closed-loop, thermosyphon could be placed in the rotor, transferring the heat from the rotor to the rotor shaft. This loop could have additional heat transfer to air passing through the core of the rotor. Further, the heat transferred to the shaft could be removed to the ambient air or an external heat exchanger utilizing the non-coupling end of the motor by the use of circulating water through the shaft, or by a rotating heat pipe as seen in [Ref. 48].

An additional method for cooling the rotor, which has been studied by numerous authors, is the use of heat pipes or closed, two-phase thermosyphons. In this case, the heat is transferred from the rotor to air circulated through the end-bell areas of the device. This method of rotor cooling greatly enhances the survivability of the device in a damage-control sense. Each heat pipe is independent of the others and damage to a few, unless all in the same group of adjacent conductor bars, would not jepardize the device; indeed, even if all were in the same group, limited operation could continue.

III. TWO-PHASE FLUID COOLING

The concept of utilizing the latent heat of vaporization to transfer heat is widely used in heat exchangers everywhere, from household and industrial boilers and space heaters to marine propulsion units. Air-conditioning equipment and heat-pump units also employ this idea to advantageously utilize the low temperature of vaporization of fluoro-carbon compounds to remove the heat from the ambient and release this through condensation under pressure, thus transferring the heat in the desired direction at the cost of the energy to pump and pressurize the gas to the point of condensation. In each of these two-phase applications, the transport of the working fluid may require a pump, or it may be accomplished by the buoyant force that exists in an acceleration field, such as that due to gravity. This is the principle that is employed in the closed two-phase thermosyphon. This device is similar to the classical "heat pipe" and the only difference is that the "pumping" method in the heat pipe uses capillary action instead of acceleration forces to pump the fluid. Thus, a "heat pipe" used in a rotating reference utilizing the acceleration forces to transport the liquid from the condenser section to the evaporator section (in lieu of a wick) is, technically, a two-phase thermosyphon. Figure 3.1 illustrates the operation of the closed two-phase thermosyphon. The evaporator end must be in the direction of the acceleration field for the liquid to be transported from the condenser. Figure 3.2 illustrates the operation of the heat pipe, which utilizes the capillary action of the wicking material to transport the liquid from the condenser to the evaporator. The remainder of the chapter shall use these definitions for a discussion of both devices.

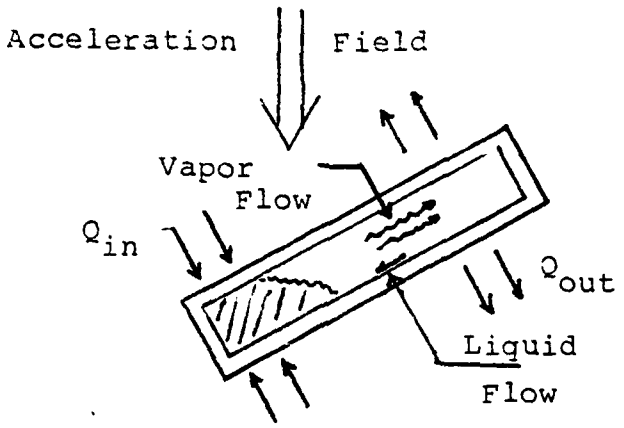

Figure 3.1 Typical Two-Phase Thermosyphon.

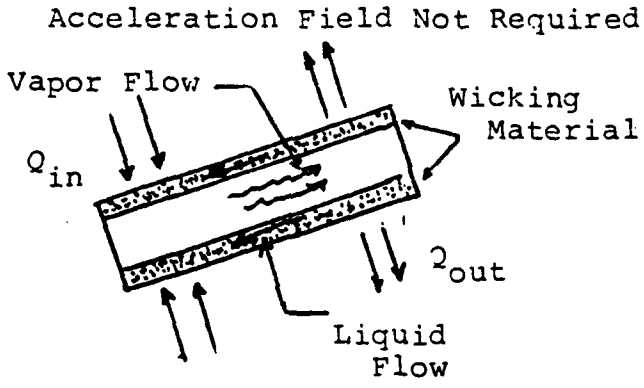

Figure 3.2 Typical Heat Pipe.

A. HISTORICAL DEVELOPMENT

The development of the heat pipe (which will apply equally to the development required for the two-phase thermosyphon) was begun by Gaugler [Ref. 49] in 1944 and by Trefethen [Ref. 50] in 1962. Trefethen was working on cooling methods for spacecraft (zero-g environment) for General Electric Company and discovered that capillary

pumping can be a very valuable area for further development. Working independently, Grover, et al. [Ref. 51] reinvented this concept; he widely published the first applications of the device and gave it its name. Kraus, et al. [Ref. 52] have reported this historical development and have given sample calculations for the design of a heat pipe. Chi [Ref. 53] also reviews the theoretical development of heat pipes, and provides the design procedures, including sample calculations, for their utilization.

B. CONVENTIONAL, CLOSED TWO-PHASE THERMOSYPHON ANALYSIS

As previously mentioned, the appealing factors associated with the two-phase utilization include: high heat fluxes associated with phase changes, lower temperature gradients associated with these processes, and reduced weight of the two-phase system over the single-phase liquid system.

Research by Cohen and Bayley [Ref. 54] (referred to and discussed by Japikse [Ref. 44]) found that the amount of liquid filling the system functionally affected to the heat transfer in both rotating and static tests. They found that heat transfer increased as the percent liquid in the system was increased to approximately 1.5% by volume, then decreased to an intermediate value, and finally increased to approximately the same value as in the 1.5% case. This was related to the following process: in the low filling situation, condensate returns to the evaporator section and forms a thin film on the walls. It is in this film that the heat transfer occurs and the phase change takes place. In the case of the completely-filled evaporator, a liquid pool region develops, and a condition of nucleate boiling exists. If the filling is insufficient, with regard to the heat flux being transported, the pool/film will not continue to the

end of the heated section and "dry-out" will occur. This "dry-cut" will assume a drop-wise instead of film-wise phase change. The geometry of the regions in which the films are likely to form, influences the results.

Lee and Mital [Ref. 55] conducted experiments with an electrically-heated, water-cooled thermosyphon using water and freon as the test fluids and varied the filling quantity, L_h/L_c, pressure (or T_{sat}), and heat flux (L_h/L_c is the ratio of the length of the heated section to the cooled section). The result of the filling quantity on heat transfer was the same as that reported by Cohen and Bayley: increasing heat transfer with filling to a point and then decreasing beyond that value to an intermediate value and increasing to the case of the completely-filled evaporator. The effect of decreasing L_h/L_c was to increase the heat transfer within the range 0.8 to 2.0 and the advantage of larger condenser area was evident. The heat-transfer coefficient was found to increase significantly with increasing mean pressure due to at least three factors:

1) since the mass flow for a given heat flux is nearly constant and density of the liquid increases with pressure, a lower pressure drop (and lower ΔT) is necessary for the same heat flux;

2) for a larger P_{sat}, P_{sat} varies much more rapidly with T_{sat} for the fluids considered, hence requiring smaller ΔT's at higher pressures; and

3) for lower pressure drops, a more favorable force balance exists on the condensate film permitting a faster liquid return.

Water was found to give heat fluxes superior to those of freon, for for the same ΔT, due to the larger values of latent heat of vaporation, and thermal conductivity.

Lee and Mital [Ref. 55] also considered the analytical problem of predicting the maximum heat-transfer rate for a laminar film, constant-wall-temperature condenser and a constant-heat-flux evaporator. Neglecting the forces due to vapor pressure drop and momentum changes, and using a force balance on the falling film, balancing the effects of gravity and fluid shear, they related the mass flow rate to the heat flux. Using a local energy balance and an overall energy balance between the condensing section and the evaporator section, the following relations for the heat transferred (q) and the saturation temperature (T_{sat}) were obtained:

$$q = \{\rho^2 R^3 h_{fg} g/2\mu\ L_h g_c\} C \qquad (3.1)$$

and

$$q = \{k(T_s - T_c)/(RL_h/L_c)\} C/D \qquad (3.2)$$

where $C = 1/8 - 1/2\ y^2 + 3/8\ y^4 - 1/2\ y^4 \ln y$,
$D = y^4 \ln y\ (1/2 \ln y^2 - 1/2) + 1/8\ y^4 + y^2 (1/2 \ln y - 1/4) = 1/8$
and $y = 1 - \delta/R$. The simplifying assumptions (forces due to vapor shear and momentum changes were neglected in the force balance) cause an error (of as much as a factor of 2) to occur, but qualitative behavior is correct as far as L_h/L_c, T_{sat} and working fluid are concerned. This development is also included in the survey by Japikse [Ref. 44]. This heat transfer is graphically presented in the Lee and Mital paper in their Figure 12, shown here as Figure 3.3. This clearly shows that the quantity of heat that can be removed by a two phase water device is large, even at a low saturation temperature. The report also indicates that for water the increasing ratio of heated length to cooled length, L+, decreases the maximum heat transfer. The heat transfer is also very sensitive to the operating pressure;

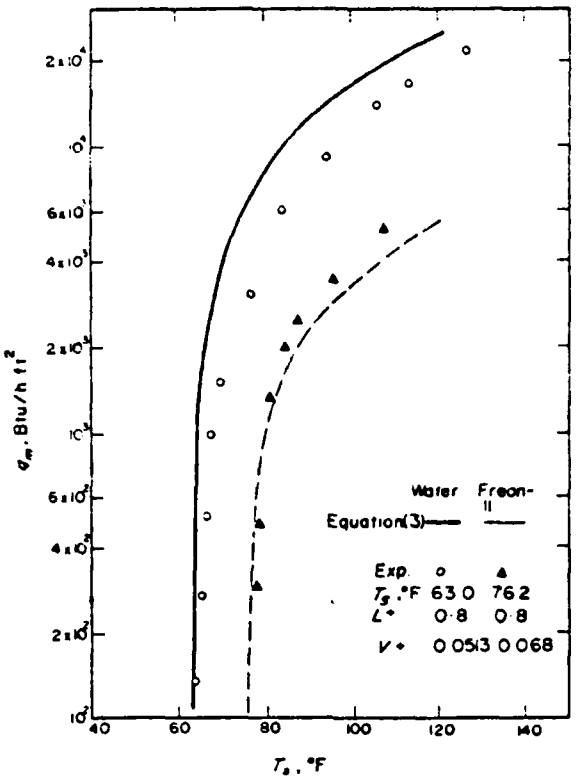

Figure 3.3 Comparison of the Experimental Results with the Analytical Prediction-from Lee & Mital paper.

the heat-transfer coefficient increases appreciably with the mean operating pressure. The temperature drop increases with the pressure drop along the length of the thermosyphon tube (and the saturation pressure gradient). As the pressure increases, the vapor specific volume decreases, resulting in a decrease in the pressure drop; the mass flow rate of the vapor is essentially constant for transferring a given heat input rate. In the previous papers, the vertically-oriented thermosyphon was considered and the current model (for some of the orientations) requires the device to be oriented in the horizontal direction (perpendicular to the applied acceleration field). Although the Lee and Mital paper was considering a vertically-oriented, two-phase thermosyphon, the general results are the same for the horizontal tube.

C. LIMITS OF OPERATION

When considering the design of a two-phase thermosyphon, or a heat pipe, limitations to the heat transfer must be considered; four of these limits are common to both devices (sonic, entrainment, boiling, and condensing). A qualitative comparison of these heat-transfer limitations as a function of the saturation temperature is given in [Ref. 48] and is shown in Figure 3.4.

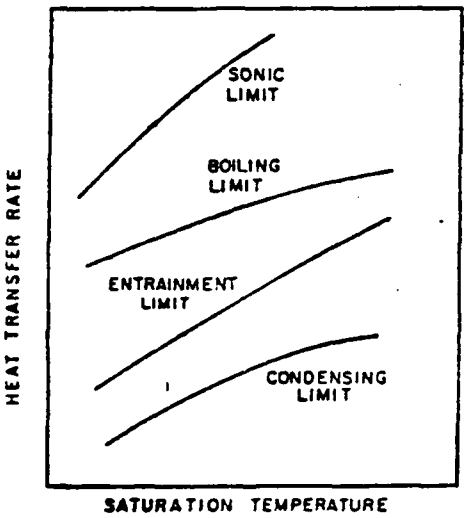

Figure 3.4 Operating Limits of Rotating Heat Pipes.

The sonic limit and the boiling limit have been readily analyzed. The entrainment and the condensation limits are not as well-known and little, if any, literature describing these phenomena exist. This is an area in which further research is needed.

1) **Sonic limit**: the vapor flow in a two-phase closed system is limited to the sonic velocity at the operating

pressure (also known as the "choking" limit). The sonic limit is represented by:

$$Q_{max} = \dot{m} h_{fg} = \rho_v A_v V_s h_{fg}, \qquad (3.3)$$

where V_s is the sonic velocity of the vapor. This limiting velocity may be determined experimentally, computed by the relationship $V_s = \{(\partial p/\partial \rho)_s\}^{1/2}$, or approximated by the perfect-gas relationship $\{\gamma R T_{sat}\}^{1/2}$.

2) **Entrainment limit:** the interfacial shear between the liquid and the vapor will hold the liquid (which is flowing in the opposite direction) back and starve the evaporator section of liquid. This counter-current flow, when the relative velocity is large, causes the interface to become unstable which results in waves at the interface. As the vapor velocity continues to grow, droplets of liquid are formed at the liquid surface as the shear force exceeds the surface-tension force. The formation of these droplets and their subsequent entrainment in the vapor stream causes the partial or total stoppage of the flow (dry-out). This phenomenon is generally governed by the Weber number (the ratio of the inertial force to the liquid surface-tension force). The Froude number is also used to characterize the phenomenon of the drop-wise entrainment of the liquid in the vapor stream. In the application considered herein, the formation of the waves is considered unlikely due to the extreme acceleration field present. Since the flow is counter-current and is in the presence of a high acceleration field the entrainment limitation thus will reduce to the "hold-up" limit. It will remain stratified until hold-up occurs, resulting in evaporator dry-out. Experimental determination of the exact correlation for the hold-up, or entrainment, limit is required for a horizontal

tube rotating around a parallel axis, thereby creating a perpendicular acceleration field many times greater than gravity. The entrainment limit is generally given by:

$$Q_{max}=h_{fg}\rho_v A_v V_E, \qquad (3.4)$$

where V_E is when the Weber number equals unity, the Froude number equals unity, or is experimentally found. In another approach, Jaster and Kosky [Ref. 56] used the ratio of the axial shear force of the vapor flow on the liquid surface to the gravitational (accelertional) body force upon the liquid (defined as "F") in order to arrive at an appropriate "hold-up" criterion. They correlated experimental data as a function of this "F" value, as the flow they were studying transiticned from stratified to annular. The result of their experiments was that the flow was stratified for "F" values below five (5) and was fully-annular above twenty-nine (29). The value of "F" set equal to five (5) was established as the criterion for the transition from stratified to annular for the co-current flow case. The same type of analogy was develcped by Collier and Wallis [Ref. 57] who balanced the inertia force and the acceleration force to scale stratification effects where their criterion was given as j* (vclumetric flux) equal to 0.25. Both of these references point out the need for further research in this area.

3) **Boiling limit**: Again, as discussed in the first section of this chapter in the general discussion on two-phase thermosyphons, the boiling limitation in the current application is due to the creation of profuse nucleation at the evaporator section and a resultant vapor film on the evaporator surface which insulates the evaporator wall, resulting in dry-out and overheating. The boiling limit is given by the Zuber-Kutateladze prediction as discussed in [Ref. 48] and is given as:

$$Q_{max} = 0.13 A_B \rho_v^{1/2} h_{fg} \{ \Omega^2 R (\rho_l - \rho_v) \sigma \}^{1/4}, \qquad (3.5)$$

where A_B is the area in the evaporator section for liquid heating.

4) **Condenser limit:** The capacity of the condenser is dependent on many parameters, such as the geometry, the working fluid, the orientation of the vessel with respect to the acceleration field, and the operating conditions. The orientation of the vessel, for the model considered, is that of a horizontal tube (perpendicular to the acceleration field) with internal condensation. The condensing limit is the capacity to condense the vapor on the inside surface of the condenser section, and this is shown in Figure 3.4. No analysis on the outer surface is presented in this thesis. Instead, the condenser limit is based on the capacity of the inside wall exposed to condensation, using an arbitrary, but reasonable, wall temperature. (Generally, the largest thermal resistance occurs between the ambient and the condenser outer surface. Therefore, heat transfer is limited by this resistance unless the outside surface area is substantially increased by the use of fins.) The condensing limit is given by an equation from [Ref. 58] by Collier for a horizontal tube with internal condensation in a gravitational field as:

$$Q_{max} = A_v \Delta T F_c \{ (\rho_l (\rho_l - \rho_v) g h_{fg} k_f^3) / D \mu_l (T_{sat} - T_w) \}^{1/4}. \qquad (3.6)$$

For the rotating reference being considered, the "g" term in equation (3.6) is replaced by the centripetal acceleration of $\Omega^2 R$. The factor "F " in this equation, allows for the fact that the rate of condensation on the stratified layer of

liquid is negligable. The value of "F " depends on the angle ϕ and is tabulated in [Ref. 58]. Its value ranges from zero, when the tube is full (no surface remains for condensation to occur), to 0.725 , when the tube empty. The angle ϕ is shown in Figure 3.5.

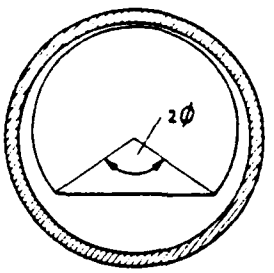

Figure 3.5 Laminar Condensation within a Horizontal Tube (from Collier).

1. Computation of Heat-Transfer Limits

The calculation of these limits is an important step in the design process.

The calculations required to analyze the configuration of the current model are not all well known. The following appear to be the most applicable to the model being evaluated:

----The sonic limit calculation is from basic principles as shown by equation (3.3) by allowing the vapor velocity to increase to the Mach value of unity.

----The boiling limit is given by the Zuber-Kutateladze prediction as discussed in [Ref. 48] and is given by equation (3.5)

----The condensing limit is given by an equation from [Ref. 58] by Collier in equation (3.6).

The literature reveals no correlation yet for the entrainment limit in the heated, horizontal tube rotating about a parallel axis with counter-current flow. Since the majority of analyses previously conducted for this type of flow have shown that the entrainment limit is typically below the sonic and above the condensing limit, the correlations previously mentioned have been plotted against the amount of fluid that is charged in the tube (percentage fill) for the three reasonably known values (sonic, boiling, and condensing limits) in Figure 3.7. Also shown is the entrainment limit computed from the Jaster and Kosky [Ref. 56] correlation developed for co-current flow.

As was previously noted, the condensing limit is the factor that is the most limiting in the design of the thermosyphon. The values of Q_{max} are increased to a maximum based on the length of the condenser, the percentage fill and the ΔT available between the constant temperature (assumed) wall and the saturation temperature of the vapor condensing on it. As already mentioned, the resistance to heat-transfer afforded by the condenser outer walls to the ambient may be quite significant. The ability to design an adequate fin arrangement and supply cooling air in sufficient quantities, while minimizing the windage losses, itself is a substantial problem. From the data obtained in this rough model, there are some self-evident points to be considered:

----The length of the condenser, from a heat-transfer point of view, determines the heat-removal potential,

----The amount of liquid fill can be optimized,

----The temperature at which the walls of the condenser are maintained and the temperature at which the thermosyphon is operated are critical as this temperature difference is the driving force in the heat transfer.

For the model being evaluated, and neglecting (as the limiting value) the entrainment limit, the closed, two-phase thermosyphon, operated at a saturation temperature at, or above, 100°C and with the condenser section held at a wall temperature of 50°C with rotation at a 0.381 m radius and 3,600 RPM can transfer the required 50 W of power with the condensing limit being the limiting value. Figure 3.7 is based on a heat load of 50 W to be equally divided between condenser sections in both end-bell regions (i.e., approximately 25 W each per condenser). For the 3600 RPM model the percentage fill may increase to approximately 40%, and still maintain the required heat flux. The effect that the RPM has with regard to the temperature rise in the heated section, makes the choice of the closed-loop thermosyphon poor for the motor application, but quite suitable for the generator. Further background on the theory of two-phase flow is available in publications by Wallis [Ref. 59] and by Collier & Wallis in [Ref. 57]. The feasibility of the design has been shown by Corman and McLaughlin [Ref. 60] and by Groll, et al. [Ref. 61] through experiments with heat-pipe cooling of electric motors in the scheme primarily recommended, although the difficulty of the liquid transport at low rotation rates was noted. A diagram of the cooling scheme such as recommended and tested by Corman & McLaughlin and Groll, et al., is shown in Figure 3.6 (reproduced from [Ref. 60]).

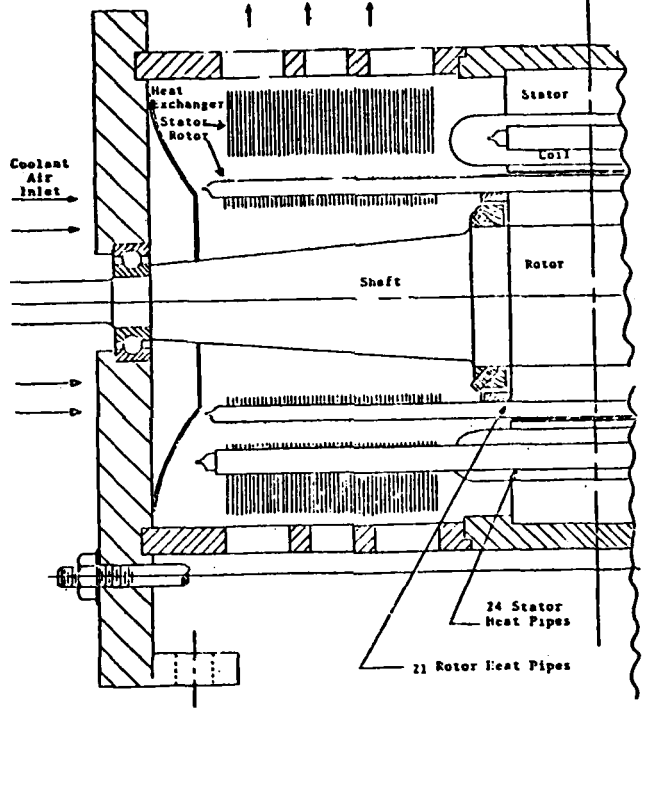

Figure 3.6 Typical Heat-Pipe Cooling Scheme.

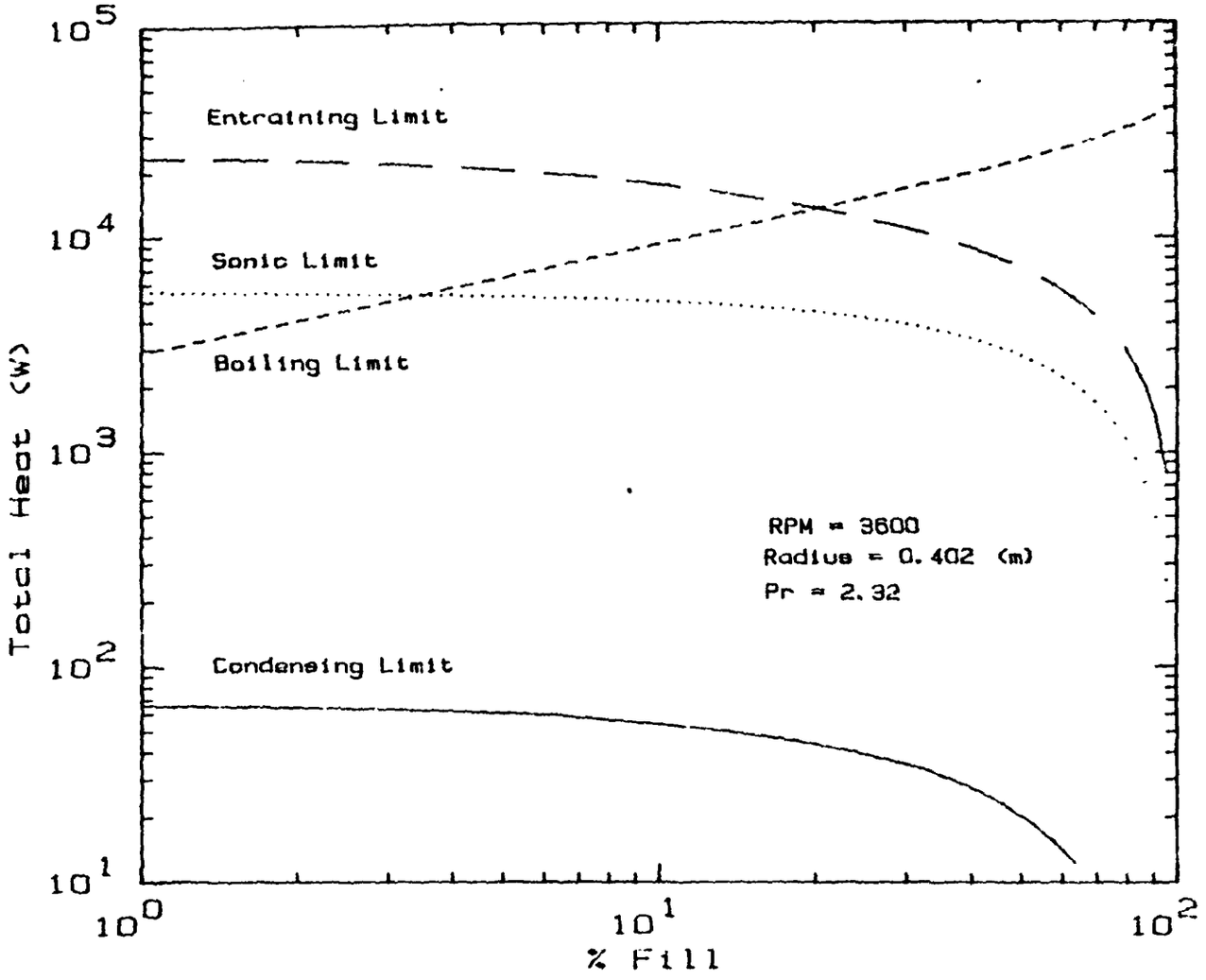

Figure 3.7 Heat-Transfer Limits in the Closed, Two-Phase Thermosyphon.

IV. CONCLUDING SUMMARY

As discussed in the paper by Greene, et al. [Ref. 62], the need for electric propulsion of minimal cost, volume, and weight is well known and motivated by the inherent advantages of this type of propulsion. A significant constraint to be overcome in the development and manufacture of these systems is the rate of heat removal from these devices. In 1976, W. D. Morris [Ref. 63] mentioned that increasing the load per unit weight of these devices demanded that the inherent heat created by the internal losses be removed via improved cooling techniques. Morris also elaborated on the "complex arrangement" of the ducting and associated equipment required to accomplish this increased cooling. Further, he stated that "There is currently insufficient technical information available with which to make confident predictions of the effect of Coriolis and centripetal acceleration on flow resistance and heat transfer in the complex coolant circuits...". Since then, Morris and his co-workers have attempted to fill the literature gap in this area, and have uncovered a great many facts regarding this flow structure; they have also uncovered a great many questions for further research.

As shown as early as 1955 in an article by Sir Claude Gibb [Ref. 64], the principle factor in the failure of two very expensive generating sets was the inability of the devices to dissipate their own heat. In the late 60's, Peach [Ref. 65] wrote of the successes that the English Electric Company had with regard to liquid cooling of the large generator rotors being used in their 500 MW devices and predicted that the devices would reach 1,000 MW with this technology. This was followed in 1970 with a second

report by Peach [Ref. 66] where he outlined the growth of U.S. generator sizes and predicted that the liquid-cooling technology would be required in the near future to support the devices being planned in this country which exceeded 1,000 MW. The losses developed in the large-scale, high-power, superconductive devices, currently being developed for large-scale implementation, require extensive use of cooling at cyrogenic temperatures in order to function in the super-conductive state in which they operate. A discussion of this application is presented by Schwartz and Foner [Ref. 67], in which a number of the schemes discussed herein are shown.

The previous chapters have discussed the ability of external, forced-convective cooling to remove the internally-developed heat loads in electrical, rotating machinery. The reduction in size, the increased efficiency, and the prolonged life cycle are all very important reasons to utilize advanced-cooling concepts. The use of turbulent flow is feasible at all RPM's; therefore, both motor and generator applications would benefit from forced-convective liquid cooling utilizing turbulent flow. Laminar-flow heat transfer is feasible only at higher RPM's, which tends to limit the application of this method in regard to motors. The actual transition from laminar to turbulent flow is not well known and further investigation is required to determine the transition point; the transition may occur at a flow and RPM acceptable for the motor application. However, the utilization of external, forced-convective cooling has some major difficulties associated with it:

1) The source of the external cooling fluid must be easily accessible, dependable (in a casualty-control sense), safe, volumetrically small, light, and should be reasonably inexpensive.

2) The fluid itself should be of high specific heat, light, inexpensive, and more importantly, non-toxic and non-flammable.

3) The method of transporting the fluid from the source, through an external heat exchanger, through the device, and back, should be extremely reliable and quite resistant to external damage. This is an area of serious consideration where the reliability of conventional, rotating seals is questionable in the least.

The alternative to the use of external, forced-convective cooling is the utilization of a closed device: (a) the closed, two-phase thermosyphon, (b) the closed, rotating-loop thermosyphon, (c) the closed rotating-loop, two-phase thermosyphon, or (d) the heat pipe. These alternatives remove the necessity of using radial rotating seals in the design of the cooling system.

The closed, two-phase thermosyphon, as shown in Figure 3.6, must have a sufficient forced-air circulation through the end-bell regions to remove the heat. This will require optimizing the length of the condenser sections, the geometry of the fins, the number of fins and the direction of air flow within the device to maximize the heat transfer while minimizing the windage losses. The closed two-phase thermosyphon is feasible at the higher RPM's that the generator operates at; additionally, this method could also be feasible in the motor application if a heat pipe (i.e., a thermosyphon whose walls are lined with a capillary wicking material) is used in lieu of the two-phase thermosyphon for the lower RPM's.

The closed, rotating-loop thermosyphon requires an additional heat exchange through the shaft of the device, possibly supplemented with forced-air convection through the hollow rotor region and by the exposed radial sections of

the loop. This shaft heat exchanger may be in the form of a rotating heat-pipe, as shown in Figures 4.1 and 4.2, where the external exchange is to either ambient forced-air, or to an external, closed water spray. The shaft heat exchanger may also be cooled by forced convection using liquid cooling, with axial, packing-type seals, external to the device as shown in Figure 4.3. This closed-loop thermosyphon could use either single-phase or two-phase operation.

The closed two-phase thermosyphon could also be extended along the shaft through a bearing plate arrangement and cooling air could be supplied external to the casing, simplifying the internal configuration, as shown in Figure 4.4.

The ability of these devices to cool effectively has been proven and their usage in this application is theoretically feasible. The exact correlations for the calculation of the performance values for these devices, especially in a rotating reference, will require further research.

The analysis herein has shown the ability of the cooling schemes discussed to remove the requisite heat load in order to extend the life of the insulation, increase the efficiency, decrease the weight and size of motors and generators. This study graphically presents the applicable correlations for the determination of the heat transfer within a rotating, electric device. It also discusses the limitations of these correlations. It has been shown that closed, two-phase systems of an inherently higher reliability are feasible, and deserve further evaluation.

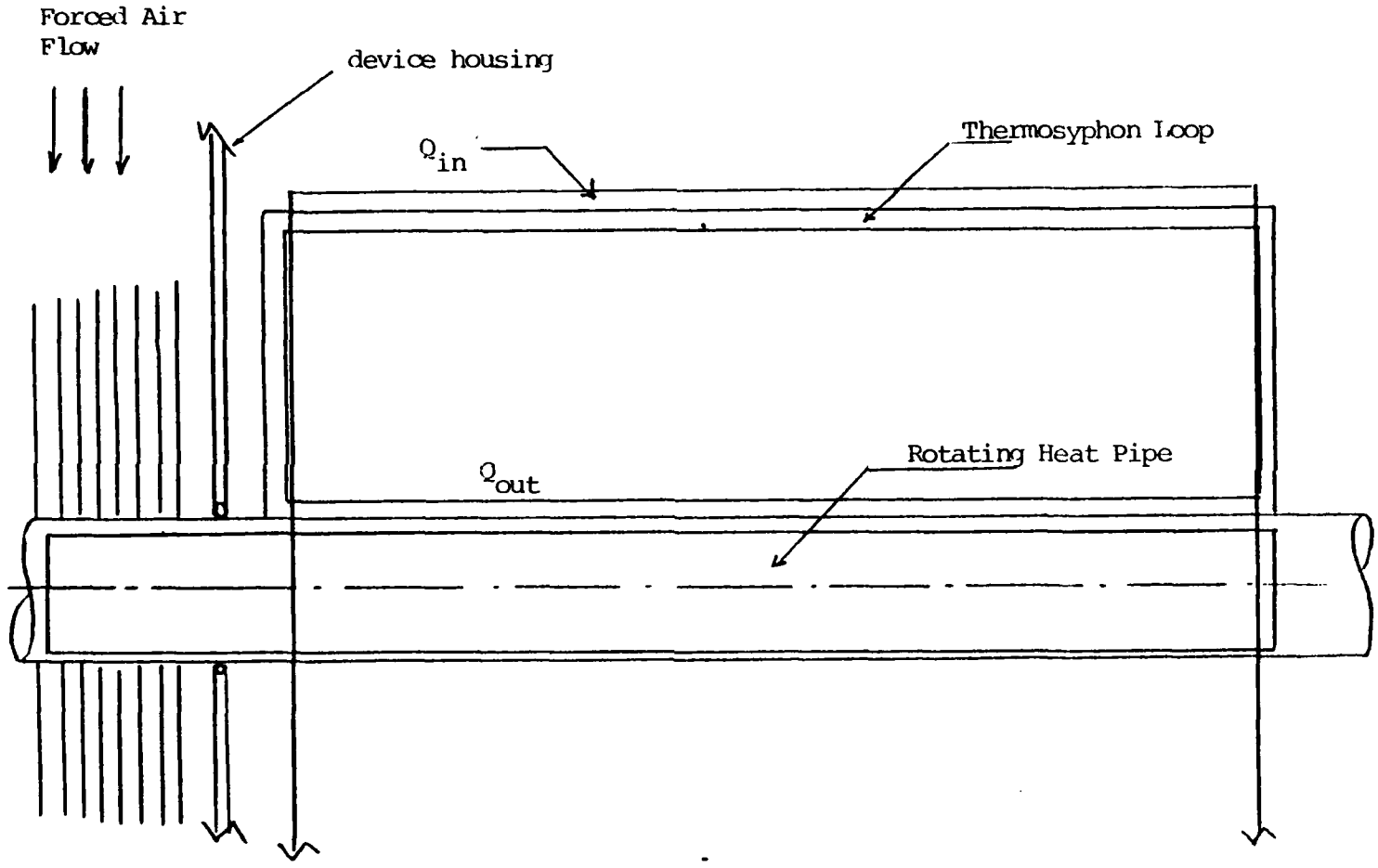

Figure 4.1 Closed-Loop Thermosyphon to Shaft Rotating Heat Pipe (Air Exchanger).

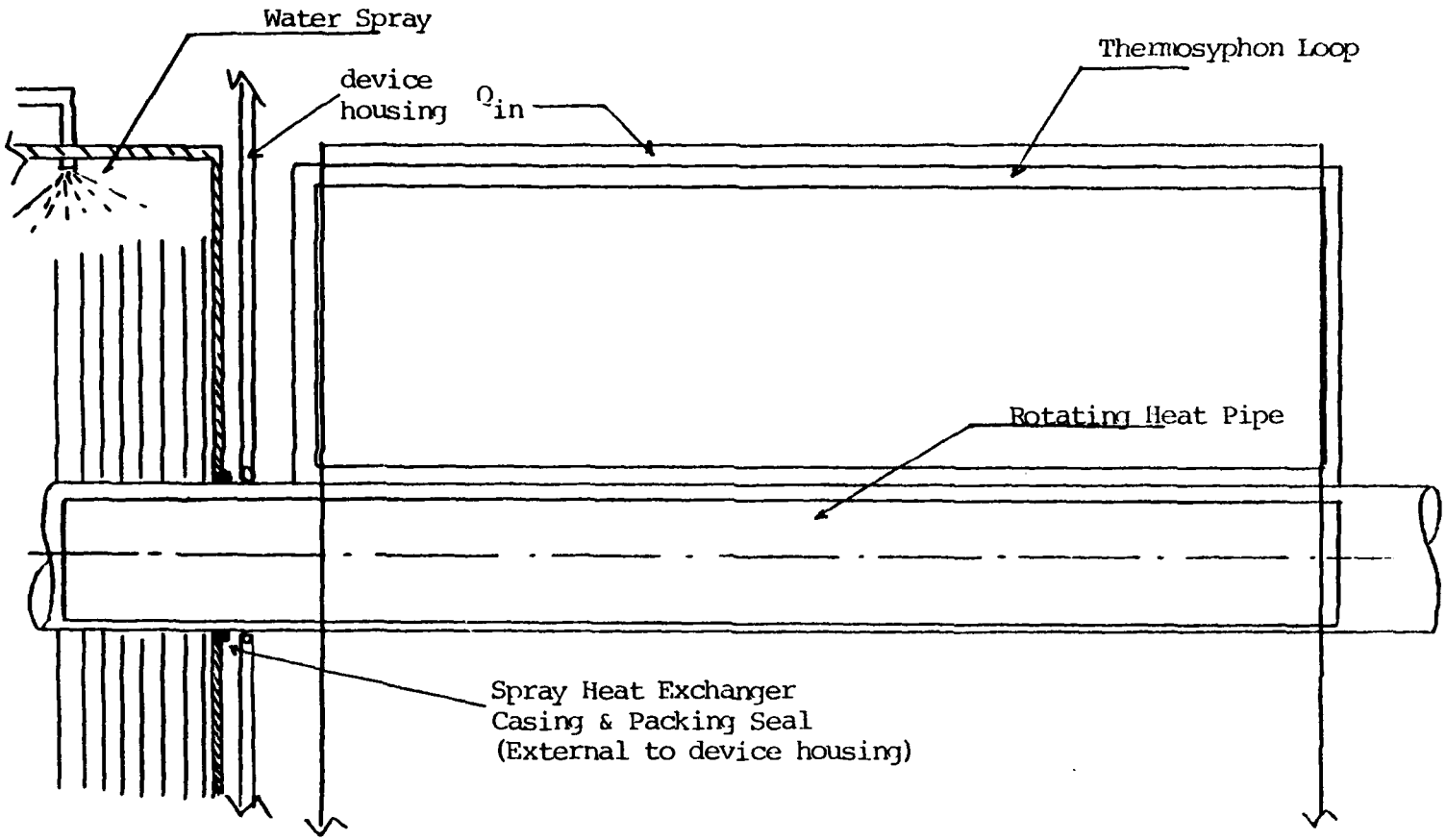

Figure 4.2 Closed-Loop Thermosyphon with Shaft Rotating Heat Pipe (Water Spray Exchanger).

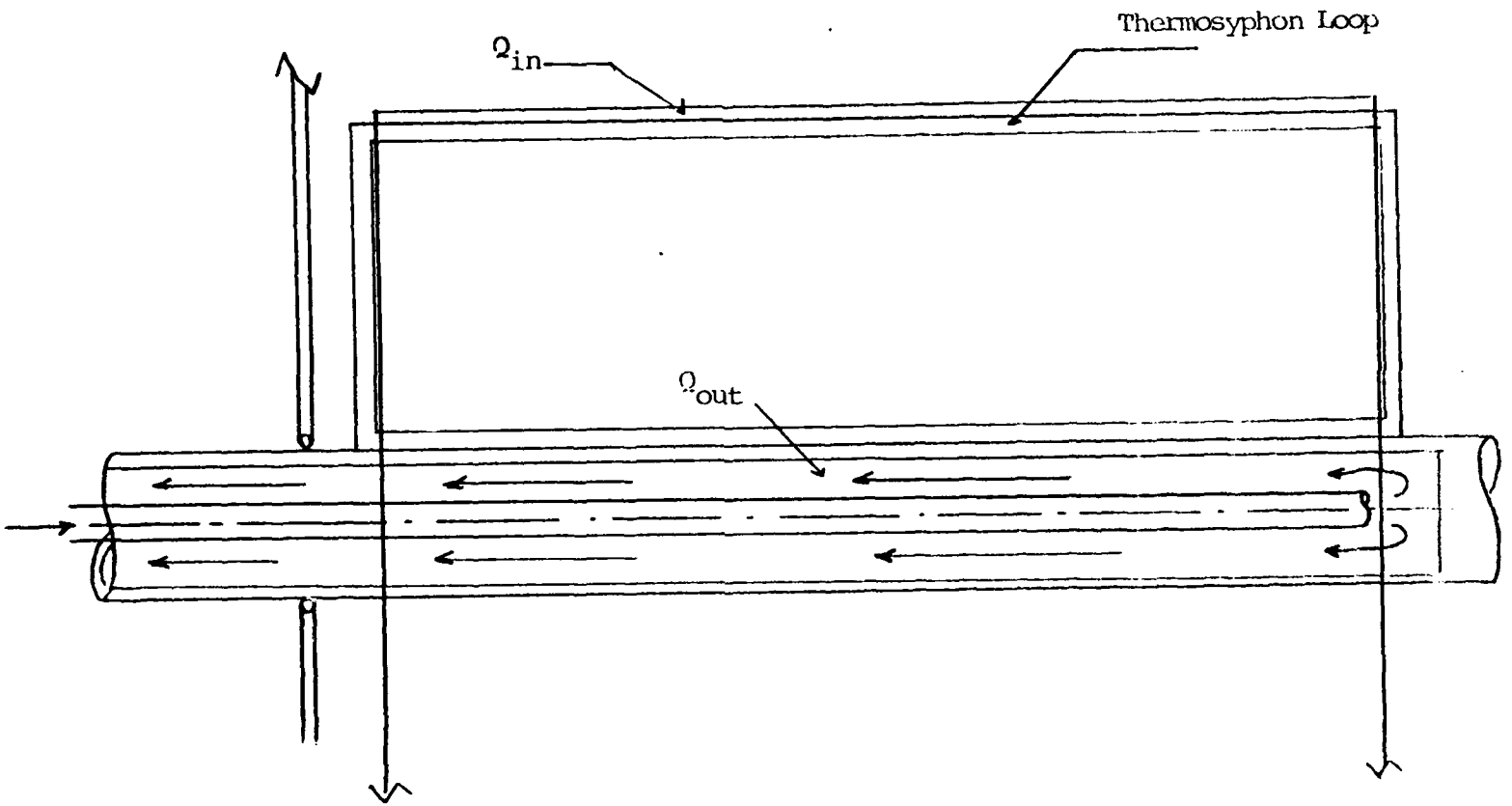

Figure 4.3 Closed-Loop Thermosyphon with Shaft Forced-Convection Liquid

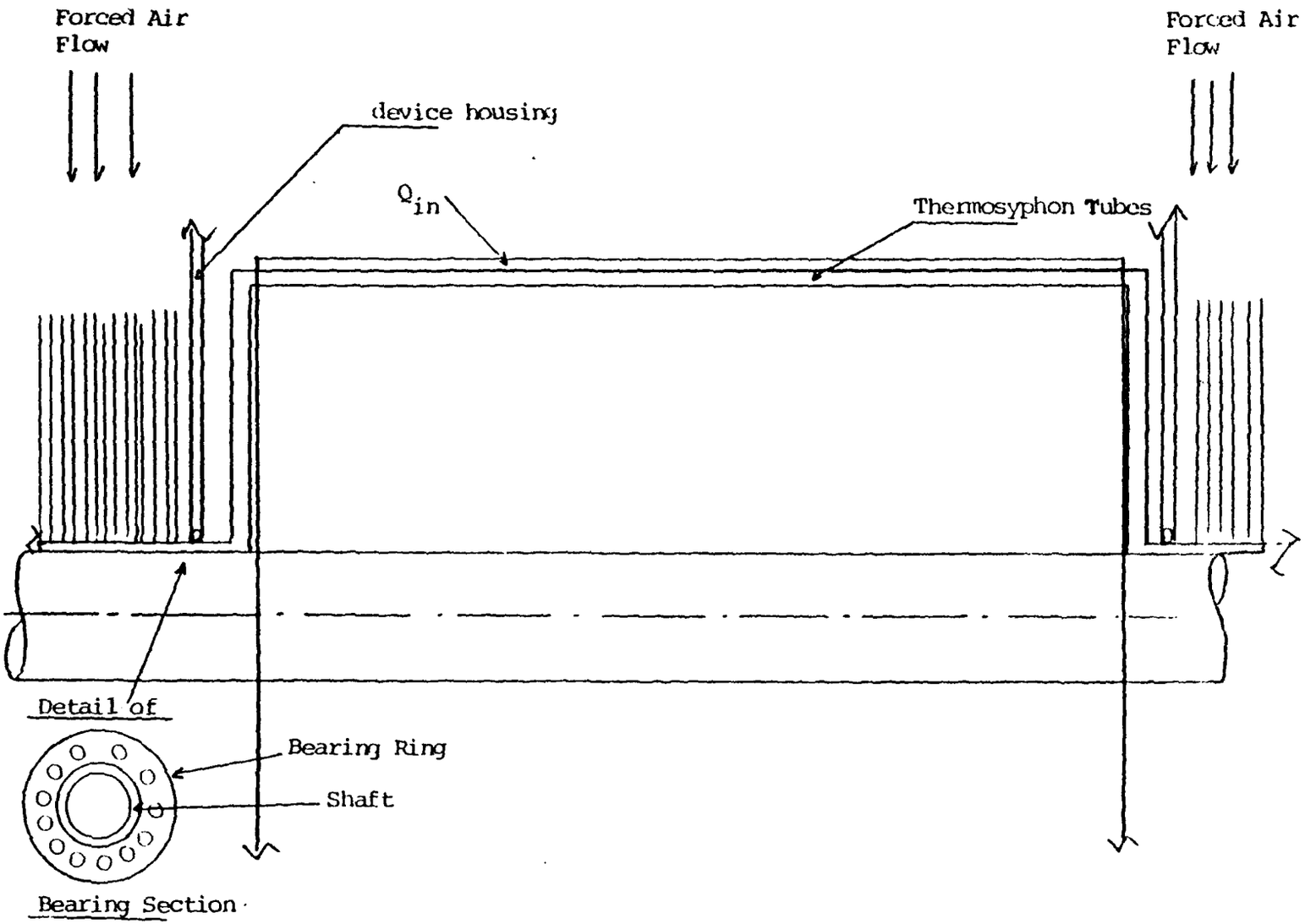

Figure 4.4 Closed Single-, or Two-Phase Thermosyphon with Radial Sections to Shaft Extending to Ambient.

V. CONCLUSIONS AND RECOMMENDATIONS

A. CONCLUSIONS

Based upon the information reviewed and analyzed in this thesis, the following conclusions are made:

1) Forced-convective liquid cooling is a practical means for improving the efficiency, reducing the size and weight, and extending the life of high-power motors and generators. The main disadvantage of forced-convective liquid cooling is the requirement of radial rotating seals.

2) Closed-loop liquid thermosyphons are feasible at high RPM. They offer improved reliability over forced-convective liquid cooling which utilizes rotating seals. However, this method requires the use the shaft as a secondary heat exchanger.

3) The closed, two-phase thermosyphon is feasible at the higher RPMs of the generators. This method requires forced-air convection through the end-bell regions or the extension of the devices along the shaft for external forced-air convection, both of which will add to the windage losses.

4) For low RPM applications, such as motors, the use of a heat pipe will be required to overcome the inability of the low acceleration field to transport the cooling fluid. Both the closed, two-phase thermosyphon and the heat-pipe require forced convection at the condenser ends to remove the heat either internal, or external to the device. This may add to the windage losses.

AD-A144 049 COOLING OF HIGH POWER GENERATORS AND MOTORS FOR ELECTRIC PROPULSION(U) NAVAL POSTGRADUATE SCHOOL MONTEREY CA J L SZATKOWSKI ET AL. MAR 84 2/2

UNCLASSIFIED F/G 13/10 NL

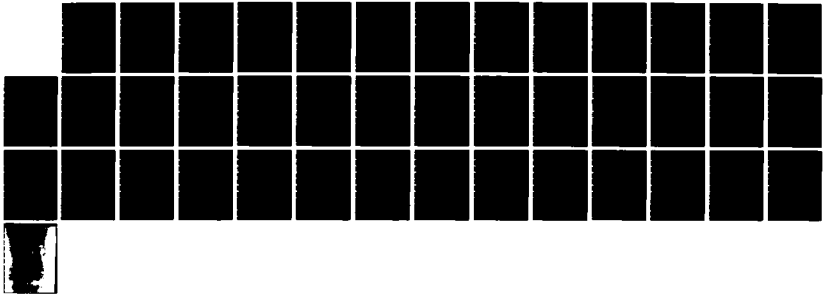

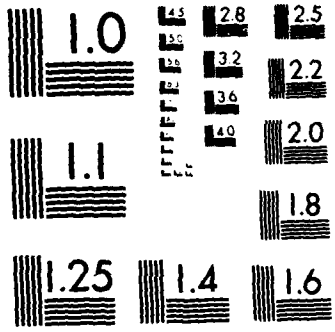

5) Correlations and theoretical analyses are not available in the literature for:

a) the counter-current entrainment limit for two-phase thermosyphons under rotation and

b) the transition from laminar to turbulent flow for rotating systems.

E. RECOMMENDATIONS

The following recommendations to continue this work are made:

1) Testing of the forced-convective liquid cooling scheme should be accomplished using the DTNSRDC test rig to confirm the analysis and the validity of the available correlations, or to obtain proper correlations for the specific geometry and utilization being projected.

2) An experimental program should be devised and conducted to determine the entrainment limitation in a horizontal, heated, channel rotated about a parallel axis with counter-current flow of liquid and vapor.

3) An experimental program should be developed to determine the optimum condenser length and proper fin arrangment for the use of both heat pipe and closed two-phase thermosyphon systems for rotor cooling. Consideration of the structural integrity must be included for the condenser end-lengths.

4) An experimental program should be developed for correlating the laminar-to-turbulent transition during forced-convective liquid cooling in a heated, horizontal, rotating pipe.

5) An experimental program should be developed to modify the inside geometry of the closed-loop thermosyphon

(and axial, closed, two-phase thermosyphon) to optimize the heat-transfer and the friction losses within the device.

6) A detailed analysis should be made of the shaft cooling potential for the rotating-loop thermosyphon with regard to the heat-transfer enhancement of the shaft to the fluid and the mechanical design of the shaft.

7) An experimental program should be developed to analyze the closed, two-phase thermosyphon with radial condenser sections and the closed-loop two-phase thermosyphon. These two devices may experience start-up balance problems.

8) Various configurations should be analyzed for their potential for heat transfer to include a combination of the systems described herein, as depicted in Figures 4.1 through 4.4.

9) The concept of modifying the geometry of the rotor windings within these devices in order to minimize heat conduction path lengths to the casing, shaft, etc., and thereby the internal temperature gradient, should also be investigated.

APPENDIX A

GOVERNING EQUATIONS FOR LAMINAR CONVECTION IN UNIFORMLY HEATED HORIZONTAL PIPES AT LOW RAYLEIGH NUMBERS

The following development, by Morton [Ref. 11], is presented herein for completeness. The steady laminar motion of a fluid in a horizontal circular pipe of radius a, the walls of which are heated uniformly so that a constant temperature gradient τ is maintained in the direction of the axis. The flow will be referred to in cylindrical coordinates (r, ϕ, z) with ϕ measured from the upward vertical and the z-axis along the axis of the pipe; the velocity components are denoted by u, v, and w. The effects of dissipation and of the pressure term in the energy equation will be neglected and that variations in the density due to the temperature differences are so small that they only effect the buoyancy term. Thermal conductivity and kinematic viscosity are assumed to be constant (which will introduce quantitative errors into the solution, but should not change its general character).

The equation of continuity is then:

$$\partial ru/\partial r + \partial v/\partial \phi + \partial rw/\partial z = 0, \qquad (A.1)$$

and the energy equation is:

$$u(\partial T/\partial r) + v/r(\partial T/\partial \phi) + w(\partial T/\partial z) = k \nabla^2 T, \qquad (A.2)$$

where $\nabla^2 = \partial^2/\partial r^2 + 1/r(\partial/\partial r) + 1/r^2(\partial^2/\partial \phi^2) + \partial^2/\partial z^2$ and T is the local fluid temperature. The momentum equations can be written in the form of equations (A.3) through (A.5).

$$u(\partial u/\partial r)+v/r(\partial u/\partial\phi)+w(\partial u/\partial z)-v^2/r = -1/\rho(\partial p/\partial r)$$

$$v(\nabla^2 u-u/r^2-2/r^2(\partial v/\partial\phi)-g(T_w-T)\cos\phi, \qquad (A.3)$$

$$u(\partial v/\partial r)+v/r(\partial v/\partial\phi)+w(\partial v/\partial z)=uv/r = -1/\rho r(\partial p/\partial\phi)$$

$$\nu(\nabla^2 v+2/r^2(\partial u/\partial\phi)-v/r^2)+ g(T_w-T)\sin\phi, \qquad (A.4)$$

$$u(\partial w/\partial r)+v/r(\partial w/\partial\phi)+w(\partial w/\partial z) =$$

$$-1/\rho(\partial p/\partial z)+\nu\nabla^2 w. \qquad (A.5)$$

In equations (A.3) and (A.4), the buoyancy force has been calculated relative to the fluid at the same level adjacent to the pipe wall and the remaining distribution of force has been absorbed into the pressure, p.

For steady convection sufficiently far from the pipe opening to avoid inlet-length effects, the temperature throughout the pipe increases uniformly with the distance along the pipe axis. Hence, the distribution of buoyancy force in sections of the pipe is independent of z; as the secondary flow is caused by the buoyancy forces, the flow field must also be independent of z. It follows that there should be a similarity solution with u,v,w, and T_w-T as functions of r and ϕ only, and with $p=\gamma z+P(r,\phi)$ (where P contains the terms absorbed into p).

The continuity equation reduces to the form:

$$\partial(ru)/\partial r + \partial v/\partial\phi = 0;$$

hence, a dimensionless Stokes stream function ψ can be introduced in such a way that:

$$ru/\nu = \partial\psi/\partial\phi, \qquad v/\nu = -\partial\psi/\partial r.$$

The main equations (A.1) through (A.5) may be reduced to non-dimensional form by the transformations $r=aR$, $w=(\nu/a)W$, and $T_w-T=\tau aPr$, where Pr is the Prandtl number (ν/α). If the pressure is eliminated between equations (A.3) and (A.4), the resulting momentum equations are:

$$\nabla_1^4\psi + 1/P\{\partial\psi/\partial R(\partial/\partial\phi)-\partial\psi/\partial\phi(\partial/\partial R)\}\nabla_1^2\psi =$$

$$Ra\{(\partial\theta/\partial R)\sin\phi + 1/R(\partial\theta/\partial\phi)\cos\phi\}, \qquad (A.6)$$

$$\nabla_1^2 W + 1/R\{(\partial\psi/\partial R)(\partial/\partial\phi)-$$

$$(\partial\psi/\partial\phi)(\partial/\partial R)\}W + 4Re = 0, \qquad (A.7)$$

and where,

$$\nabla_1^2 = \partial^2/\partial R^2 + 1/R(\partial/\partial R) + 1/R^2(\partial^2/\partial\phi^2).$$

The Rayleigh number, Ra, is given by $g\beta\tau a^4/(\alpha\nu)$ and the Reynolds number is the normal Reynolds number, Re, for Poiseuille pipe flow based on the pipe diameter and the mean velocity across a pipe section is $(a/\nu)(\gamma a^2/4\mu)$.

The solution of the energy equation depends on the temperature on the boundary condition at the wall of the pipe. Pipes will usually have reasonably-thick walls of material with thermal conductivity much higher than that of the fluid, so there will be little variation in wall temperature around the pipe circumference. This will be specially so for slow rates of heating when asymmetries of the flow will have small amplitude. Hence, write $T = T0 + z$, where T0 is the wall temperature in the section containing the origin. Although there is uniform heat transfer per unit length of pipe, the local heat transfer will be slightly greater near the bottom of the pipe than near the top. With this assumption, equation (A.2) reduces to the non-dimensional form of equation (A.8).

$$\nabla_1^2\theta + (\sigma/R)\{(\partial\psi/\partial R)(\partial\theta/\partial\phi) - (\partial\psi/\partial\phi)(\partial\theta/\partial R)\} + W = 0 \qquad (A.8)$$

The boundary conditions are:

u,v,w, and θ are zero on r=a:
u,v,w, and θ are finite on r=0.

(A.9)

Although solution of equations (A.6) through (A.8), satisfying conditions of (A.9) is considerably difficult, successive approximations to the solution can be obtained by expanding ψ, W, and θ as power series in the Rayleigh number, provided that this is numerically small. Supposing that:

$$\psi = Ra\psi_1 + Ra^2\psi_2 + \ldots,$$
$$W = W_0 + RaW_1 + Ra^2W_2 + \ldots,$$
$$\theta = \theta_0 + Ra\theta_1 + Ra^2\theta_2 + \ldots .$$

(A.10)

The leading term ψ_0 of ψ must vanish because there is no circulation when A is zero, but θ_0 is not zero since the difference in temperature between a fluid element and the neighboring wall is proportional to $\tau\theta$. When relations (A.10) are substituted in equations (A.6), (A.7), and (A.8), three sets of equations for the funtions ψ_i, W_i, and θ_i are obtained by equating coefficients of powers of Ra.

From equation (A.7), the basic equation is:

$$\nabla_1^2 W_0 + 4Re = 0, \qquad (A.11)$$

which has a solution:

$$W_0 = Re(1-r^2) \qquad (A.12)$$

which satisfies the conditions $W_0=0$ at R=1, W_0 finite at R=0. This is ordinary Poiseulle flow under a pressure gradient $-4\rho\nu^2 Re/a^3$ in an unheated pipe.

The first of the equations derived from equation (A.8) for the temperature distribution is:

$$\nabla_1^2 \theta_0 + W = 0, \tag{A.13}$$

subject to $\theta_0 = 0$ at $R=1$, θ_0 finite at $R=0$, and the solution is axially symmetrical as no account has been taken of gravity at this stage of the approximation. This is satisfied by:

$$\theta_0 = (1/16)\,Re(1-R^2)(3-R^2), \tag{A.14}$$

which is the customary solution for forced convection.

The first-order approximation for ψ satisfies the equation:

$$\nabla_1^4 \psi_1 = (\partial \theta_0 / \partial R) \sin\phi \tag{A.15}$$

obtained as the coefficient of Ra from equation A.6, and the boundary conditions $\partial\psi_1/\partial R, \partial\psi_1/\partial\phi = 0$ on $R=1$, and $R^{-1}(\partial\psi_1/\partial\phi)$, $\partial\psi_1/\partial R$ remain finite at $R=0$. If ψ_1 is assumed to have the form $\psi_1(R)\sin\phi$, the dependence of equation A.15 on ϕ is eliminated, and $\psi_1(R)$ is easily found:

$$\psi_1 = -(1/4608)\,ReR(1-R^2)^2(10-R^2)\sin\phi\,. \tag{A.16}$$

Similarly, the first-order approximation to W_1 satisfies the equation:

$$\nabla_1^2 W_1 = (1/R)(\partial\psi_1/\partial\phi)(\partial W_0/\partial R), \tag{A.17}$$

and the boundary conditions, $W_1 = 0$ at $R=1$ and W_1 finite at $R=0$. The dependence of equation A.17 on ϕ is eliminated by taking $W_1 = W_1(R)\cos\phi$, whence

$$W_1 = -(1/184320)\,Re^2 R\,(1-R^2)\,(49-51R^2+19R^4-R^6)\cos\phi. \qquad (A.18)$$

The first-order approximation to θ satisfies the equation:

$$\nabla_1^2\theta_1 = (\sigma/R)\,(\partial\psi_1/\partial\phi)\,(\partial\theta_0/\partial R) - W_1, \qquad (A.19)$$

and the boundary conditions, $\theta_1 = 0$ at $R=1$ and θ_1 finite at $R=0$. Hence,

$$\theta_1 = -(1/22118400)\,Re^2 R(1-R^2)\{(381+1325\sigma)-(354+1675\sigma)R^2+$$

$$+(146+925\sigma)R^4-(29+200\sigma)R^6+(1-2\sigma)R^8\}\cos\phi\ . \qquad (A.20)$$

This completes the approximate solution to the first order in Ra for convection in a horizontal pipe, which is heated so that there is a constant temperature gradient along the walls and uniform temperature around the girth. It may be noted from equations (A.10), (A.12), (A.14), (A.16), (A.18), and (A.20) that the full convection solution depends essentially on the product RaRe. This is clear if it is recalled that Ra is proportional to the increase in wall temperature along the pipe and Re is proportional to a characteristic velocity of the flow along the pipe. An increase in Ra means that the fluid will be carried through a larger temperature differences, and, hence, there will be increased buoyancy forces; but the same effect can be produced by an increase in Re, and hence in the velocity of the main flow.

The two most interesting consequences of such a solution are the modification of the heat transfer due to secondary flow, and the effect of heating on the tangential stress at the wall (or on the rate of flow for a given pressure gradient). However, as both W_1 and θ_1 vary with $\cos\phi$,

neither the flux nor the heat transfer across the middle section of the pipe will be changed by the first-order approximation although there will be local variations.

To find the changes in total flux and heat transfer, it is necessary to proceed to the second-order approximations, and the revelant equations for these are:

$$\nabla_1^4 \psi_2 = (1/R)\{\partial(\nabla_1^2\psi_1, \psi_1)/\partial(R,\phi)\} + (\partial\theta_1/\partial R)\sin\phi + (1/R)(\partial\theta_1/\partial\phi)\cos\phi ,$$

$$\nabla_1^2 W_2 = (1/R)\{\partial(W_1, \psi_1)/\partial(R,\phi)\} + (1/R)\{\partial(W_0, \psi_2)/\partial(R,\phi)\},$$

$$\nabla_1^2 \theta_2 = (\sigma/R)\{\partial(\theta_1, \psi_1)/\partial(R,\phi)\} + (\sigma/R)\{\partial(\theta_0, \psi_2/\partial(R,\phi)\} - W_2 . \quad \text{(A.21)}$$

The only difficulty in solving these equations is numerical tediom and the remaining second-order solutions are presented in [Ref. 11].

APPENDIX B

SINGLE-PHASE ANALYSIS (COMPUTER PROGRAM AND RESULTS)

The following program was written to give the results of the various correlations for the heat transfer for the forced, single-phase convection in the rotating reference as disscussed in Chapter II. The program is so written that modification to include other correlations is quite easy. It was written in HP-Basic for the HP-9826 computer. Sub-programs for the graphics are not shown. Sample runs are included immediately following the listing.

```
1000! FILE NAME:     a:S
1010! CREATED:       January 11, 1984
1020! LAST REVISED:  February 5, 1984
1030!
1040  COM /Cmin/ Xmin,Ymin,Sfx,Sfy
1050  PRINTER IS 1
1060  BEEP
1070  PRINT USING "2X,""Default values: """
1080  D=4.763E-3     ! Tube diameter   (m)
1090  L=.8230        ! Tube length     (m)
1100  R=.4021        ! Radius of rotor (m)
1110  PRINT USING "4X,""Tube diameter   = "",Z.4DE,"" (m)""":D
1120  PRINT USING "4X,""Tube length     = "",DD.D,"" (m)""":L
1130  PRINT USING "4X,""Radius of rotor = "",Z.3D,"" (m)""":R
1140  BEEP
1150  INPUT "OK TO ACCEPT DEFAULT VALUES (1=Y,0=N)?",Id
1160  BEEP
1170  INPUT "LIKE A HARD COPY (1=Y,0=N)?",Ihc
1180  IF Ihc=1 THEN
1190  PRINTER IS 701
1200  ELSE
1210  PRINTER IS 1
1220  END IF
1230  IF Id=1 THEN 1300
1240  BEEP
1250  INPUT "ENTER TUBE DIAMETER (m)",D
1260  BEEP
1270  INPUT "ENTER TUBE LENGTH (m)",L
1280  BEEP
1290  INPUT "ENTER RADIUS OF ROTOR (m)",R
1300  PRINT USING "10X,""*** Geometric Variables *** """
1310  PRINT USING "14X,""Tube diameter (D) = "",Z.3DE,"" (m)""":D
1320  PRINT USING "14X,""Tube length (L)   = "",DD.DD,"" (m)""":L
1330  PRINT USING "14X,""L/D               = "",5D.D":L/D
1340  PRINT USING "14X,""Rotor radius (R)  = "",Z.3D,"" (m)""":R
1350  PRINT
1360  PRINT USING "10X,""Computed values are: """
1370  PRINTER IS 1
1380  BEEP
1390  PRINT USING "2X,""SELECT OPTION:"""
1400  PRINT USING "4X,""1  Single point"""
1410  PRINT USING "4X,""2  Nu versus RPM"""
1420  PRINT USING "4X,""3  Nu versus Re"""
1430  PRINT USING "4X,""4  Nu versus Prod"""
1440  INPUT Op
1450  IF Op>3 THEN
1460  PRINT USING "4X,""SELECT OPTION:"""
1470  PRINT USING "4X,""2  VARY RPM"""
1480  PRINT USING "4X,""3  VARY Re"""
1490  INPUT Opx
1500  IF Opx=2 THEN Op=2
1510  IF Opx=3 THEN Op=3
1520  END IF
1530  IF Op>1 THEN
1540  BEEP
1550  Jv=0
1560  PRINTER IS 1
1570  PRINT USING "4X,""SELECT OPTION:"""
1580  PRINT USING "4X,""  1=Dittus-Boelter, 2=Nakayama, 3=Nakayama & Fujioka"""
```

```
1590  PRINT USING "4X,""  4=Woods & Morris, 5=Stephenson, 6=Woods&Morris, 7=Am
mar,8=Nakayama""
1600  INPUT Ian
1610  BEEP
1620  INPUT "LIKE TO PLOT (1=Y,0=N)?",Okplot
1630   IF Okplot=1 THEN
1640   CALL Plot(Jj,Jc,Jd,X,Y,Type,Cx)
1650   BEEP
1660   INPUT "SOLID=1,DASH-DASH=2,DOT-DOT=3",Type
1670   END IF
1680  END IF
1690  Nstep=100
1700  IF Op=2 THEN
1710  BEEP
1720  INPUT "ENTER RPM RANGE (MIN,MAX)",Rpml,Rpmh
1730  Rpm=Rpml
1740  ELSE
1750  BEEP
1760  INPUT "ENTER RPM OF ROTOR",Rpm
1770  END IF
1780  BEEP
1790  INPUT "ENTER OPTION (1=Q,2=Mf,3=Dt)",Io
1800  IF Ihc=1 THEN PRINTER IS 701
1810  IF Ihc=0 THEN PRINTER IS 1
1820  PRINT
1830  PRINT USING "10X,""*** Operating Variables *** """
1840  PRINT
1850  PRINT USING "10X,""Input variables are: """
1860  IF Io=1 THEN
1870  BEEP
1880  INPUT "ENTER COOLANT MASS FLOW RATE (kg/s)",Mf
1890  BEEP
1900  PRINT USING "14X,""Coolant mass flow rate = "",Z.3DE,"" (kg/s)""";Mf
1910  INPUT "ENTER INLET AND OUTLET TEMPS (C)",T1,To
1920  PRINT USING "14X,""Coolant inlet temp      = "",DD.DD,"" (C)""";T1
1930  PRINT USING "14X,""Coolant outlet temp     = "",DD.DD,"" (C)""";To
1940  END IF
1950  IF Io=2 THEN
1960  BEEP
1970  INPUT "ENTER HEAT LOAD (W)",Q
1980  PRINT USING "14X,""Heat load               = "",4D.DD,"" (W)""";Q
1990  BEEP
2000  INPUT "ENTER INLET AND OUTLET TEMPS (C)",T1,To
2010  PRINT USING "14X,""Coolant inlet temp      = "",DD.DD,"" (C)""";T1
2020  PRINT USING "14X,""Coolant outlet temp     = "",DD.DD,"" (C)""";To
2030  END IF
2040  IF Io=3 THEN
2050  IF Jj>0 THEN 2200
2060  BEEP
2070  INPUT "ENTER HEAT LOAD (W)",Q
2080  PRINT USING "14X,""Heat load               = "",4D.DD,"" (W)""";Q
2090  BEEP
2100  IF Op<3 THEN
2110  INPUT "ENTER COOLANT MASS FLOW RATE (kg/s)",Mf
2120  PRINT USING "14X,""Coolant mass flow rate = "",Z.4DE,"" (kg/s)""";Mf
2130  ELSE
2140  INPUT "ENTER MASS FLOW RATES (MIN,MAX)",Mfl,Mfh
2150  Mf=Mfl
2160  END IF
2170  BEEP
2180  INPUT "ENTER COOLANT INLET TEMP (C)",T1
```

```
2190  PRINT USING "14X,""Coolant inlet temp      = "",DD.DD,"" (C)""":T
2200  END IF
2210  END IF
2220  Ta=(To+T1)*.5
2230  Cp=FNCpw(Ta)
2240  Mu=FNMuw(Ta)
2250  K=FNKw(Ta)
2260  Pr=FNPrw(Ta)
2270  Rho=FNRhow(Ta)
2280  Nuv=Mu/Rho
2290  IF Io=1 THEN
2300  Q=Mf*Cp*(To-T1)
2310  PRINT USING "14X,""Heat load (Q)           = "",4D.D,"" (W)""":Q
2320  END IF
2330  IF Io=2 THEN
2340  Mf=Q/(Cp*(To-T1))
2350  PRINT USING "14X,""Coolant mass flow rate = "",Z.4DE,"" (kg/s)""":Mf
2360  END IF
2370  IF Io=3 THEN
2380  Toc=T1+Q/(Mf*Cp)
2390  IF ABS(To-Toc)>.01 THEN
2400  To=(To+Toc)*.5
2410  GOTO 2220
2420  END IF
2430  IF Jj=0 THEN PRINT USING "14X,""Coolant outlet temp     = "",3D.DD,"" (C)""
":To
2440  END IF
2450  IF Jj=0 THEN
2460  PRINT
2470  PRINT USING "10X,""Fluid properties evaluated at "",DD.DD, "" (C) are:""":
Ta
2480  PRINT USING "14X,""Specific heat (Cp)      = "",4D.D,"" (J/kg.K)""":Cp
2490  PRINT USING "14X,""Viscosity (Mu)          = "",Z.4DE,"" (N.s/m^2)""":Mu
2500  PRINT USING "14X,""Thermal cond (k)        = "",Z.4D,"" (W/m.K)""":K
2510  PRINT USING "14X,""Prandtl number (Pr)     = "",Z.3D":Pr
2520  PRINT USING "14X,""Density (Rho)           = "",4D.D,"" (kg/m^3)""":Rho
2530  PRINT USING "14X,""Kinematic vis (Nuv)     = "",Z.4DE,"" (m^2/s)""":Nuv
2540  Beta=FNBeta(Ta)
2550  PRINT USING "14X,""Coef ther exp (Beta)    = "",Z.4DE,"" (1/K)""":Beta
2560  PRINT
2570  PRINT USING "10X,""*** Calculations ***""""
2580  PRINT
2590  PRINT USING "10X,""Preliminary calculations:""""
2600  END IF
2610  Re=4*Mf/(PI*D*Mu)
2620!
2630! Friction Factors for stationary reference
2640  IF Re<2*1.E+4 THEN 2670
2650  F=.184/Re^.2  !I&D Eqn 8.21
2660  GOTO 2690
2670  F=.316/Re^.25  !I&D Eqn 8.20
2680!
2690  Qpp=Q/(PI*D*L)
2700  Qp=Qpp*PI*D
2710  Vm=4*Mf/(Rho*PI*D^2)
2720  Dps=F*Rho*Vm^2*L/(2*D)
2730  Omega=Rpm*2*PI/60
2740  Ro=Vm/(Omega*D)
2750  Jay=Omega*D^2/Nuv  !From STEPH-Rotational Re
2760  Kw=FNKw(Ta)
2770  Dtt=(To-T1)/L
```

```
2780  Gr=R*(Omega 2)*Beta*((D/2) 4)*Dtt/Nuv 2
2790  Ra=Gr*Pr
2800  Gamma=(Re (22/13))*((Gr*(Pr .6)) (-12/13))
2810  Ty=Re/(Gamma^2.5)
2820!
2830! Laminar Value
2840  Nulam=48/11
2850!
2860! Turbulent Value from Dittus-Boelter
2870  Nudb=.023*Re^.8*Pr^.4
2880!
2890! Stephenson Correlation
2900  Nus=(Pr^.4/.367)^.0071*Re^.88*Jay^.023 !Air,Turb-EQN2.23-corrected for wat
er
2910!
2920! Nakayama Correlation for turbulent conditions
2930  Nunak=(Re^.8)*(Pr^.4)*(Tg^(1/30))*(1+.014/(Tg)^(1/6))*.033  ! Eqn 2.9 (Tur
blent)
2940  Ty=Nunak/(Re^.8*Pr^.4)
2950!
2960! Nakayama Correlation for laminar conditions
2970  J2=J*2
2980  Sq=2/11*(1+SQR(1+77/4*(1/Pr^2)))
2990  Cf=1-.486*((3*Sq-1)^.4/(Sq*(Sq*Pr*SQR(5)+2)))*J2/(Ra*Re)^.6
3000  Nunak1=48/11*.191/Sq*(3*Sq-1)^.2*(Ra*Re)^.2*1/(1+(1/10*Sq*Pr))
3010!
3020! Nakayama/Fuzioka Correlation for Radial Pipes
3030  Nunf=(.014/.023)*(Re/Ro^2.5)^.124*Nudb  !TURB-EQN 2.21
3040  Mus=Mu !Temp Value Mus=Mu
3050!
3060! Sieder-Tate Correlation for Turbulent
3070  Nust=.027*Re^.8*Pr^.3333*(Mu/Mus)^.14
3080  Prod=Ra*Re*Pr
3090!
3100! Woods-Morris Correlation for Laminar
3110  Nuwm=.262*Prod^.173*48/11 ! Eqn 2.22-WM3
3120  J1=Jay/8
3130!
3140! Woods-Morris Correlation for Radial Pipes
3150  Nuwm2=.015*Re^.78*J1^.25 !from wm2
3160  IF J;=0 THEN
3170  PRINT USING "14X,""Reynolds number (Re)    = "",Z.3DE":Re
3180  PRINT USING "14X,""Friction factor (stat) = "",Z.3DE":F
3190  PRINT USING "14X,""Heat flux (Qpp)         = "",Z.3DE,"" (W/m^2)""":Qpp
3200  PRINT USING "14X,""Mean fluid vel (Vm)     = "",Z.2DE,"" (m/s)""":Vm
3210  PRINT USING "14X,""RPM                     = "",4D.DD,":Rpm
3220  END IF
3230  IF Ihc=0 THEN PRINTER IS 1
3240  PRINT
3250  IF J;=0 THEN PRINT USING "10X,""Results: """
3260  IF Okplot=0 OR (Okplot=1 AND Nstep<11) THEN
3270  PRINT USING "10X,""     Nudb     Nunak    Nunf     Nuwm      Nus     Nuwm2"""
3280  PRINT USING "13X,6(3D.DD,2X)":Nudb,Nunak,Nunf,Nuwm,Nus,Nuwm2
3290  PRINT USING "14X,""     Ra          Ro      Ra*Re*Pr      Mf          Nak1 """
3300  PRINT USING "14X,4(Z.2DE,2X),3D.DD,DD.DDD,Z.DD":Ra,Ro,Prod,Mf,Nunak1
3310  PRINT USING "14X,""    RaRe      Tg        Ty"""
3320  PRINT USING "13X,D.2DE,2X,Z.3DE,2X,Z.DDD":Ra*Re,Tg,Ty
3330  END IF
3340  IF Okplot=1 THEN
3350  IF Ian=1 THEN Y=Nudb
3360  IF Ian=2 THEN Y=Nunak
```

```
3370  IF Ian=3 THEN Y=Nunf
3380  IF Ian=4 THEN Y=Nuwm
3390  IF Ian=5 THEN Y=Nus
3400  IF Ian=6 THEN Y=Nuwm2
3410  IF Ian=7 THEN Y=Nulam
3420  IF Ian=8 THEN Y=Nunakl
3430  IF Op=2 AND Opx<>2 THEN X=Rpm
3440  IF Op=3 AND Opx<>3 THEN X=Mf
3450  IF Opx=2 OR Opx=3 THEN X=Prod
3460  Jj=Jj+1
3470  CALL Plot(Jj,Jc,Jd,X,Y,Type,Cx)
3480  END IF
3490  IF Op=2 THEN
3500  Rpm=Rpm*10^(Cx/Nstep)
3510  IF Rpm>Rpmh THEN 3590
3520  GOTO 2730
3530  END IF
3540  IF Op=3 THEN
3550  Mf=Mf*10^(Cx/Nstep)
3560  IF Mf>Mfh THEN 3590
3570  GOTO 2040
3580  END IF
3590  BEEP
3600  INPUT "ANOTHER RUN (1=Y,0=N)?",Ir
3610  PRINT "PU"
3620  IF Ir=1 THEN 1350
3630  INPUT "WANT TO LABEL?(1=Y,0=N)",Il
3640  IF Il=1 THEN CALL Label
3650  END
```

```
1000  DEF FNPvst(Tsteam)
1010  DIM K(8)
1020  DATA -7.691234564,-26.08023595,-168.1705546,64.23295504,-119.9546225
1030  DATA 4.16711732,20.9750378,1.25,6
1040  READ K(*)
1050  T=(Tsteam+273.15)/647.3
1060  Sum=0
1070  FOR N=0 TO 4
1080  Sum=Sum+K(N)*(1-T)^(N+1)
1090  NEXT N
1100  Br=Sum/(T*(1+K(5)*(1-T)+K(6)*(1-T)^2))-(1-T)/(K(7)*(1-T)^2+K(8))
1110  Pr=EXP(Br)
1120  P=22120000*Pr
1130  RETURN P
1140  FNEND
1150  DEF FNHfg(T)
1160  Hfg=2477200-2450*(T-10)
1170  RETURN Hfg
1180  FNEND
1190  DEF FNMuw(T)
1200  A=247.8/(T+133.15)
1210  Mu=2.4E-5*10^A
1220  RETURN Mu
1230  FNEND
1240  DEF FNVvst(Tt)
1250  P=FNPvst(Tt)
1260  T=Tt+273.15
1270  X=1500/T
1280  F1=1/(1+T*1.E-4)
1290  F2=(1-EXP(-X))^2.5*EXP(X)/X^.5
1300  B=.0015*F1-.000942*F2-.0004882*X
1310  K=2*P/(461.52*T)
1320  V=(1+(1+2*B*K)^.5)/K
1330  RETURN V
1340  FNEND
1350  DEF FNCpw(T)
1360  Cpw=4.21120858-T*(2.26826E-3-T*(4.42361E-5+2.71428E-7*T))
1370  RETURN Cpw*1000
1380  FNEND
1390  DEF FNRhow(T)
1400  Ro=999.52946+T*(.01269-T*(5.482513E-3-T*1.234147E-5))
1410  RETURN Ro
1420  FNEND
1430  DEF FNPrw(T)
1440  Prw=FNCpw(T)*FNMuw(T)/FNKw(T)
1450  RETURN Prw
1460  FNEND
1470  DEF FNKw(T)
1480  X=(T+273.15)/273.15
1490  Kw=-.92247+X*(2.8395-X*(1.8007-X*(.52577-.07344*X)))
1500  RETURN Kw
1510  FNEND
1520  DEF FNTanh(X)
1530  P=EXP(X)
1540  Q=EXP(-X)
1550  Tanh=(P-Q)/(P+Q)
1560  RETURN Tanh
1570  FNEND
1580  DEF FNHf(T)
```

```
1590  Hf=T*(4.203849-T*(5.88132E-4-T*4.551603'7E-6))
1600  RETURN Hf*1000
1610  FNEND
1620  DEF FNTvap(P)
1630  Tu=110
1640  Tl=10
1650  Ta=(Tu+Tl)*.5
1660  Pc=FNPvst(Ta)
1670  IF ABS((P-Pc)/P)>.001 THEN
1680  IF Pc<P THEN Tl=Ta
1690  IF Pc>P THEN Tu=Ta
1700  GOTO 1650
1710  END IF
1720  RETURN Ta
1730  FNEND
1740  DEF FNBeta(T)
1750  Rop=FNRhow(T+.1)
1760  Rom=FNRhow(T-.1)
1770  Beta=-2/(Rop+Rom)*(Rop-Rom)/.2
1780  RETURN Beta
1790  FNEND
1800  DEF FNAlpha(T)
1810  Alpha=FNKw(T)/(FNRhow(T)*FNCpw(T))
1820  RETURN Alpha
1830  FNEND
1840  DEF FNSigma(T)
1850  Tt=647.3-T
1860  A=.001*Tt^2*(.1160936807/(1+.83*Tt))
1870  B=.001121404688-5.75280518E-6*Tt
1880  C=1.28627465E-8*Tt^2-1.14971929E-11*Tt^3
1890  Sigma=A+B+C
1900  RETURN Sigma
1910  FNEND
```

```
*** Geometric Variables ***
    Tube diameter (D) = 4.763E-03 (m)
    Tube length (L)   =    .22 (m)
    L/D               =   172.6
    Rotor radius (R)  = 0.402 (m)

Computed values are:

*** Operating Variables ***

Input variables are:
    Heat load              =   50.00 (W)
    Coolant inlet temp     = 45.00 (C)
    Coolant outlet temp    = 45.72 (C)
    Coolant mass flow rate = 1.6329E-02 (kg/s)

Fluid properties evaluated at 45.36 (C) are:
    Specific heat (Cp)     = 4224.7 (J/kg.K)
    Viscosity (Mu)         = 5.8661E-04 (N.s/m^2)
    Thermal cond (k)       = 0.6380 (W/m.K)
    Prandtl number (Pr)    = 3.884
    Density (Rho)          =  990.0 (kg/m^3)
    Kinematic vis (Nuv)    = 5.9255E-07 (m^2/s)
    Coef ther exp (Beta)   = 4.1266E-04 (1/K)

*** Calculations ***

Preliminary calculations:
    Reynolds number (Re)   = 7.441E+03
    Friction factor (stat) = 3.402E-02
    Heat flux (Qpp)        = 4.060E+03 (W/m^2)
    Mean fluid vel (Vm)    = 9.26E-01 (m/s)
    RPM                    = 3600.00

Results:
    Nudb     Nunak     Nunf     Nuwm      Nus     Nuwm2
    49.52    55.30   111.80    31.56    44.84   102.34
      Ra        Ro      Ra*Re*Pr       Mf        Nak1
    7.39E+03  5.16E-01  2.14E+08  1.63E-02    44.90
      RaRe       Tg        Tv
   5.50E+07  7.506E-05  0.026
```

APPENDIX C

THERMOSYPHON ANAIYSIS (COMPUTER PROGRAM AND RESULTS)

The following program was written to give the results of the correlation for the heat transfer for the rotating, closed-loop thermosyphon discussed in Chapter III. It was written in HP-Basic for the HP-9826 computer. Sub-programs for the graphics and the thermophysical properties are not shown. A sample run is included immediately following the listing.

```
1000! FILE NAME:     IHSY
1010! CREATED:       Feburary 26, 1988
1020!
1030  COM /Cmin/ Xmin,Ymin,Sfx,Sfy
1040  PRINTER IS 1
1050  BEEP
1060  PRINT USING "2X,""Default values: """
1070  D=4.763E-3      ! Tube diameter    (m)
1080  L=.8230         ! Tube length      (m)
1090  R=.4021         ! Radius of rotor (m)
1100  Kff=0           ! Friction Factor for bends
1110  Lt=2*L+2*R
1120  PRINT USING "4X,""Tube diameter    = "",Z.4DE,"" (m)""":D
1130  PRINT USING "4X,""Tube length      = "",DD.D,"" (m)""":L
1140  PRINT USING "4X,""Ckt Length (Lt) = "",DD.D,"" (m)""":Lt
1150  PRINT USING "4X,""Radius of rotor = "",Z.3D,"" (m)""":R
1160  BEEP
1170  INPUT "OK TO ACCEPT DEFAULT VALUES (1=Y,0=N)?",Id
1180  BEEP
1190  INPUT "LIKE A HARD COPY (1=Y,0=N)?",Ihc
1200  IF Ihc=1 THEN PRINTER IS 701
1210  IF Id=1 THEN 1280
1220  BEEP
1230  INPUT "ENTER TUBE DIAMETER (m)",D
1240  BEEP
1250  INPUT "ENTER TUBE LENGTH (m)",L
1260  BEEP
1270  INPUT "ENTER RADIUS OF ROTOR (m)",R
1280  PRINT USING "10X,""*** Geometric Variables *** """
1290  PRINT USING "14X,""Tube diameter (D) = "",Z.3DE,"" (m)""":D
1300  PRINT USING "14X,""Tube length (L)   = "",DD.DD,"" (m)""":L
1310  PRINT USING "14X,""Ckt length (Lt)   = "",DD.DD,"" (m)""":Lt
1320  PRINT USING "14X,""L/D               = "",5D.D":L/D
1330  PRINT USING "14X,""Rotor radius (R)  = "",Z.3D,"" (m)""":R
1340  PRINT
1350  PRINT USING "10X,""Computed values are: """
1360  PRINTER IS 1
1370  BEEP
1380  PRINT USING "2X,""SELECT OPTION:"""
1390  PRINT USING "4X,""1  Single point"""
1400  PRINT USING "4X,""2  Nu versus RPM"""
1410  INPUT Op
1420  IF Op>1 THEN
1430  BEEP
1440  Jj=0
1450  PRINTER IS 1
1460  INPUT "LIKE TO PLOT (1=Y,0=N)?",Okplot
1470  BEEP
1480  INPUT "Nudb=1,Nunak1=2,Nuwm=3,Nus=4,Nul=5",Ian
1490  IF Okplot=1 THEN
1500  CALL Plot(Jj,X,Y,Dt,Tc)
1510  INPUT "LIKE A LABEL?(1=Y,0=N)",Il
1520  IF Il=1 THEN CALL Label
1530  END IF
1540  END IF
1550  Nstep=11
1560  IF Op=2 THEN
1570  BEEP
1580  INPUT "ENTER RPM RANGE (MIN,MAX)",Rpmi,Rpmn
```

```
1590  Rpm=Rpm1
1600  ELSE
1610  BEEP
1620  INPUT "ENTER RPM OR RETURN",Rpm
1630  END IF
1640  BEEP
1650  IF Ihc=1 THEN PRINTER IS 701
1660  IF Ihc=0 THEN PRINTER IS 1
1670  PRINT
1680  PRINT USING "10X,""*** Operating Variables *** """
1690  PRINT
1700  PRINT USING "10X,""Input variables are: """
1710  BEEP
1720  INPUT "ENTER HEAT LOAD (W)",Q
1730  PRINT USING "14X,""Heat load              = "",4D.DD,""  (W)""":Q
1740  BEEP
1750  INPUT "ENTER COLD SIDE TEMP (C)",Tc
1760  PRINT USING "14X,""Cold side temp         = "",4D.DD,"" (C)""":Tc
1770  Dt=5
1780  Th=Tc+Dt
1790  Ta=(Tc+Th)*.5
1800  Dtt=Dt/L
1810  PRINT
1820  Cp=FNCpw(Ta)
1830  Mu=FNMuw(Ta)
1840  K=FNKw(Ta)
1850  Pr=FNPrw(Ta)
1860  Rho=FNRhow(Ta)
1870  Nuv=Mu/Rho
1880  Beta=FNBeta(Ta)
1890  Omega=Rpm*2*PI/60
1900  Th=Tc+Dt
1910  Ta=Tc+Dt/2
1920  PRINTER IS 1
1930  PRINT "TA = ",Ta
1940  Rhoh=FNRhow(Th)
1950  PRINT "RHOH=",Rhoh
1960  Rhoc=FNRhow(Tc)
1970  PRINT "RHOC=",Rhoc
1980  Rhom=FNRhow(Ta)
1990  Drho=Rhoc-Rhoh
2000  IF Drho<0 THEN GOTO 3140
2010  PRINT "dro=",Drho
2020  Mu=FNMuw(Ta)
2030  Cp=FNCpw(Ta)
2040  Beta=FNBeta(Ta)
2050  Pr=FNPrw(Ta)
2060  Nuv=Mu/Rhom
2070  PRINT "MU,CP  =",Mu,Cp
2080  Mf=Q/(Cp*Dt)
2090  Re=4/PI*Mf/(Mu*D)
2100  Gr=R*(Omega^2)*Beta*((D/2)^4)*Dtt/Nuv^2
2110  Ra=Gr*Pr
2120  Prod=Ra*Re*Pr
2130  Nuwm=.262*Prod^.173*48/11
2140  Dtwp=Q/(K*Nuwm*PI*L)
2150  PRINT "DTWP =",Dtwp
2160  Dtw=Dtwp
2170  Grr=R*Omega^2*Beta*D^3*Dtw/Nuv^2
2180  Nu=Pr/Grr*Lt/R*D/L*Rhom/Rhoh*(Kff+(256/Re*Lt/D))*Re^3
2190  Dtwc=Q/(PI*L*K*Nu)
```

```
2200  IF ABS(Dtuc-Dtw)>.10 THEN
2210  IF Rpm>3000 THEN
2220  Dt=Dt+.5
2230  GOTO 1900
2240  END IF
2250  IF Rpm>1000 THEN
2260  Dt=Dt+1
2270  GOTO 1900
2280  END IF
2290  IF Rpm>500 THEN
2300  Dt=Dt+1.5
2310  GOTO 1900
2320  END IF
2330  IF Rpm>=300 THEN
2340  Dt=Dt+4
2350  GOTO 1900
2360  END IF
2370  END IF
2380  Vm=4*Mf/(Rhom*PI*D^2)
2390  Ro=Vm/(Omega*D)
2400  Jay=Omega*D^2/Nuv  !From STEPH-Rotational Re
2410  Dtt=(Th-Tc)/L
2420  Gr=R*(Omega^2)*Beta*((D/2)^4)*Dtt/Nuv^2
2430  Ra=Gr*Pr
2440!
2450! Laminar Value
2460  Nulam=48/11
2470!
2480! Turbulent Value from Dittus-Boelter
2490  Nudb=.023*Re^.8*Pr^.4
2500!
2510! Stephenson Correlation
2520  Nus=(Pr^.4/.867)*.0071*Re^.88*Jay^.023 !Air,Turb-EQN2.23-corrected for wat
er
2530!
2540! Nakayama Correlation for laminar conditions
2550  J2=J*2
2560  Sq=2/11*(1+SQR(1+77/4*(1/Pr^2)))
2570  Cf=1-.486*((3*Sq-1)^.4/(Sq*(Sq*Pr+SQR(5)+2)))*J2/(Ra*Re)^.6
2580  Nunakl=48/11*.191/Sq*(3*Sq-1)^.2*(Ra*Re)^.2*1/(1+(1/10*Sq*Pr))
2590  Mus=Mu !Temp Value Mus=Mu
2600  Prod=Ra*Re*Pr
2610!
2620! Woods-Morris Correlation for Laminar
2630  Nuwm=.262*Prod^.173*48/11 ! Eqn 2.22-WM3
2640  J1=Jay/8
2650!
2660! Woods-Morris Correlation for Radial Pipes
2670  Nuwm2=.015*Re^.78*J1^.25 !from wm2
2680  IF Ihc=0 THEN
2690  PRINTER IS 1
2700  ELSE
2710  PRINTER IS 701
2720  END IF
2730  IF Jj=0 THEN
2740  IF Jj=0 THEN PRINT USING "10X,""Results: """
2750  PRINT USING "10X,""Fluid properties evaluated at "",DDD.DD,"" (C) are:""":
Ta
2760  PRINT USING "14X,""Specific heat (Cp)      = "",4D.DE,""(J/kg.K)""":Cp
2770  PRINT USING "14X,""Viscosity (Mu)          = "",Z.4DE,"" (N.s/m^2)""":Mu
```

```
2780  PRINT USING "14X,""Thermal cond (k)        = "",Z.4D,"" (w/m.k)""";k
2790  PRINT USING "14X,""Prandtl number (Pr)     = "",Z.3DE";Pr
2800  PRINT USING "14X,""Density (Rho)           = "",4D.2D,"" kg/m 3)""";Rho
2810  PRINT USING "14X,""Kinematic visc (Nu)     = "",Z.4DE,"" (m^2/s)""";Nuv
2820  PRINT USING "14X,""Coef therm exp(beta)    = "",Z.4DE,"" (1/K)""";Beta
2830  PRINT USING "14X,""Reynolds number (Re)    = "",Z.3DE";Re
2840  PRINT USING "14X,""Mean fluid vel (Vm)     = "",Z.2DE,"" (m/s)""";Vm
2850  PRINT USING "14X,""Mass flow rate          = "",Z.2DE,"" (kg/s)""";Mf
2860  PRINT USING "14X,""Temperature (hotside)   = "",DDD.DD,""(C)""";Th
2870  PRINT USING "14X,""RPM                     = "",DDDDD.,";Rpm
2880  END IF
2890  PRINT
2900  IF Okplot=0 OR (Okplot=1 AND Nstep<11) THEN
2910  PRINT USING "10X,""    Nudb     Nunak1    Nuwm      Nus      """"
2920  PRINT USING "13X,6(3D.DD,2X)":Nudb,Nunak1,Nuwm,Nus
2930  PRINT USING "14X,""    Ra         Ro      Ra*Re*Pr      Mf      """"
2940  PRINT USING "14X,4(Z.2DE,2X),3D.DD":Ra,Ro,Prod,Mf
2950  END IF
2960  IF Okplot=1 THEN
2970  IF Ian=1 THEN Y=Nudb
2980  IF Ian=2 THEN Y=Nunak1
2990  IF Ian=3 THEN Y=Nuwm
3000  IF Ian=4 THEN Y=Nus
3010  IF Ian=5 THEN Y=(48/11)
3020  X=Rpm
3030  Jj=Jj+1
3040  CALL Plot(Jj,X,Y,Dt,Tc)
3050  PRINTER IS 1
3060  END IF
3070  IF Op=2 THEN
3080  Dt=5
3090  Rpm=Rpm+10^.1*
3100  IF Rpm>Rpmh THEN 3130
3110  GOTO 1890
3120  END IF
3130  BEEP
3140  INPUT "ANOTHER RUN (1=Y,0=N)?",Ir
3150  PRINT "PU"
3160  IF Ir=1 THEN 1360
3170  INPUT "WANT TO LABEL?(1=Y,0=N)",Il
3180  IF Il=1 THEN CALL Label
3190  END
```

*** Geometric Variables ***
Tube diameter (D) = 4.763E-03 (m)
Tube length (L) = .82 (m)
Ckt length (Lt) = 2.45 (m)
L/D = 172.8
Rotor radius (R) = 0.402 (m)

Computed values are:

*** Operating Variables ***

Input variables are:
Heat load = 50.00 (W)
Cold side temp = 45.00 (C)

Results:
Fluid properties evaluated at 62.75 (C) are:
Specific heat (Cp) = 4310.1E+00(J/kg.K)
Viscosity (Mu) = 4.4172E-04 (N.s/m 2)
Thermal cond (k) = 0.6404 (W/m.k)
Prandtl number (Pr) = 2.902E+00
Density (Rho) = 989.1 9kg/m 3)
Kinematic vis (Nuv) = 4.4991E-07 (M'2/S)
Coef therm exp(Beta) = 5.3940E-04 (1/K)
Reynolds number (Re) = 1.978E+02
Mean fluid vel (Vm) = 1.87E-02 (m/s)
Mass flow rate = 3.27E-04 (kg/s)
Temperature (hotside) = 80.50(C)
RPM = 3600.

Nudb	Nunair	Nuwm	Nus
2.42	51.80	34.41	1.65

Ra	Ro	Ra*Re*Pr	Mf
6.13E+05	1.04E-02	3.52E+08	3.27E-04

APPENDIX D

CLOSED TWO-PHASE THERMOSYPHON ANALYSIS (COMPUTER PROGRAM AND RESULTS)

The following program was written to give the results of the correlations for the sonic, boiling, and condensing limits as discussed in Chapter IV. It was written in HP-Basic for the HP-9826 computer. Sub-programs for the graphics and the thermophysical properties are not shown. A sample run is included immediately following the listing.

```
1000! FILE NAME:     HEAT
1010! DATE:          March 5, 1986
1020! LAST REVISED: March 10, 1986
1030! 2170.CALCS: 4000.PLOT: 5250.FNS: 6100.LABEL:
1040!
1050  COM /Cmin/ Xmin,Ymin,Sfx,Sfy
1060  PRINTER IS 1
1070  BEEP
1080  PRINT USING "2X,""Default values: """
1090  D=4.762E-3     ! Tube diameter    (m)
1100  Le=.6223/2     ! Tube length(Evap)(m)
1110  Lc=.5*Le
1120  L=Le+Lc
1130  R=.402         ! Radius of rotor (m)
1140  PRINT USING "4X,""Tube diameter     = "",Z.4DE,"" (m)""";D
1150  PRINT USING "4X,""Tube length(Evap)= "",DD.D,"" (m)""";Le
1160  PRINT USING "4X,""Tube Length(Cond)= "",DD.D,"" (m)""";Lc
1170  PRINT USING "4X,""Radius of rotor  = "",Z.3D,"" (m)""";R
1180  BEEP
1190  INPUT "OK TO ACCEPT DEFAULT VALUES (1=Y,0=N)?",Ic
1200  BEEP
1210  INPUT "LIKE A HARD COPY (1=Y,0=N)?",Ihc
1220  IF Ihc=1 THEN
1230  PRINTER IS 701
1240  ELSE
1250  PRINTER IS 1
1260  END IF
1270  IF Ic=1 THEN 1360
1280  BEEP
1290  INPUT "ENTER TUBE DIAMETER (m)",D
1300  BEEP
1310  INPUT "ENTER TUBE LENGTH(Evap) (m)",Le
1320  BEEP
1330  INPUT "ENTER TUBE LENGTH(Cond) (m)",Lc
1340  BEEP
1350  INPUT "ENTER RADIUS OF ROTOR (m)",R
1360  PRINT USING "10X,""*** Geometric Variables *** """
1370  PRINT USING "14X,""Tube diameter (D) = "",Z.3DE,"" (m)""";D
1380  PRINT USING "14X,""Tube length(Evap) (Le)  = "",Z.3D,"" (m)""";Le
1390  PRINT USING "14X,""Tube length(Cond) (Lc)  = "",Z.3D,"" (m)""";Lc
1400  PRINT USING "14X,""Rotor radius (R)        = "",Z.3D,"" (m)""";R
1410  PRINT
1420  PRINTER IS 1
1430  BEEP
1440  PRINT USING "2X,""SELECT OPTION:"""
1450  PRINT USING "4X,""1  Q versus %Fill"""
1460  PRINT USING "4X,""2  ??????????"""
1470  INPUT Op
1480  IF Op>1 THEN
1490  BEEP
1500  PRINTER IS 1
1510  PRINT USING "4X,""NOT IMPLEMENTED YET"""
1520  GOTO 1440
1530  ELSE
1540  BEEP
1550  G=0
1560  Jr=0
1570  Pct=.
1580  INPUT "LIKE TO PLOT (1=Y,0=N)?",Okplot
```

```
1590   IF [illegible] THEN
1600   CALL Plot(Jj,Cc,Ca,X,Y,Type,Cx)
1610   Jj=1
1620   BEEP
1630   INPUT "1=SOLID,2=DASH-DASH,3=[illegible]",Type
1640   END IF
1650  END IF
1660  Nstep=100
1670  BEEP
1680  INPUT "ENTER OPTION (1=S,2=E,3=B,4=C)",Io
1690  IF Io=2 THEN
1700  BEEP
1710  INPUT "1=WALLIS,2=JASTER",Ie
1720  END IF
1730  IF Ihc=1 THEN PRINTER IS 701
1740  IF Ihc=0 THEN PRINTER IS 1
1750  BEEP
1760  INPUT "ENTER Tsat (C)",Tsat
1770  PRINT USING "14X,""Tsat(C)                     = "",DDD.D";Tsat
1780  BEEP
1790  INPUT "ENTER RPM",Rpm
1800  PRINT USING "14X,""RPM                         = "",4D";Rpm
1810  BEEP
1820  INPUT "ENTER COND. WALL TEMPERATURE",Tw
1830  PRINT USING "14X,""T wall                      = "",DDD.D";Tw
1840  At=PI*D^2/4
1850  Tsatk=Tsat+273.15
1860  Cp=FNCpw(Tsat)
1870  Mul=FNMuw((Tsat+Tw)/2)
1880  Muv=FNMuv(Tsat)
1890  K=FNKw(Tsat)
1900  Pr=FNPrw(Tsat)
1910  Rhol=FNRhow(Tsat)
1920  Hfg=FNHfg(Tsat)
1930  Beta=FNBeta(Tsat)
1940  Sigma=FNSigma(Tsat)
1950  Rhov=1/FNVvst(Tsat)
1960  Nuv=Muv/Rhov
1970  Rsn=1.327
1980  Cv=Cp/Rsn
1990  Rgc=461.52  ! (J/kg.K)
2000  Omega=Rpm*2*PI/60
2010  Accel=Omega^2*R
2020  IF Jj=0 THEN
2030  PRINT
2040  PRINT USING "10X,""Fluid properties evaluated at "",DDD.DD,"" (C) are:""""
 ";Tsat
2050  PRINT USING "14X,""Specific heat (Cp)      = "",4D.D,"" (J/kg.K)"""";Cp
2060  PRINT USING "14X,""Ratio of Specific Heats= "",D.DDD";Rsn
2070  PRINT USING "14X,""Viscosity (Mu)          = "",Z.4DE,"" (N.s/m^2)"""";Mul
2080  PRINT USING "14X,""Thermal cond (k)        = "",Z.4D,"" (W/m.K)"""";K
2090  PRINT USING "14X,""Prandtl number (Pr)     = "",Z.3D";Pr
2100  PRINT USING "14X,""Enthalpy (Hfg)          = "",Z.4DE";Hfg
2110  PRINT USING "14X,""Density (Rhol)          = "",4D.D,"" (kg/m^3)"""";Rhol
2120  PRINT USING "14X,""Density (Rhov)          = "",Z.4D,"" (kg/m^3)"""";Rhov
2130  PRINT USING "14X,""Coef ther exp (Beta)    = "",Z.4DE,"" (1/K)"""";Beta
2140  PRINT USING "14X,""Omega                   = "",4D.D,"" (1/s)"""";Omega
2150  PRINT USING "14X,""Surface Tension         = "",Z.4DE,""  (N/m)"""";Sigma
2160  END IF
2170!
2180! PCF = KFILL
```

```
2190!
2200  M=Rho.*Lt*Pi*Rs^2*100*9.2^3
2210  Av=(M/(Lt*(Rhov-Rhol)))-((Rhol/(Rhov-Rhol))*At)
2220!
2230! SONIC CALCULATION
2240  IF Io=1 THEN
2250  IF Jj=0 THEN
2260  PRINT
2270  PRINT USING "10X,""Sonic Limit Calculations:"""
2280  PRINT USING "10X,""% Fill     Total Heat"""
2290  END IF
2300  Qm=Rhov*Hfg*(M/(Lt*(Rhov-Rhol))-Rhol/(Rhov-Rhol)*At)*SQR(Rgc*Tsatk)
2310  Mf=Qm/Hfg
2320  X=Pcf
2330  Y=Qm
2340  IF Qm<=0 THEN GOTO 2400
2350  IF Qkplot=1 THEN
2360  CALL Plot(Jj,Jc,Jd,X,Y,Type,Cx)
2370  ELSE
2380  PRINT USING "12X,3D.3X,Z.3DE":Pcf,Qm
2390  END IF
2400  IF Pcf>=100 THEN GOTO 3730
2410  IF Qkplot=1 THEN
2420  Pcf=Pcf*10^.02
2430  ELSE
2440  Pcf=Pcf+1
2450  Jj=Jj+1
2460  END IF
2470  GOTO 2200
2480  END IF
2490!
2500! ENTRAINMENT CALCULATIONS
2510  IF Io=2 THEN
2520!
2530  IF Jj=0 THEN
2540  PRINT
2550  PRINT USING "10X,""Entraining Limit Claculations:"""
2560  PRINT USING "10X,""% Fill     Total Heat"""
2570  END IF
2580! WALLIS CORRELATION J*=.25
2590  IF Ie=1 THEN
2600  IF Av=0 THEN GOTO 2990
2610  Jv=.25/Rhov^.5*(Omega^2*R*D*(Rhol-Rhov))^.5
2620  Qm=Rhov*Jv*At*Hfg
2630  END IF
2640!
2650! JASTER CORRELATION
2660  IF Ie=2 THEN
2670  IF Pcf=0 THEN Pcf=1
2680  T1=(1/(1-(Pcf/100)))-1
2690! T1=(1/(Pcf/100))-1
2700  T2=T1*(Rhol/Rhov)^(2/3)
2710  IF T1<0 THEN 2990
2720  Xx2=(Mul/Muv)^.25*T1^1.75*(Rhol/Rhov)^((2/3)*1.75-1)
2730  Xx=1/(1+T2)
2740! Xx=.5
2750! Xx2=(Mul/Muv)^.25*Rhov/Rhol
2760  IF G=0 THEN G=1
2770  Rel=(1-Xx)*(G*D/Mul)
2780  Rev=Xx*G*D/Muv
2790  Fv=.079/Rev^.25
```

```
2800  IF Re<=1250 THEN Cd=80/(Re^.5)
2810  IF Re>1250 THEN Cd=.0504*(Re)^.375
2820  Num=10*SQR(2)*(Rhol*Rhov)^1.5*Mu^2*Qc*Omega^2*R
2830  Den=(1+Xx^2)^.25)^5*Rhol*(Rhol-Rhov)^2)
2840  Gc=(Num/Den)^(1/3)
2850  IF ABS((G-Gc)/Gc)>.01 THEN
2860  G=(G+Gc)/2
2870  GOTO 2760
2880  END IF
2890  Qm=Xx*G*At*Hfg
2900  END IF
2910  X=Pcf
2920  Y=Qm
2930  IF Qm<=0 THEN GOTO 2990
2940  IF Okplot=1 THEN
2950  CALL Plot(Jj,Jc,Jd,X,Y,Type,Cx)
2960  ELSE
2970  PRINT USING "12X,3D.3X,Z.4DE,4X,Z.3DE":Pcf,Qm,G
2980  END IF
2990  IF Pcf>=100 THEN GOTO 3730
3000  IF Okplot=1 THEN
3010  Pcf=Pcf*10^.02
3020  ELSE
3030  Pcf=Pcf+10
3040  END IF
3050  Jj=Jj+1
3060  IF Ie=2 THEN GOTO 2580
3070  IF Ie=1 THEN GOTO 2200
3080  END IF
3090!
3100! BOILING CALCULATIONS
3110  IF Io=3 THEN
3120  IF Jj=0 THEN
3130  PRINT
3140  PRINT USING "10X,""Boiling Limit Calculations:"""
3150  PRINT USING "10X,""% Fill     Total Heat        QDP"""
3160  END IF
3170  IF Pcf>100 THEN GOTO 3730
3180  Ab=D*Le*ACS(1-Pcf/50)
3190  Qm=Ab*.13*Rhov^.5*Hfg*(Omega^2*R*(Rhol-Rhov)*Sigma)^.25
3200  X=Pcf
3210  Y=Qm
3220  IF Qm<=0 THEN 3280
3230  IF Okplot=1 THEN
3240  CALL Plot(Jj,Jc,Jd,X,Y,Type,Cx)
3250  ELSE
3260  PRINT USING "12X,3D.3X,Z.4DE,3X,Z.4DE":Pcf,Qm,Qm/Ab
3270  END IF
3280  IF Pcf>100 THEN GOTO 3730
3290  Jj=Jj+1
3300  IF Okplot=1 THEN
3310   Pcf=Pcf*10^.02
3320   ELSE
3330   Pcf=Pcf+1
3340  END IF
3350  GOTO 2200
3360  END IF
3370!
3380! CONDENSATION CALCULATIONS
3390  IF Io=4 THEN
```

```
3400  IF Jj=0 THEN
3410  PRINT
3420  PRINT USING "10X,""Condensing Limit Calculations:"""
3430  PRINT USING "10X,""% Fill     Total Heat"""
3440  END IF
3450  Dt=Tsat-Tw
3460  Hfgp=Hfg*(1+.68*(Cp*Dt/Hfg))
3470  Tgg=(Rhol*(Rhol-Rhov)*Omega^2*R*Hfgp*K^3/(U*Mul*Dt))^.25
3480  DEG
3490  Phi=180-ACS(1-(Pcf/50))
3500  IF Phi>=0 AND Phi<=110 THEN F=FNF1(Phi)
3510  IF Phi>110 AND Phi<=150 THEN F=FNF2(Phi)
3520  IF Phi>150 AND Phi<=180 THEN F=FNF3(Phi)
3530  IF Phi>180 THEN PRINT "ERROR,PHI>180!!!"
3540  RAD
3550  Qm=Av*Dt*F*Tgg
3560  X=Pcf
3570  Y=Qm
3580  IF Qm<=0 THEN GOTO 3700
3590  IF Okplot=1 THEN
3600  CALL Plot(Jj,Jc,Jd,X,Y,Type,Cx)
3610  ELSE
3620  PRINT USING "12X,3D.8X,3D.D":Pcf,Qm
3630  END IF
3640  IF Okplot=1 THEN
3650  Pcf=Pcf*10^.02
3660  ELSE
3670  Pcf=Pcf+1
3680  END IF
3690  Jj=Jj+1
3700  IF Pcf>=100 THEN GOTO 3730
3710  GOTO 2200
3720  END IF
3730  BEEP
3740  INPUT "ANOTHER RUN (1=Y,0=N)?",Ir
3750  IF Ir=1 THEN 1200
3760  BEEP
3770  INPUT "WANT TO LABEL?(1=Y,0=N)",Il
3780  IF Il=1 THEN CALL Label
3790  END
```

*** Geometric Variables ***
Tube diameter (D) = 4.750E-03 (m)
Tube length(Evap) (Le) = .4[illegible] (m)
Tube length(Cond) (Lc) = .2[illegible] (m)
Rotor radius (R) = 0.402 (m)

Tsat(C)= 80
RPM = 3600
T wall= 45

Fluid properties evaluated at 80.00 (C) are:
Specific heat (Cp) = 4451.9 (J/kg.K)

Ratio of Specific Heats= 1.327
Viscosity (Mu) = 4.4336E-04 (N.s/m 2)
Thermal cond (k) = 0.6638 (W/m.K)
Prandtl number (Pr) = 2.319
Enthalpy (Hfg) = 2.3057E+06
Density (Rhol) = 971.8 (kg/m^3)
Density (Rhov) = .3 (kg/m 3)
Coef ther exp (Beta) = 6.4578E-04 (1/K)
Omega = 377.0 (1/S)
Surface Tension = 7.7048E-02 (N/m)

Condensing Limit Calculations:

% Fill	Total Heat
1	66.1
2	64.7
3	63.4
4	62.2
5	61.1
6	60.1
7	58.1
8	56.8
9	55.5
10	54.4
11	53.2
12	52.1
13	51.0
14	49.9
15	48.9
16	47.9
17	46.9
18	45.9
19	45.0
20	44.0
21	43.1
22	42.2
23	41.3
24	40.5
25	39.6
26	38.8
27	37.9
28	37.1
29	36.3
30	35.5
31	34.7
32	33.9
33	33.4
34	32.5
35	31.7
36	30.8
37	30.0
38	29.2
39	28.4
40	27.6
41	26.9
42	26.1
43	25.4
44	24.6
45	23.9
46	23.2
47	22.5
48	21.8

49	[illegible]
50	20.4
51	[illegible]
52	[illegible]
53	[illegible]
54	17.9
55	17.2
56	[illegible]
57	16.0
58	15.4
59	14.9
60	14.3
61	[illegible]
62	[illegible]
63	12.6
64	[illegible]
65	11.6
66	11.1
67	10.6
68	10.1
69	9.6
70	9.1
71	[illegible]
72	8.2
73	7.7
74	7.3
75	[illegible]
76	6.5
77	[illegible]
78	5.6
79	[illegible]
80	[illegible]
81	[illegible]
82	[illegible]
83	[illegible]
84	[illegible]
85	[illegible]
86	[illegible]
87	[illegible]
88	[illegible]
89	[illegible]
90	[illegible]
91	[illegible]
92	[illegible]
93	[illegible]
94	[illegible]
95	[illegible]
96	[illegible]
97	[illegible]
98	[illegible]
99	[illegible]

LIST OF REFERENCES

1. Kane, J.R., General Considerations in Marine Engineering, in Marine Engineering, R.L. Harrington, editor, SNAME, New York, 1971

2. Jacobsen, W.E., Electric Propulsion Drives, in Marine Engineering, R.L. Harrington, editor, SNAME, New York, 1971

3. Rueter, W., Weiler, D.J., Keane, Jr., R.G., "Naval Ship Design: Past, Present, and Future," SNAME 1979 Spring Meeting/STAR Symposium, Houston, TX, April 1979

4. Harrington, R.L., "Economic Considerations in Shipboard Design Trade-off Studies," Marine Technology, April 1969

5. Gott, E., Svensson, S.O., "Gas Turbine Propulsion- An Engineering Comparison of Mechanical Versus Electric Drive," ASME paper 74-GT-34, 1974

6. Robinson, S.M., Electric Ship Propulsion, Simmons-Boardman, 1922

7. Naval Sea Systems Command, extracts from the Electric Drive presentation to OPNAV, June 1983

8. Skilling, H.H., Electromechanics, Wiley, 1962

9. Luke, G.E., "Surface Heat Transfer in Electric Machines with Forced Air Flow," presented to A.I.E.E. Annual Meeting, June, 1926

10. Kostikov, O.N., Malykhin, E.I., Us, Z.P., Yakovlev, A.I., "Influence of Internal Heat Transfer on the Thermal State of Totally Enclosed Low-Power Electric Motors," Elektrotekhnika, v. 50, #9, 1979

11. Morton, B.R., "Laminar Convection in Uniformly Heated Horizontal Tubes at Low Rayliegh Numbers," Q.Jl.Mech.Appl.Math., 1959, v 12, pp 410-420

12. Kays, W.M., "Numerical Solutions for Laminar-Flow Heat Transfer in Circular Tubes," Trans. Amer. Soc. Mech. Engrs., 1955, v 77, p 1265

13. Kreith, F., "Convection Heat Transfer in Rotating Systems," Recent Advances in Heat Transfer, 1968, v 5, p 129

14. Morris, W.D., "Laminar Convection in a Heated Vertical Tube Rotating about a Parallel Axis," J. Fluid Mech., 1965, v 21 pt 3, p 453

15. Mori, Y., Nakayama, W., "Convective Heat Transfer in Rotating Radial Circular Pipes (1st Report, Laminar Region)," Int. J. Heat Mass Transfer, 1968, v 11, pp 1027-1040

16. Mori, Y., Fukada, T., Nakayama, W., "Convective Heat Transfer in a Rotating Radial Circular Pipe (2nd Report, Turbulent Region)," Int. J. Heat Mass Transfer, 1971, v 14, pp 1807-1824

17. Ito, H., Nanbu, K., "Flow in Rotating Straight Pipes of Circular Cross Section," Journal of Basic Engineering, September 1971, pp 383-394

18. Kuo, C.Y., Iida, H.T., Taylor, J.H., Kreith, F., "Heat Transfer in Flow Through Rotating Ducts," Journal of Heat Transfer, 1960, v 82, p 139

19. Taylor, G.I., "Stability of a Viscous liquid contained between two rotating cylinders," Phil. Trans., 1923, v 223 (Series A), p 289

20. Taylor, G.I., "Fluid Friction between two rotating cylinders," Proc. Royal Society, 1936, v 157 (Series A), p 561

21. Oliver, D.R., "The effect of convection on viscous-flow heat transfer in horizontal tubes," Chem. Eng. Sci., 1962, v 17, pp 335-350

22. Colburn, A.P., "A Method of Correlating Forced Convection Heat Transfer Data and a Comparison with Fluid Friction," Trans. Amer. Inst. Chem. Eng., 1933, Vol 29, p 174

23. Martinelli, R.C., Southwell, C.J., Alves, G., Craig, H.L., Weinberg, E.B., Lansing, N.F., Boelter, L.M.K., "Heat Transfer and Pressure Drop for a Fluid Flowing in the Viscous Region Through a Vertical Pipe," Trans. Amer. Inst. Chem. Eng., 1942, v 38, p 493

24. Pattenden, R.F., "Heat Transfer from a Rotating Tube with Controlled Fluid Flow," Journal Mech. Engng. Science, 1960, v 6, #2, p 144

25. Mori, Y., Futagami, K., Tokuda, S., Nakamura, M., "Forced Convective Heat Transfer in Uniformly Heated Horizontal Tubes," Int. J. Heat Mass Transfer, 1966, v 9, pp 453-463

26. Mori, Y., Nakayama, W. "Study on forced convective heat transfer in curved pipes (1st Report, laminar region)," Int. J. Heat Mass Transfer, 1965, v 8, p 67

27. Mori, Y., Nakayama, W. "Study on forced convective heat transfer in curved pipes (2nd Report, Turbulent region)," Int. J. Heat Mass Transfer, 1967, v 10, p 37

28. Mori, Y., Nakayama, W., "Forced Convective Heat Transfer in a Straight Pipe Rotating Around a Parallel Axis (1st Report, Laminar Region)" Int. J. Heat Mass Transfer, 1967, v 10, pp 1179-1194

29. Nakayama, W.,"Forced Convective Heat Transfer in a Straight Pipe Rotating Around a Parallel Axis (2nd Report, Turbulent Region)," Int. J. Heat Mass Transfer, 1968, v 11, pp 1185-1201

30. Siegwarth, D.P., Mikesell, R.D., Readal, T.C., Hanratty, T.J., "Effect of Secondary Flow on the Temperature Field and Primary Flow in a Heated Horizontal Tube," Int. J. Heat Mass Transfer, 1969, v 12, pp 1535-1552

31. Woods, J.L., Morris, W.D., "A Study of Heat Transfer in a Rotating Cylindrical Tube," Journal of Heat Transfer, 1980, v 102, p 612

32. Morris, W.D., Woods, J.L., "Heat Transfer in the Entrance Region of Tubes that Rotate about a Parallel Axis," Journal of Mech. Engng. Science, 1978, v 20, #6, p 319

33. Davidson, D.F., "Heat Transfer Rig for Hydorgen-cooled Generator Field Windings," Proc. Instn. Mech. Engrs., 1969-70, v 184 pt 3E, p 31

34. Petukhov, B.S., Polyakov, A.F., "Heat Transfer and Resistance in Rotating Pipe (survey), Izvestiya Akademii Nauk SSSR, Energetika i Transport, 1977, v 15, # 3, pp 116-133

35. Mori, Y., Nakayama, W., "Secondary Flows and Enhanced Heat Transfer in Rotating Pipes and Ducts," presented at ICHMT 14th Symposium, 1982, Dubrovnik, Yugoslavia

36. Lambrecht, D., "Problems of FLow and Heating in Turbo-generators with Water-cooled Rotor Winding," Proc. Instn. Mech. Engrs., 1969-70, v 184 pt 3E, p 41

37. Sakamoto, M., Fukui, S., "Convective Heat Transfer of a Rotating Tube Revolving About an Axis Parallel to Itself" Intl. Heat Transfer Conference Proceedings, 1070, 4th, v 3, FC7.2

38. Woods, J.L., Morris, W.D., "An Investigation of Laminar Flow in the Rotor Windings of Directly-cooled Electrical Machines," Journal of Mech. Engng. Science, 1974, v 16, # 6, p 408

39. Nakayama, W., Fuzioka, K., "Flow and Heat Transfer in

the Water-cooled Rotor Winding of a Turbine Generator," IEEE Trans. on Power Apparatus and Systems, 1978, v PAS-97, #1, p 225

40. Morris, W.D., " Flow and Heat Transfer in Rotating Coolant Channels," AGARD-CP-229, Conf. Proc., 1977, p 38-1

41. Marto, P.J., "Recent Developments in Heat and Mass Transfer in Rotating Machinery," Naval Postgraduate School Report, October 1982

42. Johnson, A.R., Morris, W.D., "Pressure Loss Measurments in Circular Ducts which Rotate about a Parallel Axis," presented at ICHMT 14th Symposium, 1982, Dubrovnik, Yugoslavia

43. Stephenson, P.L., "An Experimental Study of Flow and Heat Transfer in a Duct Rotating about a Parallel Axis," presented at ICHMT 14th Symposium, 1982, Dubrovnik, Yugoslavia

44. Japikse, D., "Advances in Thermosyphon Technology," Recent Advances in Heat Transfer, 1963, v 9, p 1

45. Davies, T.H., Morris, W.D., "Heat Transfer Characteristics of a Closed Loop Rotating Thermosyphon," Proc. Intl. Heat Transfer Conf., 3rd, 1966, v 2, p 172

46. Bayley, F.J., Lock, G.S.H., "Heat Transfer Characteristics of the Closed Thermosyphon, Journal of Heat Transfer, 1965, vol 87, #1, pp. 30-40

47. Bayley, F.J., Martin, B.W., "A Review of Liquid Cooling of High-Temperature Gas-Turbine Rotor Blades," Proc. Instn. Mech. Engnrs., 1970-71, vol 185, #18, pp. 219-227

48. Marto, P.J., "Rotating Heat Pipes," Heat and Mass Transfer in Rotating Machinery, Hemispere, 1983, pp. 609-632

49. Gaugler, R.S., Heat Transfer Devices, U.S.Patent 2350348, 1944

50. Trefethen, L., "On the Surface Tension Pumping of Liquids or a Possible Role of the Candlewick in Space Exploration," GE Tech. Inf. Ser. No. 615-D114, General Electric Company, Schenectady, N.Y., Feburary 1962

51. Grover, G.M., Cotter, T.P., and Erickson, G.F., "Structures of Very High Thermal Conductivity," Journal of Applied Physics, 1964, vol 35, pp. 1190-1191

52. Kraus, A.D., Bar-Cohen, A., "Thermal Analysis and Control of Electronic Equipment," Hemisphere, Washington, DC, 1983

53. Chi, S.T., Heat Pipe Theory and Practice, Hemisphere, Washington, DC, 1976

54. Cohen, H., Bayley, F.J., " " Proc. Inst. Mech. Engnrs., 1955, vol 169, #53, p. 1063

55. Lee, Y., Mital, U., "A Two-Phase Closed Thermosyphon" Intl. J. Heat Mass Transfer, 1972, vol 15, pp 1695-1707

56. Jaster, H., Kosky, P.G., "Condensation Heat Transfer in a Mixed Flow Regime", Intl. J. Heat Mass Transfer, 1976, vol 19, pp 95-99

57. Collier, J.G., Wallis, G.B., Two-Phase Flow and Heat Transfer, Notes for a Short Course, 24 July-4 Aug. 1967, Stanford University.

58. Collier, J.G., Convective Boiling and Condensation McGraw-Hill(UK), 1972

59. Wallis, G.B., One-dimensional Two-phase Flow, McGraw-Hill, 1969

60. Corman, J.C., McLaughlin, M.H., "Thermal Design-Heat Pipe Cooled Electric Motor," General Electric Report # 71-C-140, prepared for U.S. Army under DAAK 02-69-C-0510, May 1971

61. Groll, M., Krahling, H., Munzel, W.D., "Heat Pipes for Cooling of an Electric Motor, 3rd Int'l Heat Pipe Conf., Palo Alto, CA., 22-24 May 1978

62. Greene, D.L., Mole, C.J., Welch, W.P., Seng, W.R., "Analysis of a High- Power Water-Cooled Electric Propulsion System," SNAME Transactions, 1978, vol 86, pp 140-162

63. Morris, W.D., "Experimental Observations on the Thermal Performance of a Rotating Coolant Circuit with Reference to the Design of Electrical Machine Rotors", Inst. Mech Engnrs., 1976, vol 190, pp 561-570

64. Gibb, Sir Claude, "Report on Investigation into the Failure of Two 100-MW Turbo-generators," Instn. Mech Engnrs., General Mtg., 15 Feburary 1955, pp 511-538

65. Peach, N., "Generator Rotors can be Water-cooled", Power, August 1968, pp 80-81

66. Peach, N., "Largest Generators are Water-cooled", Power, August 1970, pp 34-36

67. Schwartz, B.B., Foner, S., "Superconductor Applications: SQUIDs and Machines," Proceedings of a NATO Advanced Study Institute on Small-scale Applications of Superconductivity, Plenum Press, 1976, pp 34-36

INITIAL DISTRIBUTION LIST

		No. Copies
1.	Defense Technical Information Center Cameron Station Alexandria, Virginia 22314	2
2.	Library, Code 0142 Naval Postgraduate School Monterey, California 93943	2
3.	Chairman, Department of Mechanical Engineering Code 69 Naval Postgraduate School Monterey, California 93943	1
4.	Dr. P.J. Marto, Code 69Mx Department of Mechanical Engineering Naval Postgraduate School Monterey, California 93943	5
5.	Dr. A.S. Wanniarachchi, Code 69Wa Department of Mechanical Engineering Naval Postgraduate School Monterey, California 93943	1
6.	Lt. J.L. Szatkowski, USN c/o 952 Harrop St. Ogden, Utah 84404	2
7.	Mr. Joseph Odom, Code 56Z31 Naval Sea Systems Command 2221 Jefferson Davis Hwy. Arlington, Virginia 20360	1
8.	Mr. M. Superczynski, Code 2712 Naval Ship Research and Development Center Annapolis, Maryland 21402	2